BELLE2-NOTE-XX-YYYY-ZZZ
Version X.Y
January 15, 2025

Search for $D^0 \to$ invisible final states in Belle II experiment

Chanho Kim*, Youngjoon Kwon†,

Yonsei University

Abstract

We measured the branching fraction of $D^0 \to K^-\pi^+$ control mode decay and the upper limit of Branching fraction of D^0 to invisible final states signal mode on 1 ab^{-1} generic MC which contains mixed, charged, $q\bar{q}(q = u, d, s, c)$ events. the measurement of absolute branching fraction of the signal and control mode is performed with charm tagging method. the results are shown in the below.

Contents

List of Figures

List of Tables

1 Motivation

In standard model, the decay D^0 to the invisible final states correspond to the $D^0 \to \nu\bar{\nu}$ decay and its Feynmann diagrams are shown in Figure 1. however as shown in the figure 2, the $D^0 \to \nu\bar{\nu}$ is helicity suppressed with expected branching fraction of 10^{-30} order, which is beyond current collider experiment. but the Br($D^0 \to$ invisible) can be enhanced in some of dark matter model. if signal is observed, then it would be a sign of new physics. in other words, the search for D^0 to the invisible final states is very sensitive to new physics.

The previous research in Belle exepriment had result of upper limit estimation of Branching fraction. its value is 9.4×10^{-5} at 90% conference level on 924fb^{-1} data samples.

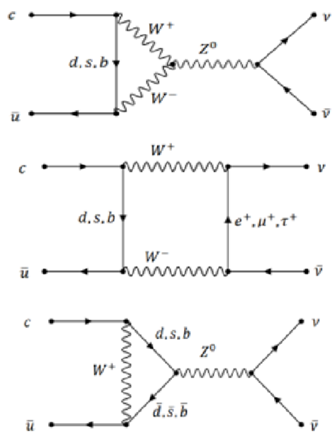

Figure 1: Feynman diagram of signal MC

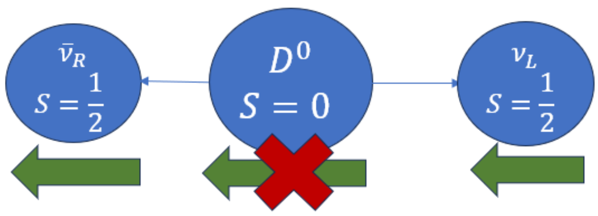

Figure 2: Scheme of helicity suppresing

2 Data Sample

The analysis is based on the 1ab^{-1} MC15 run independent samples that contains mixed, charged and $q\bar{q}(q = u, d, s, c)$ events and the signal MC which have 20M $e^+e^- \to c\bar{c} \to D_{tag}X_{frag}D^{*+}_{sig}$ and $D^{*+}_{sig} \to D^0_{sig}\pi^{\pm}$ and $D^0_{sig} \to \nu\bar{\nu}$ event and 20M $D^0 \to K^-\pi^+$ events as control sample.

3 Charm tagger : Inclusive D^0 reconstruction

3.1 Overview

Since the signal D^0 is invisible, so direct reconstruction of signal D^0 is not possible. so, we need to reconstruct the signal D^0 indirectly. To obtain the inclusive D^0 sample, the process followed by $e^+e^- \to c\bar{c}$ which we are going to reconstruct is

$$e^+e^- \to c\bar{c} \to D_{tag}^{(*)} X_{frag} D^{*+}, D^{*+} \to D^0\pi^+$$

Through this process, one of the c quark hadronizes into $D_{tag}^{(*)}$, which is going to be reconstructed as tag side. $D_{tag}^{(*)}$ includes ground state $D_{tag}(D^0, D^+, D_s^+$ and $\Lambda_c^+)$ and excited state $D_{tag}^*(D^{*0}, D^{*+}$ and $D_s^{*+})$. Since the CM energy of KEKB is above the $c\bar{c}$ mass threshold, for the $e^+e^- \to c\bar{c}$ production, besides two hadrons with c flavor would be generated from the 2 c jets, other unflavored mesons would also be generated from fragmentation, which is denoted as X_{frag}. X_{frag} consists of any number of pions or γ, and even number of Kaons. The information of recoil D^* is the missing momentum against the reconstructed $D_{tag}^{(*)}$ and X_{frag}. We use the inverse mass constrained fit to improve the resolution of recoil D^* momentum and to suppress background from many fragmenation particle combinations. With tagging on a extra slow π^+ from recoil D^{*+}, we can finally reconstruct the inclusive D^0. The yield of inclusive D^0 is obtained by the fit on missing mass distribution recoiling against $D_{tag}^{(*)}, X_{frag}$ and π_s^+.

One example of the signal events that consist of $D_{tag}^* = D^{*+}(\to D^+(\to K^-\pi^+\pi^+)\pi^0)$ and $X_{frag} = K^+K^-$ is the below figure. In this example, I reconstructed $D^{*+} \to D^+(\to K^-\pi^+\pi^+)\pi^0$ and K^+K^- directly and then reconstruct signal side D^{*-} by calculating missing momentum against of this D_{tag}^* and X_{frag}.

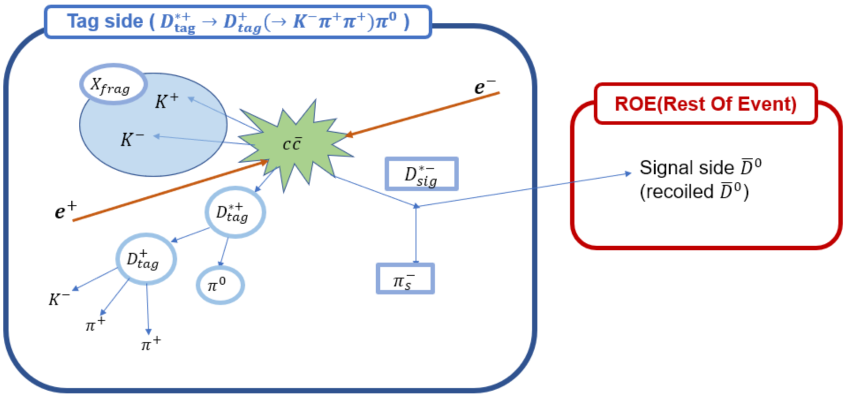

Figure 3: one example of signal events

Measurement of absolute branching fraction of D^0 to an exclusive final state f is determined by this formula:

$$\mathrm{Br}(D^0 \to f) = \frac{N_{excl}(D^0 \to f)}{N_{incl}^{D^0} \cdot \epsilon(D^0 \to f|incl.D^0)}$$

where $N_{incl}^{D^0}$ represents the total number of inclusive D^0 reconstructed by the charm tagger, $N_{excl}(D^0 \to f)$ is signal yield of exclusive $D^0 \to f$ decay, and the $\epsilon(D^0 \to f|incl.D^0)$ is the signal side selection efficiency of $D^0 \to f$ decay with a given inclusive D^0 sample. Basically, the signal side selection is usually constraints on the remaining detector information for specific D^0. For instance, we will require there is no remaining detector information at signal side for $D^0 \to \nu\bar{\nu}$ study.

In order to get better statistics, we reconstruct as many tag side decay channels as possible. for this reason, one of the main background source is from mis-reconstruction of tag side. So, the BDT is also being used for suppressing background from mis-reconstructed tag side.

This signal event reconstruction procedure is called as Charm Tagger and basf2 release-06 is used for MC production and basf2 light-2405-quaxo version is used for reconstruction.

3.2 D_{tag} recontruction

The first step is to reconsttruct the ground state charm hadron D_{tag}. I used 4 types of D_{tag} and totally 51 decay channels are reconstructed and all these channels are listed in Table 1. All reconstructions except for $D^0 \to K_S^0\pi^0$, $D^+ \to \pi^+\pi^0$ and $\Lambda_c^+ \to \Sigma^+\pi^0$ were done with vertex fit. applying vertex fit on these 3 channels is not possible due to degree of freedom issue for vertex fit.

D^0 decay	$Br(\%)$	D^+ decay	$Br(\%)$	Λ_c^+ decay	$Br(\%)$	D_s^+ decay	$Br(\%)$
$K^-\pi^+$	3.9	$K^-\pi^+\pi^+$	9.4	$pK^-\pi^+$	5.0	$K^+K^-\pi^+$	5.5
$K^-\pi^+\pi^0$	13.9	$K^-\pi^+\pi^+\pi^0$	6.1	$pK^-\pi^+\pi^0$	3.4	$K_S^0K^+$	1.5
$K^-\pi^+\pi^+\pi^-$	8.1	$K_S^0\pi^+$	1.5	pK_s^0	1.1	$K_S^0K_S^0\pi^+$	5.4
$K^-\pi^+\pi^+\pi^-\pi^0$	4.2	$K_S^0\pi^+\pi^0$	6.9	$\Lambda^0\pi^+$	1.1	$K^+K^-\pi^+\pi^0$	5.6
$K_S^0\pi^+\pi^-$	2.9	$K_S^0\pi^+\pi^+\pi^-$	3.1	$\Lambda^0\pi^+\pi^0$	3.6	$K_S^0K^-\pi^+\pi^+$	1.5
$K_S^0\pi^+\pi^-\pi^0$	5.4	$K^+K^-\pi^+$	1.0	$\Lambda^0\pi^+\pi^+\pi^-$	2.6	$K^+\pi^-\pi^+K_S^0$	1.0
$K^-\pi^+\pi^0\pi^0$	8.9	$K^-K^+\pi^+\pi^0$	0.7	$p^+\pi^-\pi^+$	0.5	$\pi^+\pi^-\pi^+$	1.0
$\pi^-\pi^+$	0.1	$\pi^-\pi^+\pi^+$	0.3	$p^+K^-K^+$	0.1	$\pi^+K_S^0$	0.1
$\pi^-\pi^+\pi^-\pi^+$	0.8	$\pi^-\pi^+\pi^+\pi^0$	1.2	$p^+K^-\pi^+\pi^0\pi^0$	0.1	$\pi^+\pi^0K_S^0$	0.5
$\pi^-\pi^+\pi^0$	1.5	$K^+K_S^0K_S^0$	0.3	$p^+\pi^-\pi^+\pi^-\pi^+$	0.2	$K^-K^+\pi^+\pi^-\pi^+$	0.7
$\pi^-\pi^+\pi^0\pi^0$	1.0	$\pi^+\pi^0$	0.1	$p^+K_S^0\pi^0$	2.0		
K^-K^+	0.4			$p^+K_S^0\pi^+\pi^-$	1.6		
$K^-K^+\pi^0$	0.3			$\pi^+\pi^-\Sigma^+$	4.5		
$K^-K^+K_S^0$	0.4			$\pi^+\pi^-\pi^0\Sigma^+$	1.2		
$\pi^0K_S^0$	1.2			$\pi^0\Sigma^+$	1.2		
sum	53.1	sum	30.5	sum	28.2	sum	22.8

Table 1: D_{tag} decay channels (note : $\pi^+\pi^-\pi^0\Sigma^+$ not measured yet)

3.2.1 Preselection for final state particles

- Selection for charged tracks
  - dr < 1.0 and |dz| < 3.0 and thetaInCDCAcceptance
- PID selection for Charged hadrons (π^+, K^+ and p^+)

- π^+ : 15 candidates with highest pionID after pionID > 0.01
- K^+ : 10 candidates with highest kaonID after kaonID > 0.1
- p^+ : 10 candidates with highest protonID after protonID > 0.1

• selection for π^0, K_S^0, Σ^+ and Λ^0

- K_S^0 : 0.468 GeV/c^2 < M < 0.506 GeV/c^2 and goodBelleKshort == 1
- Σ^+ : 1.08 GeV/c^2 < M < 1.28 GeV/c^2
- π^0 :
  * standard eff40 May2020 π^0
  * beamBackgroundSuppression > 0.5 and fakePhotonSuppression > 0.1 for each daughter γ
- Λ^0 :
  * 1.111 GeV/c^2 < M < 1.121 GeV/c^2
  * dr > 0.1
  * $\chi^2 < 100$
  * cosAngleBetweenMomentumAndVertexVectorInXYPlane > 0.99

3.2.2 Preselection for D_{tag} candidate

For D_{tag} reconstruction, I applied some selections on mass and momentum variables and if vertex fit was applied, selection on χ^2. this is just preselection so just only some basic selections were applied such as roughly mass cut covering the nominal mass and selection on p* for suppressiong charm particle from B meson decay and accept only reasonable scaled momentum(xp) value. the below table is about this preseletion.

D^0	1.81 GeV/c^2 < M < 1.91 GeV/c^2 p* > 2.3 GeV and xp > 0.0 $\chi^2 < 20$
D^+	1.81 GeV/c^2 < M < 1.91 GeV/c^2 p* > 2.3 GeV and xp > 0.0 $\chi^2 < 20$
Λ_c^+	2.23 GeV/c^2 < M < 2.33 GeV/c^2 p* > 2.3 GeV and xp > 0.0 $\chi^2 < 20$
D_s^+	1.91 GeV/c^2 < M < 2.0 GeV/c^2 p* > 2.3 GeV and xp > 0.0 $\chi^2 < 20$
Note	selection about χ^2 is only on those reconstructed channels with vertex fit

Table 2: preselection for D_{tag} reconstruction

3.3 D^*_{tag} reconstruction

Table 3: D^*_{tag} decay channels

D^{*+} decay	Br(%)	D^{*0} decay	Br(%)	D_s^{*+} decay	Br(%)
$D^0\pi^+$	67.7	$D^0\pi^0$	61.9	$D_s^+\gamma$	93.5
$D^+\pi^0$	30.7	$D^0\gamma$	38.1		
sum	98.4	sum	100.0	sum	93.5

For reconstruction of D^*_{tag}, I used totally 5 channels listed in the table 3. in this step, $\pi^0, \pi^\pm$ and γ are used for reconstruction and I also did π^0 veto to suppress background in case of using γ.

- Selection for $\pi^\pm$, π^0 and γ to reconstruct D^*_{tag}
  - $\pi^\pm$: same selection criteria with preselection on first step of charm tagger
  - π^0 : same selection criteria with preselection on first step of charm tagger
  - γ :
    * |clusterTiming| < 200 ns and $\left|\frac{\text{clusterTiming}}{\text{clusterErrorTiming}}\right| < 2.0$
    * beamBackgroundSuppression > 0.5 and fakePhotonSuppression > 0.1
    * E > 0.1 GeV

- Selection for π^0 veto on $D^{*0} \to D^0\gamma$ and $D_s^+ \to D_s^+\gamma$:
  The γ used in reconstruction of $D^{*0} \to D^0\gamma$ and $D_s^+ \to D_s^+\gamma$ can be from $\pi^0 \to \gamma\gamma$. so I would like to suppress background from $\pi^0 \to \gamma\gamma$ decay by vetoing γ candidate that can be from π^0.

  To do π^0 veto, the procedure is like this :
  I made combination using γ_{sig} from $D^{*0} \to D^0\gamma$ and $D_s^+ \to D_s^+\gamma$
  and γ_{roe} in rest of event and check whether that combination is π^0 like
  by checking $\mathrm{M}_{\gamma_{\mathrm{sig}}\gamma_{\mathrm{roe}}}$ and if that combination is in π^0 selection,
  then veto $D^{*0} \to D^0\gamma$ and $D_s^+ \to D_s^+\gamma$ candidates.

  - γ_{roe} :
    * standard loose photon:
      inCDCAcceptance and clusterErrorTiming < 10^6
      clusterE1E9 > 0.4 or E > 0.075
    * should be in Rest Of Event (isRestOfEvent == 1)
    * beamBackgroundSuppression > 0.5 and fakePhotonSuppression > 0.1
  - π^0 (combination of γ_{sig} and γ_{roe}):
    * 0.115 GeV/c^2 < $\mathrm{M}_{\gamma_{\mathrm{sig}}\gamma_{\mathrm{roe}}}$ < 0.150 GeV/c^2
    * $\left|\frac{E_{\gamma_1}-E_{\gamma_2}}{E_{\gamma_1}+E_{\gamma_2}}\right| < 0.5$
    * select one π^0 candidate with smallest dM

3.3.1 Preselection for D^*_{tag} candidate

Table 4: Selections of D^*_{tag}

D^*_{tag}	Mass [GeV/c^2]	ΔM [GeV/c^2]
$D^{*+} \to D^0\pi^+$	$1.96 \sim 2.06$	$0.14 \sim 0.15$
$D^{*+} \to D^+\pi^0$	$1.96 \sim 2.06$	$0.1375 \sim 0.1465$
$D^{*0} \to D^0\pi^0$	$1.95 \sim 2.05$	$0.1375 \sim 0.1465$
$D^{*0} \to D^0\gamma$	$1.95 \sim 2.05$	$0.125 \sim 0.160$
$D^{*+}_s \to D^+_s\gamma$	$2.06 \sim 2.16$	$0.125 \sim 0.16$
Note	xp > 0.0 for all D^*_{tag}	vertex fit on $D^{*+} \to D^0\pi^+$

3.4 FastBDT: background suppression from $D^{(*)}_{tag}$ reconstruct

Since there are so much $D^{(*)}_{tag}$ decay channels for tag side reconstruction, the mis-reconstructed $D^{(*)}_{tag}$ can be one of the main source of backgrounds. so I used fastBDT to suppress the background from reconstruction of $D^{(*)}_{tag}$. I totally trained 51 BDTs for D_{tag} and 5 BDTs for D^*_{tag} for this charm tagger.

The training is done on 1ab^{-1} MC15 run independent generic MC sample. in order to avoid bias in training, the size of signal and background sample for each trainings was set up as same.

3.4.1 Input variables of FastBDT

- Input variables for D_{tag} training
  - PID for charged tracks : pionID for π^+, kaonID for K^+, protonID for p^+
  - dr(flightlength), dz (these variables used for the decay with vertex fit applied)
  - Mass : M
  - scaled momentum : xp
  - angle variables :
    - cosAngleBetweenMomentumAndVertexVectorInXYPlane
    - cosToThrustOfEvent
    - cosHelicityAngle(only for 2 body or 3 body decays)
  - variables for π^0, K^0_S, Λ^0 and Σ^+ :
    - Energy Asymmetry between two daughters : $\left|\frac{E_{d_1}-E_{d_2}}{E_{d_1}+E_{d_2}}\right|$
    - Angle between momentum of two daughters
- Input variables for D^*_{tag} training
  - PID for charged tracks : pionID for π^+
  - momentum of γ
  - dr(flightlength), dz (these variables used for the decay with vertex fit applied)

– ΔM($=M_{D^*_{tag}} - M_{D_{tag}}$)
– scaled momentum : xp
– angle variables :
  * cosAngleBetweenMomentumAndVertexVectorInXYPlane
  * cosToThrustOfEvent
  * cosHelicityAngle
– variables for π^0 :
  * Energy Asymmetry between two daughters : $\left|\frac{E_{\gamma_1} - E_{\gamma_2}}{E_{\gamma_1} + E_{\gamma_2}}\right|$
  * Angle between momentum of two daughters

3.4.2 BDT Input variable distribution

In this section, there are BDT input variables for training about $D^0 \to \pi^+\pi^- K^0_S$ in tag side. All the other training informations will be appendix section.

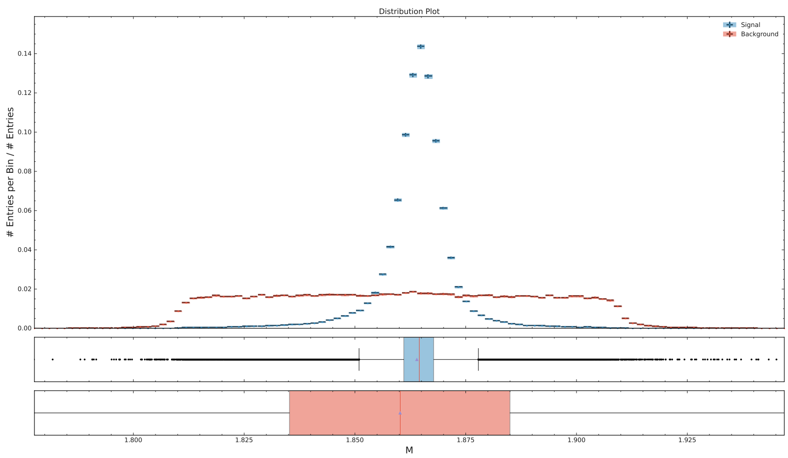

Figure 4: BDT Input variable: Mass

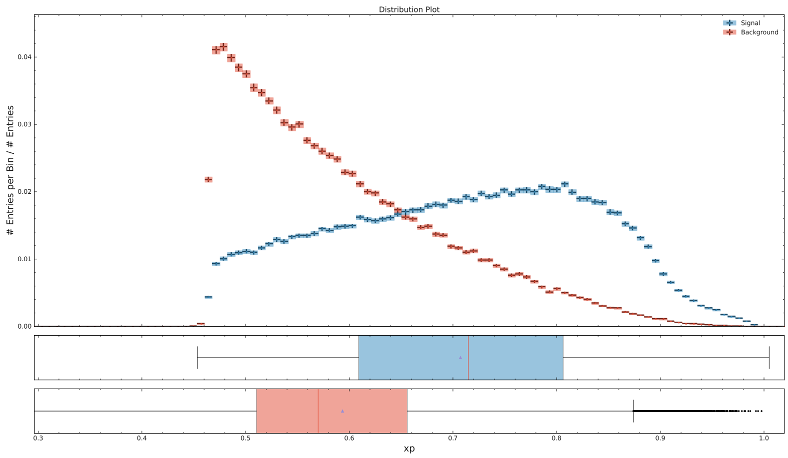

Figure 5: BDT Input variable: xp(scaled momentum)

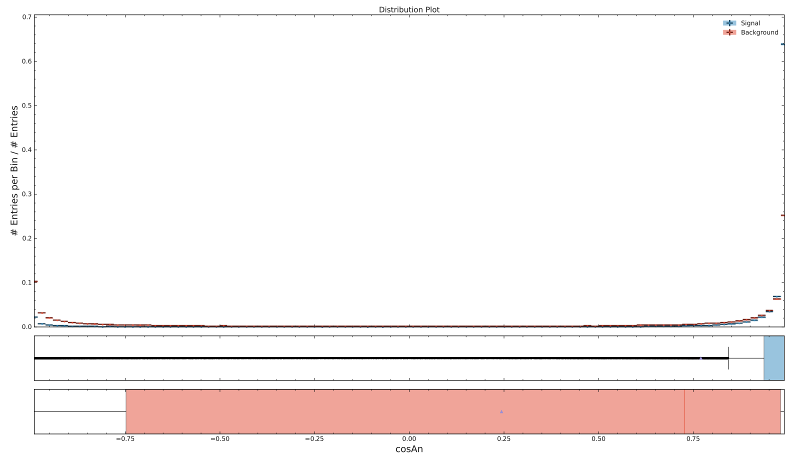

Figure 6: BDT Input variable: cosAngleBetweenMomentumAndVertexVectorInXYPlane

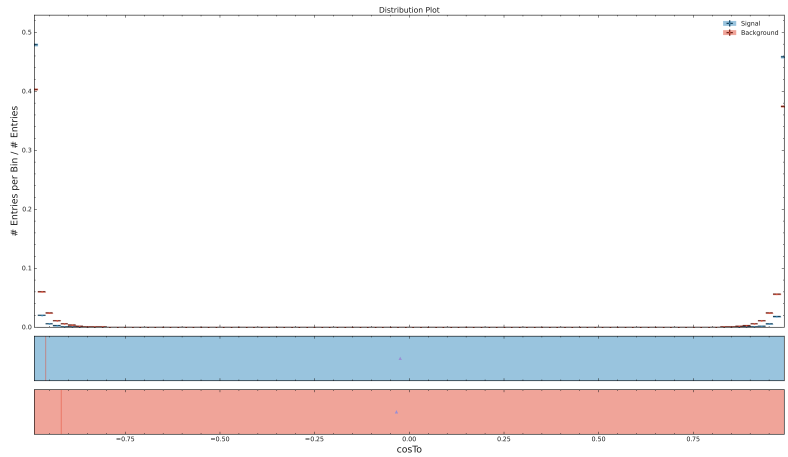

Figure 7: BDT Input variable: cosToThrustOfEvent

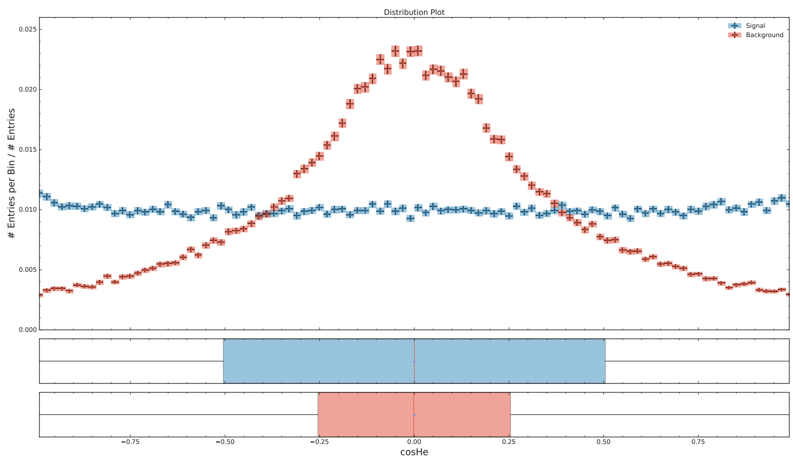

Figure 8: BDT Input variable: cosHelicityAngleMomentum

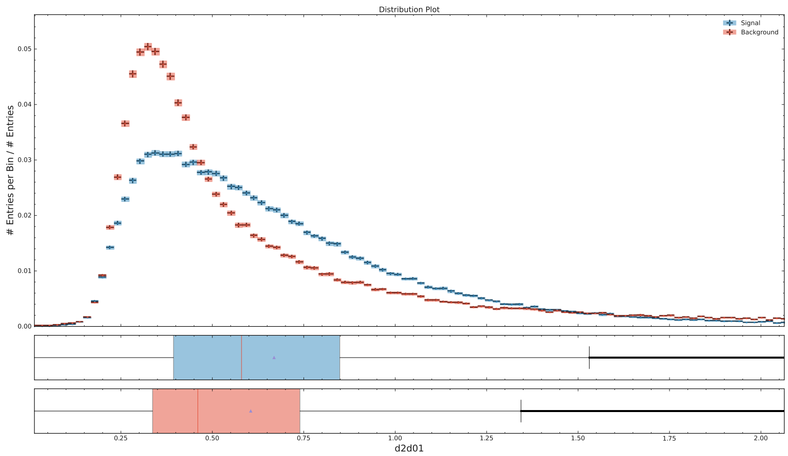

Figure 9: BDT Input variable: angle between 2 daughters of K_S^0

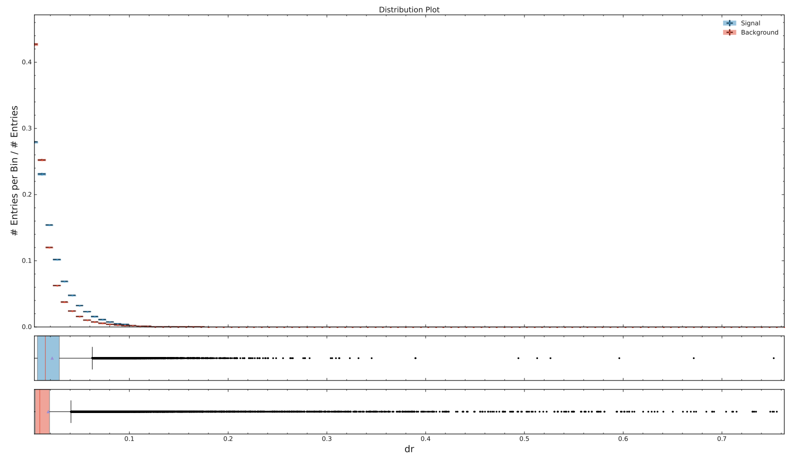

Figure 10: BDT Input variable: dr

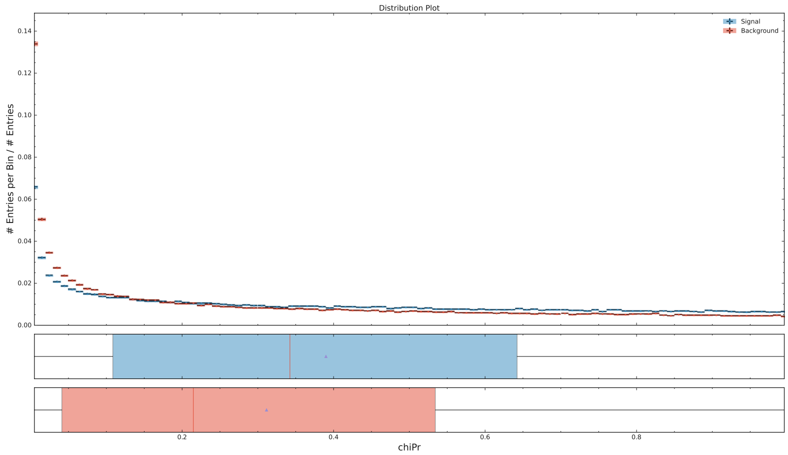

Figure 11: BDT Input variable: chiProb

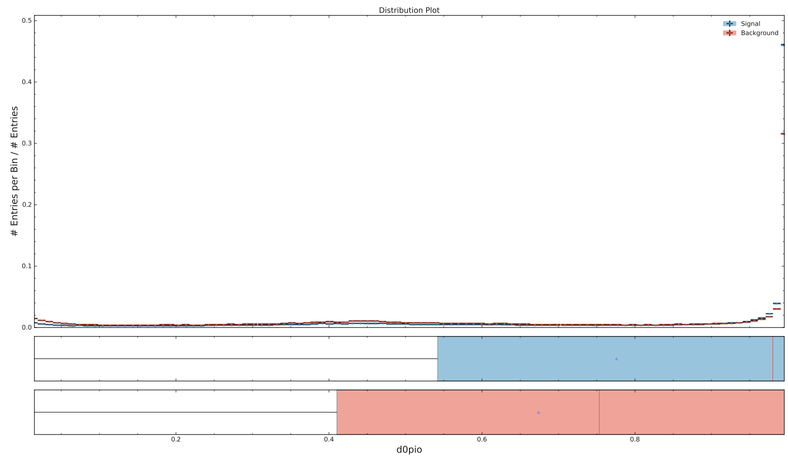

Figure 12: BDT Input variable: pionID

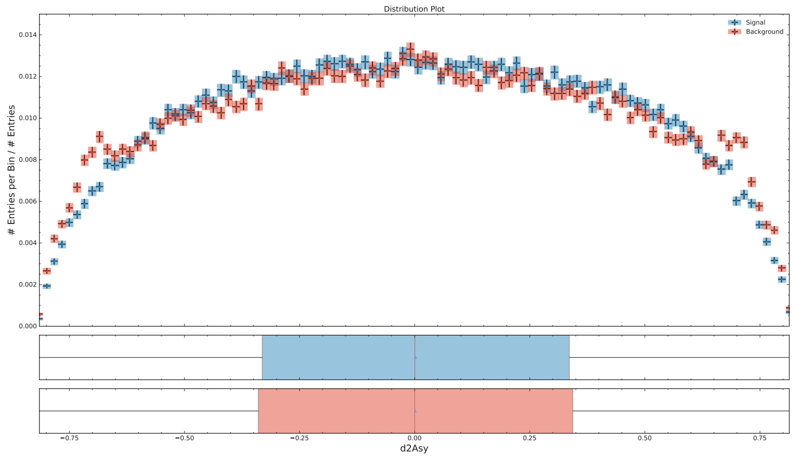

Figure 13: BDT Input variable: Energy Asymmetry

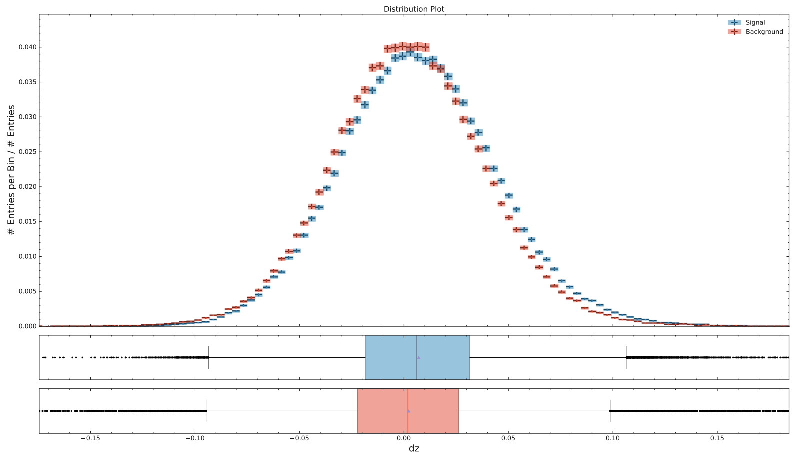

Figure 14: BDT Input variable: dz

3.4.3 Check correlation on BDT Input variables

As first trial, as many variables as possible are used for BDT input variables and then with checking correlation and importance of variables some variables are removed in BDT input varible lists.

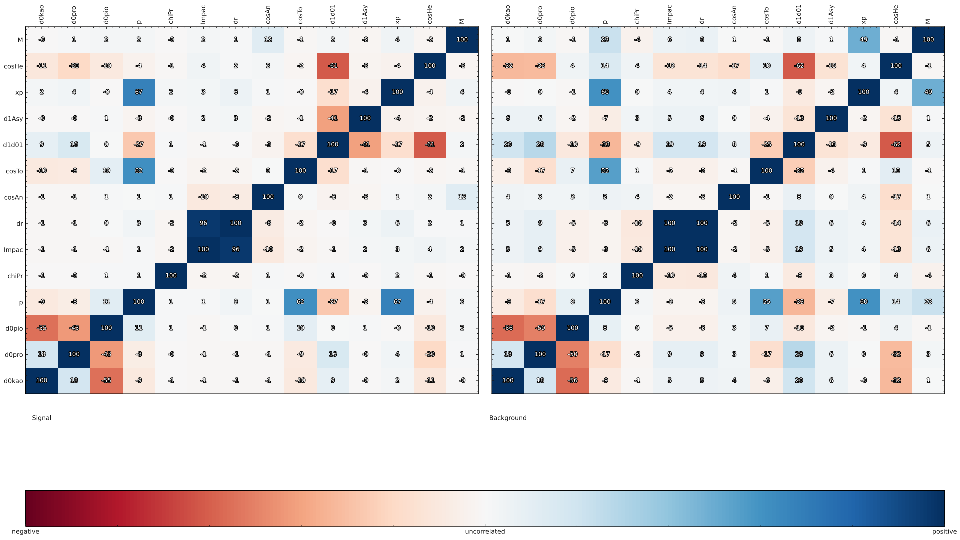

Figure 15: high correlation in old training $\Lambda_c^+ \to p^+ K_S^0 \pi^0$

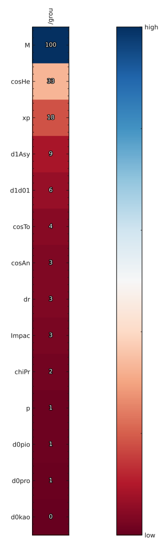

Figure 16: importance of BDT variables of training $\Lambda_c^+ \to p^+ K_S^0 \pi^0$

All the pionID, kaonID and protonID for each pion, kaon and proton candidate were used in training, but it seems not so worthful but just had correlations each variables. so the PID variables are reduced by removing redundant kaonID, protonID for pion candidate and pionID, protonID for kaon candidate and pionID, kaonID for proton candidate. In case of high correlation above 50 commonly in many tag channels, variables with low importance are removed. For example, there were high correlation over Q, E, p, xp variables and xp had greater importance so Q, E, p are removed in BDT input variables.

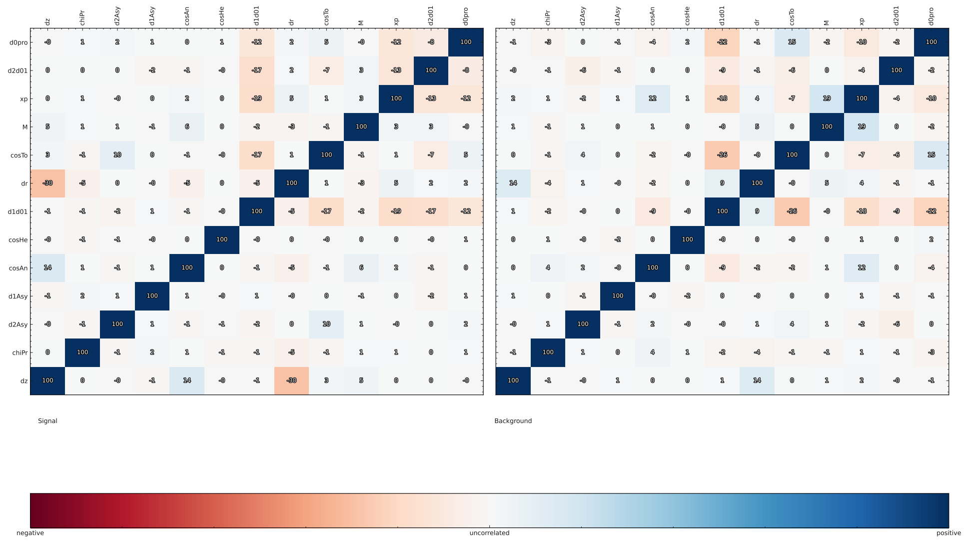

Figure 17: correlation plot in new training $\Lambda_c^+ \to p^+ K_S^0 \pi^0$

3.4.4 Optimizations of FastBDT setup and selection on FastBDT output

There are hyper parameters in BDT such as number of trees, cuts and depth. so I also optimized those hyper parameter by doing grid search about those parameters for each BDTs.

Another optimization is about the selection on BDT output. it is by calculating the FoM(Figure of Merit). the definition of FoM is $\frac{S}{\sqrt{S+B}}$.

These optimizations are done on all 56 BDTs.

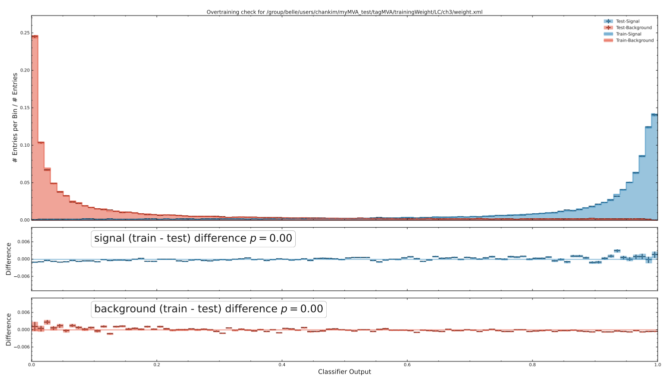

Figure 18: training result $\Lambda_c^+ \to p^+ K^- \pi^+ \pi^0$ as example

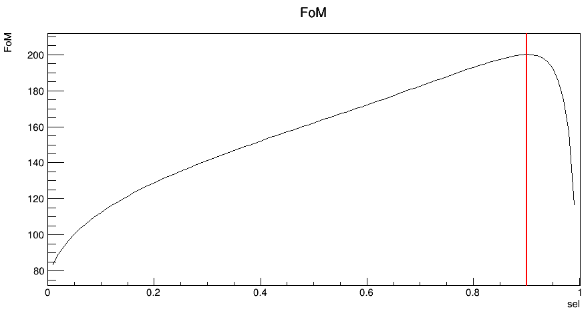

Figure 19: optimization on BDT output for $\Lambda_c^+ \rightarrow p^+K^-\pi^+\pi^0$ as example

3.5 X_{frag} reconstruction

Table 5: Fragmentation according to tag side

D^{*+} *or* D^+	D^{*0} *or* D^0	Λ_c^+	D_s^{*+} *or* D_s^+
nothing(K^+K^-)	$\pi^+(K^+K^-)$	$\pi^+\bar{p}$	K_S^0
$\pi^0(K^+K^-)$	$\pi^+\pi^0(K^+K^-)$	$\pi^+\pi^0\bar{p}$	$\pi^0K_S^0$
$\pi^+\pi^-(K^+K^-)$	$\pi^+\pi^+\pi^-(K^+K^-)$	$\pi^+\pi^-\pi^+\bar{p}$	π^+K^-
$\pi^+\pi^-\pi^0(K^+K^-)$			$\pi^+\pi^-\pi^0K_S^0$
			π^+K^-
			$\pi^+\pi^0K^-$
			$\pi^+\pi^-\pi^+K^-$

All fragmentation channels are selected with conserving baryon quantum number and strangness quantum number and charge according to $D_{tag}^{(*)}$ particle so that the signal side can contain $D^{*\pm}$. Totally 24 channels are used as fragmentations and listed in table 5.

3.5.1 Preselection for X_{frag}

- Selection for fragmentation particles ($\pi^+,\ K^+$ and p^+ and π^0)
  - π^+ : pionID > 0.1 and p > 0.1 GeV
  - K^+ : kaonID > 0.9 and p > 0.1 GeV
  - p^+ : protonID > 0.9 and p > 0.1 GeV
  - K_S^0 : same with K_S^0 in charm tagger with p > 0.1 GeV
  - π^0 :
    - same with preselection of π^0 in charm tagger
    - additionally p > 0.1 GeV
    - additionally $\left|\frac{E_{\gamma_1}-E_{\gamma_2}}{E_{\gamma_1}+E_{\gamma_2}}\right| < 0.9$

3.6 Reconstruction of signal side D^*

There are many possible combinations in X_{frag} and it means there can be many backgrounds from possible combination of particles in fragmentation. so I applied inverse mass constrained fit on $M_{miss}(D^{(*)}_{tag} X_{frag})$ to m_{D^*}, the nominal mass of $D^{*\pm}$, and choose only one candidate with highest chiProb calculated from this mass constrained fit.

3.7 Reconstruction of signal side D^0 from recoiled $D^{*\pm}$

With tagging π_s^+, singal D^0 momentum is calculated by $p_{miss}(D^{(*)}_{tag} X_{frag}) - p(\pi_s^+)$. one thing to be careful is that there can be also multiple candiates from multiple π_s^+ candidates. so I choosed one recoiled signal side D^0 with largest opening angle between momentums of $D^{(*)}_{tag}$ and signal side D^0 in center of mass frame.

3.8 Charm tagger execution

- Procedure of Charm Tagger execution
  - Preparation of $\pi^+, K^+, p^+, \pi^0, K^0_S, \Lambda^0, \Sigma^+$
  - Reconstruction of D_{tag} with tag side decay channels
  - Optimized selection with FoM on BDT output about D_{tag}
  - Reconstruction of D^*_{tag}
  - Optimized selection with FoM on BDT output about D^*_{tag}
  - Reconstruction recoiled signal side $D^{*\pm}$ with $D^{(*)}_{tag}$ and X_{frag}
  - inverse mass constrained fit on recoiled signal side $D^{*\pm}$ mass
  - Selection of best candidate of recoiled signal side $D^{*\pm}$ with chiProb
  - Reconstruction of recoiled signal side D^0 with tagging $\pi_s^\pm$
  - Selection of best canadiate of recoiled signal side D^0 with opening angle between D^*_{tag} and recoiled signal D^0 in center of mass frame

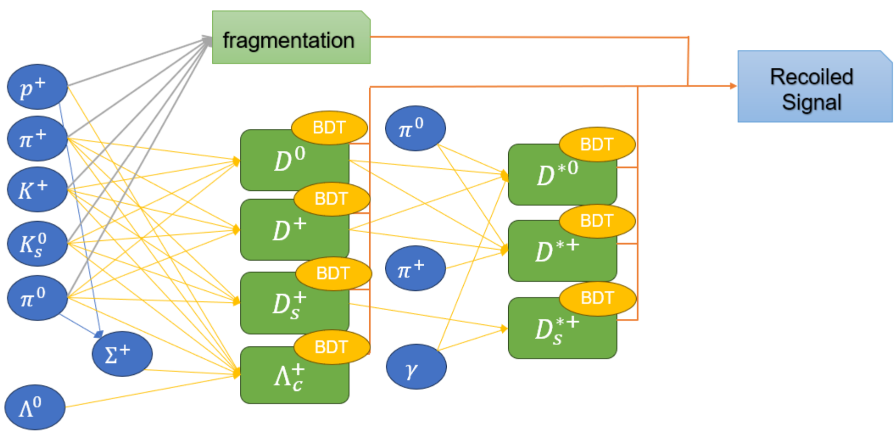

Figure 20: Scheme of Charm tagger execution

3.9 D^0 from charm tagger

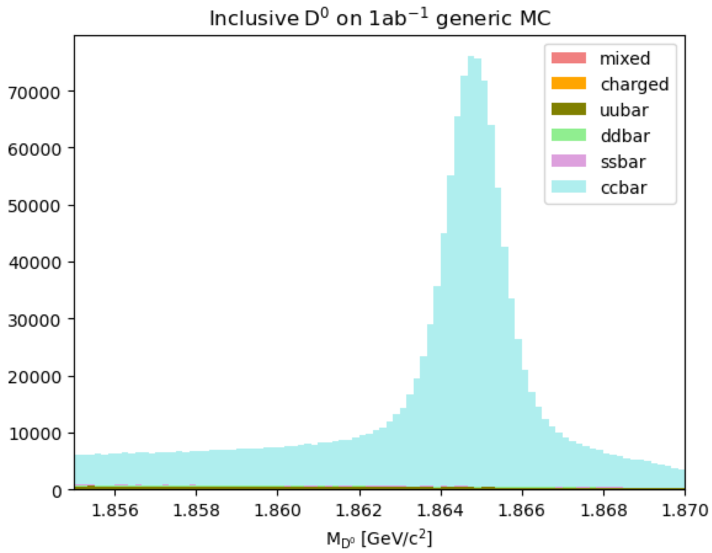

Figure 21: Recoiled signal D^0 from charm tagger on 1ab^{-1} generic MC

- Inclusive D^0 : D^0 from charm tagger can have any decays since there are no requirements on signal side. so D^0 from charm tagger is inclusive D^0.
  - tagging efficiency: 0.18%
- Exclusive D^0 : exclusive D^0 from charm tagger is subset of inclusive D^0 from charm tagger by requiring some selections on the signal side(=rest of event of $D^{(*)}_{tag}X_{frag}\pi^{\pm}_{s}$). For this, I checked number of tracks, $\pi^0, K^0_S, K^0_L, \Lambda^0$, and if possilbe, directly reconstructed signal D^0.
  - track selection : dr < 1.0 and $|\text{dz}| < 3.0$
  - K^0_S selection : same with tag preselection
  - Λ^0 selection : same with tag preselection
  - π^0 selection :
    - $0.115\ \text{GeV/c}^2 < \text{M} < 0.155\ \text{GeV/c}^2$
    - $|\text{clusterTiming}| < 200$ ns and $\left|\frac{\text{clusterTiming}}{\text{clusterErrorTiming}}\right| < 2.0$ for daughter γ
    - beamBackgroundSuppression > 0.5 and fakePhotonSuppression > 0.1 for daughter γ
  - K^0_L selection :
    - $0.468\ \text{GeV/c}^2 < \text{M} < 0.508\ \text{GeV/c}^2$ and $0.5\ \text{GeV} < \text{E} < 10.0\ \text{GeV}$
    - klmClusterKlId > 0.2 and nKLMClusterTrackMatches $== 0$

4 Skimming

Skim is needed for efficient data use since the data size is very huge. so, there are some skim selections such as cuts on PID and mass and momentum variables that are covering the selections in step of reconstruction.

- Selection for charged tracks on skim
  - dr < 1.0 and |dz| < 3.0 and thetaInCDCAcceptance
- PID selection for Charged hadrons (π^+, K^+ and p^+)
  - π^+ : 15 candidates with highest pionID after pionID > 0.01
  - K^+ : 10 candidates with highest kaonID after kaonID > 0.1
  - p^+ : 10 candidates with highest protonID after protonID > 0.1
- selection for π^0, K_S^0, Σ^+ and Λ^0 on skim
  - K_S^0 : 0.468 GeV/c^2 < M < 0.506 GeV/c^2 and goodBelleKshort == 1
  - Σ^+ : 1.08 GeV/c^2 < M < 1.28 GeV/c^2
  - π^0 :
    * 0.115 GeV/c^2 < M < 0.160 GeV/c^2
    * E > 0.05 GeV for daughter γ
  - Λ^0 :
    * 1.111 GeV/c^2 < M < 1.121 GeV/c^2
    * dr > 0.1 and χ^2 < 100
    * cosAngleBetweenMomentumAndVertexVectorInXYPlane > 0.99
- Skim selection for tag side D^0: 1.72 GeV/c^2 < M < 2.02 GeV/c^2 and $p^* > 2.0$ GeV
- Skim selection for tag side D^+: 1.72 GeV/c^2 < M < 2.02 GeV/c^2 and $p^* > 2.0$ GeV
- Skim selection for tag side D_s^+: 1.82 GeV/c^2 < M < 2.12 GeV/c^2 and $p^* > 2.0$ GeV
- Skim selection for tag side Λ_c^+: 2.18 GeV/c^2 < M < 2.38 GeV/c^2 and $p^* > 2.0$ GeV
- Skim selection for $D^{*+} \to D^0\pi^+$: 0.135 GeV/c^2 < ΔM < 0.155 GeV/c^2
- Skim selection for $D^{*+} \to D^+\pi^0$: 0.130 GeV/c^2 < ΔM < 0.160 GeV/c^2
- Skim selection for $D^{*0} \to D^0\pi^0$: 0.130 GeV/c^2 < ΔM < 0.160 GeV/c^2
- Skim selection for $D^{*0} \to D^0\gamma$: 0.120 GeV/c^2 < ΔM < 0.165 GeV/c^2
- Skim selection for $D_s^{*+} \to D_s^+\gamma$: 0.120 GeV/c^2 < ΔM < 0.165 GeV/c^2
- Skim selection for signal side $D^{*\pm}$ and D^0
  - 1.81 GeV/c^2 < M_{D^*} < 2.21 GeV/c^2 for signal side $D^{*\pm}$
  - 0.08 GeV/c^2 < $M_{D^*} - M_{D^0}$ < 0.27 GeV/c^2 and $p^* > 2.0$ GeV for signal D^0

5 Signal extraction

For signal extraction, I used recoil mass(M_{D^0}) for extraction of signal yield of inclusive D^0 and also used both of recoil mass(M_{D^0}) and extra remained energy in ECL (E_{ECL}) for extraction of signal yield of exclusive D^0.

About E_{ECL} calculation, some constraints are applied to remove cluster energy from beam background.

- $|\text{clusterTiming}| < 200$ ns and $\left|\frac{\text{clusterTiming}}{\text{clusterErrorTiming}}\right| < 2.0$ for γ
- beamBackgroundSuppression > 0.5 and fakePhotonSuppression > 0.1 for γ
- dr < 1.0 and $|\text{dz}| < 3.0$ for e^-
- electronID > 0.6 for e^-
- isFromECL > 0 and isRestOfEvent $== 1$ for γ and e^-

5.1 Fit strategy

1D fit on M_{D^0} and 2D fit on (M_{D^0}, E_{ECL}) were performed for signal extraction of inclusive or exclusive D^0. the fit region is 1.855 GeV/c^2 $< M_{D^0} <$ 1.870 GeV/c^2 for inclusive D^0 fit and 1.855 GeV/c^2 $< M_{D^0} <$ 1.870 GeV/c^2 and $E_{ECL} < 2.1$ GeV for exclusive D^0 fit.

- each component PDF about M_{D^0} for inclusive D^0:
  - signal PDF on M_{D^0}: combination of 2 gaussians and 1 bifurcated gaussian with same mean
    Note : The signal PDF shape is fixed on fit result about $D^0 \to \nu\bar{\nu}$ signal MC
  - background PDF on M_{D^0}: combination of argus and linear function
- each component PDF about M_{D^0} for exclusive D^0:
  - signal PDF on M_{D^0}: signal PDF from Inclusive D^0 fit
  - flat background PDF on M_{D^0}: combination of argus and linear function
  - peak background PDF on M_{D^0}: 3 gaussians with same mean
- each component PDF about E_{ECL} for exclusive D^0:
  - signal PDF: histogram PDF from exclusive D^0 on signal MC
  - flat background PDF: histogram PDF from sideband on background only MC
    sideband: 1.855 GeV/c^2 $< M_{D^0} <$ 1.870 GeV/c^2
  - peak background PDF:
    * (a) : histogram PDF in peak region
      peak region: 1.860GeV/c^2 $< M_{D^0} <$ 1.870GeV/c^2
    * (b) : histogram PDF in sideband
    * peak background histogram PDF = (1 + w)*(a) - w*(b)
      (w: floating variable between 0 and 1)

5.1.1 Inclusive D^0

For signal extraction of inclusive D^0, one-dimensional extended binned maximum likelihood fit is performed on the recoil mass($M_{D^0} \equiv M_{miss}(D_{tag}^{(*)} X_{frag} \pi_s^{\pm})$). Fit is perforemd with maximizing this likelihood function defined as

$$L = \frac{e^{-\Sigma_j N_j}}{N!} \prod_{i=1}^{N} (\Sigma_j N_j P_j(M_{D^0}^i)),$$

The N is total number of candiates, N_j is the number of events in component j, $M_{D^0}^i$ is M_{D^0} value of i-th candidate and P_j is one-dimensinal probability density function corresponding to the j component.

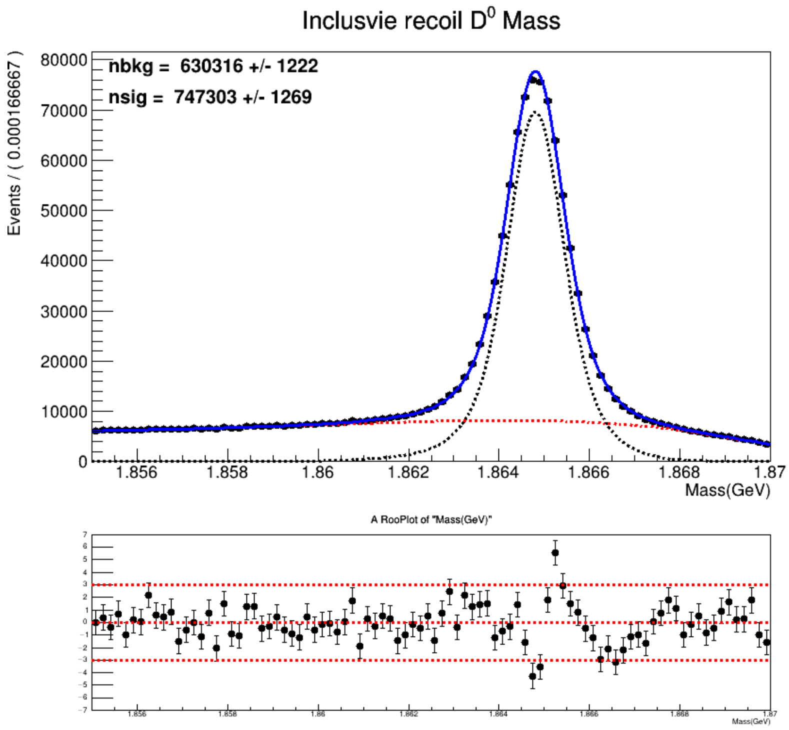

Figure 22: fit result of inclusive D^0 on 1ab^{-1} generic MC

5.1.2 Exclusive D^0

For signal extraction of exclusive D^0, two-dimensional extended binned maximum likelihood fit is performed on (M_{D^0}, E_{ECL}). two dimensional likelihood function is defined as

$$L = \frac{e^{-\Sigma_j N_j}}{N!} \prod_{i=1}^{N} (\Sigma_j N_j P_j(M_{D^0}, E_{ECL}))$$

N is total number of events in this fit, i means i-th candidate and P_j is probability density function of j component such as signal or flat background or peak background.

6 $D^0 \to \nu\bar{\nu}$

6.1 Selection criterion for $D^0 \to \nu\bar{\nu}$

- Exclusive selection for $D^0 \to \nu\bar{\nu}$ signal MC:
  no remaining tracks, $\pi^0, K_S^0, K_L^0, \Lambda^0$ in signal side

6.2 Signal MC study: signal efficiency

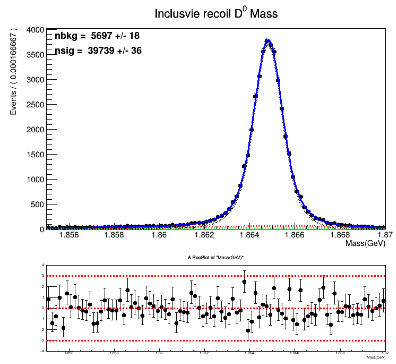

Figure 23: inclusive D^0 on signal MC

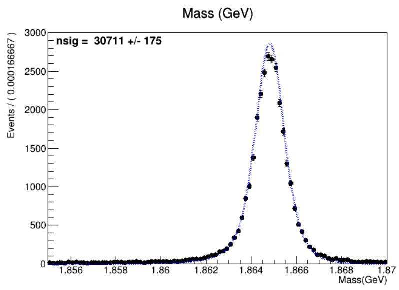

Figure 24: M_{D^0} of exclusive D^0 on signal MC

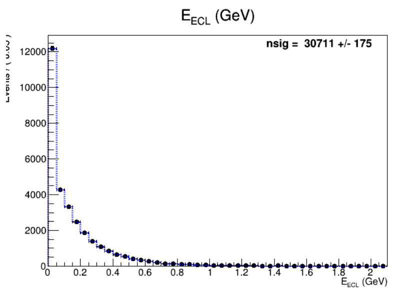

Figure 25: E_{ECL} of exclusive D^0 on signal MC

- signal efficiency : 0.77282 ± 0.00446

6.3 2D fit result about $D^0 \to \nu\bar{\nu}$

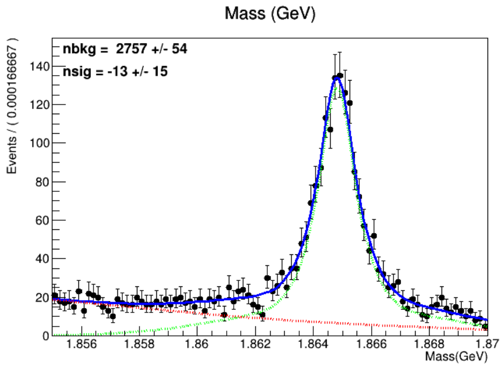

Figure 26: M_{D^0} of exclusive D^0 on generic MC

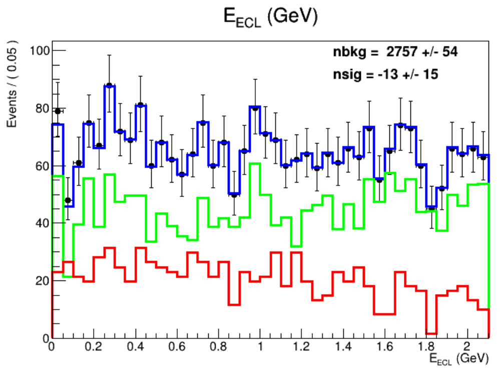

Figure 27: E_{ECL} of exclusive D^0 on generic MC

7 Control Sample study : validation of charm tagger

Following this analysis procedure, it is also possible to measure branching fraction of other decay. so, I tried to measure Br($D^0 \to K^-\pi^+$) with this charm tagger on purpose of validation of charm tagger.

7.1 Selection criterion for $D^0 \to K^-\pi^+$

- 2 remaining tracks and no $\pi^0, K_S^0, K_L^0, \Lambda^0$ in signal side
- 1 directly reconstructed $D^0 \to K^-\pi^+$ in signal side
  - selection for K^+: kaonID > 0.6 and electronID < 0.95 and muonID < 0.95
  - selection for π^+: pionID > 0.4 and electronID < 0.95 and muonID < 0.95
  - 1.80 GeV/c$^2 <$ M < 1.92 GeV/c^2

– vertex fit applied and choose one candidate with highest chiProb

- $|\Delta\text{E}(= \text{recoiled } E_{D^0}$ - $E_{K\pi})| < 0.1$ GeV

7.2 Signal efficiency

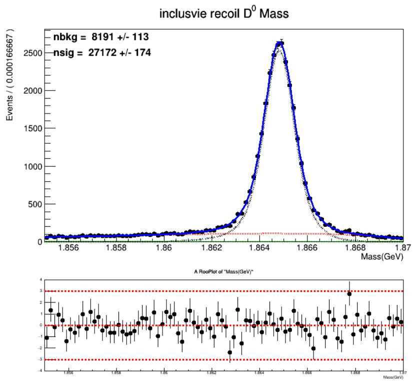

Figure 28: inclusive D^0 on $D^0 \to K^-\pi^+$ signal MC

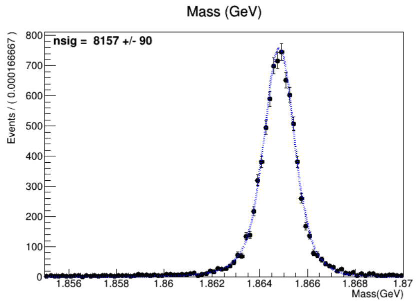

Figure 29: M_{D^0} of exclusive D^0 on $D^0 \to K^-\pi^+$ signal MC

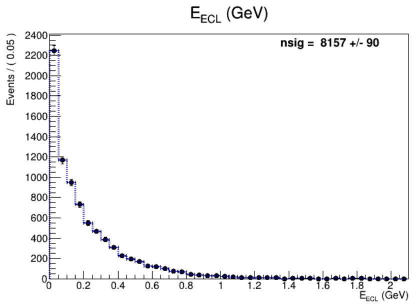

Figure 30: E_{ECL} of exclusive D^0 on $D^0 \to K^-\pi^+$ signal MC

- signal efficiency : 0.30020 ± 0.00383

7.3 Measurement of Br($D^0 \to K^-\pi^+$)

The branching fraction calculation is based on this formula:

$$\text{Br}(D^0 \to K^-\pi^+) = \frac{N_{sig}^{excl}}{N_{sig}^{incl} \times \epsilon_{sig}}$$

N_{sig}^{incl} is signal yield of inclusive D^0 on generic MC and N_{sig}^{excl} is signal yield of exclusive $D^0 \to K^-\pi^+$ on generic MC and ϵ_{sig} is signal efficiency calculated on $D^0 \to K^-\pi^+$ signal MC study.

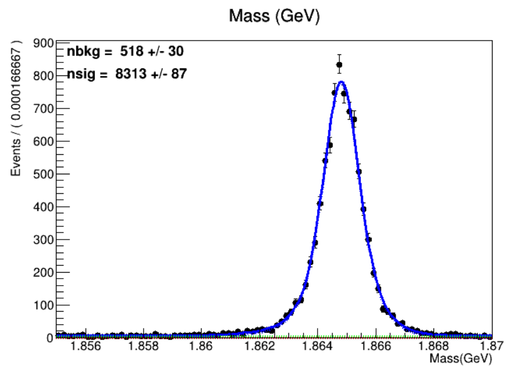

Figure 31: M_{D^0} of exclusive $D^0 \to K^-\pi^+$ on generic MC

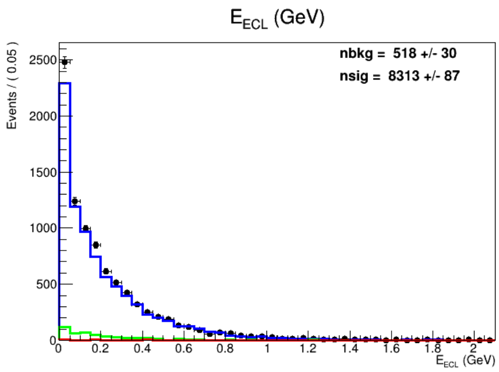

Figure 32: E_{ECL} of exclusive $D^0 \to K^-\pi^+$ on generic MC

based on these fit results, the measured Br($D^0 \to K^-\pi^+$) is 0.03706 ± 0.00061.

8 ToyMC study : check the stability of fitter

Checking the fit result with pull distribution, almost fit results seems okay, but the inclusive D^0 fit result on generic MC shows a few points are out of 3σ range. so, Toy ensemble test and Linearity test are performed on this fit result. the bias from these tests will be considered as systematic uncertainty in future.

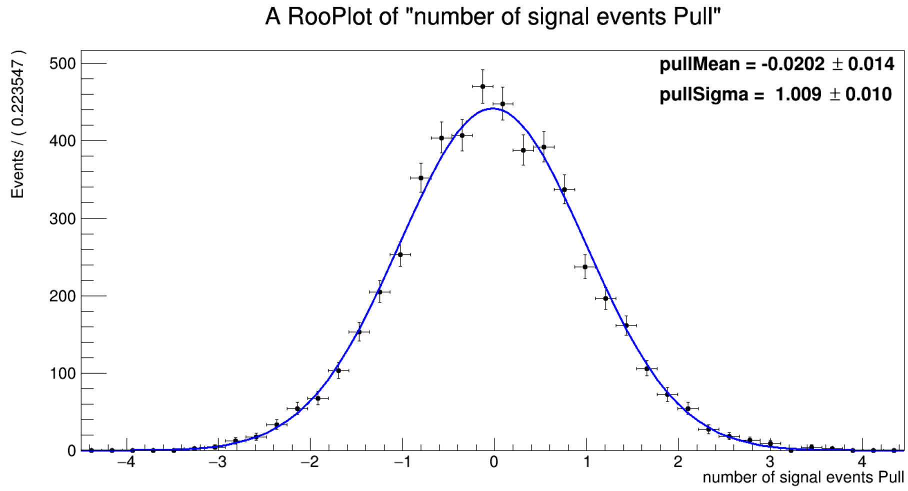

Figure 33: Toy ensemble test about N_{sig} on inclusive D^0 fit result on generic MC

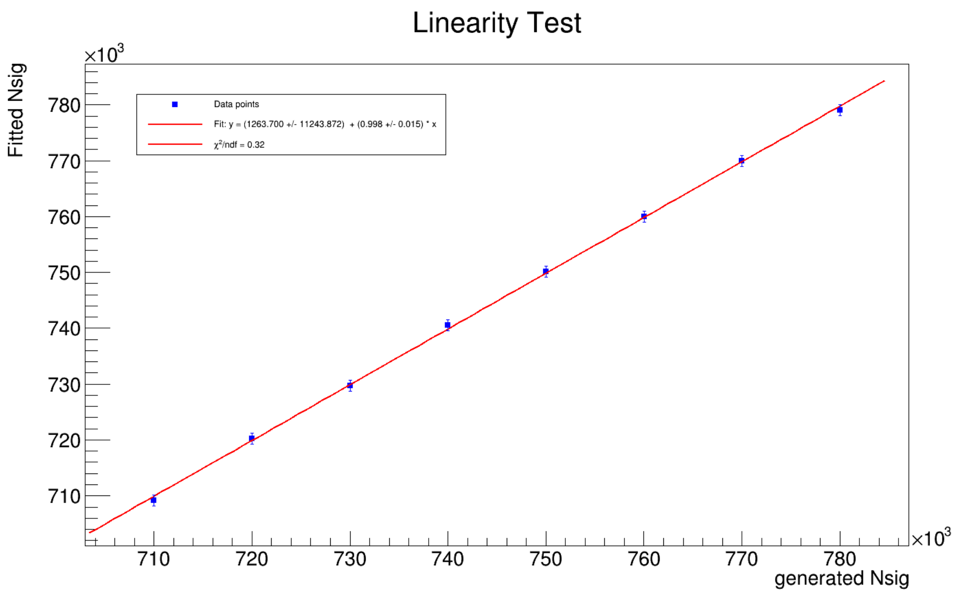

Figure 34: Linearity test about N_{sig} on inclusive D^0 fit result on generic MC

9 Systematic uncertainties

- Charm tagger: tagging efficiency
- Number of Inclusive D^0
- Fit bias
- Signal PDF
- Flat background PDF
- Peak background PDF
- Reconstruction efficiency uncertainty
- Veto on remaining detector information (tracks,$\pi^0, K_S^0, K_L^0, \Lambda^0$)
- Study veto efficiency dependence on $D_{tag}^{(*)}/X_{frag}$

10 Upper Limit estimation

Since $D^0 \to \nu\bar{\nu}$ does not exist in generic MC, the signal yield should be zero. As shown in the figure 12 and figure 13, the signal yield from fit is consistent with the zero yield within 1σ. so, estimation of 90% Upper limit of Branching fraction was tried with 2 methods. one is bayesian approach and the other is frequentist approach.

Bayesian approach is based integrating the likelihood function shown below:

$$\int_0^N \mathcal{L}(n)\,dn = 0.9 \int_0^\infty \mathcal{L}(n)\,dn,$$

where $\mathcal{L}(n)$ is likelihood of fit result with condition that the number of signal yield is fixed at n. the systematic uncertainty is not considered yet. it will be included in future.

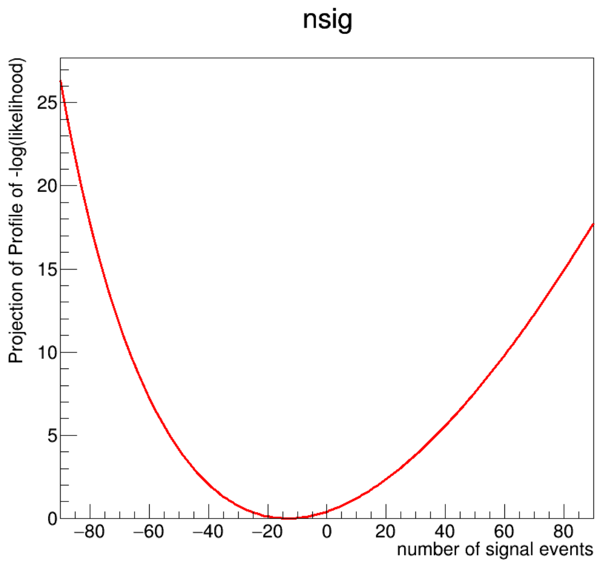

Figure 35: Negative log likelihood function

the estimated upper limit from bayesian approach is 2.0×10^{-5}.

Another method is frequentist approach which is called as CLs method. this calculation is by RooStat Profile likelihood calculator based on frequentist statistics. The plot shows p-value of background only hypothesis(CL_b) as function of signal yield(N_{sig}) and signal+background(CL_{s+b}) and $\mathrm{CL}_s(\equiv \mathrm{CL}_{\mathrm{s+b}}/\mathrm{CL}_{\mathrm{b}})$ model. the colored area shows one and two σ expected CL_s value around the median value(black dashed line), asuuming data corresponds to the background only hypothesis.

the estimated upper limit from this frequentist approach is 3.8×10^{-5}.

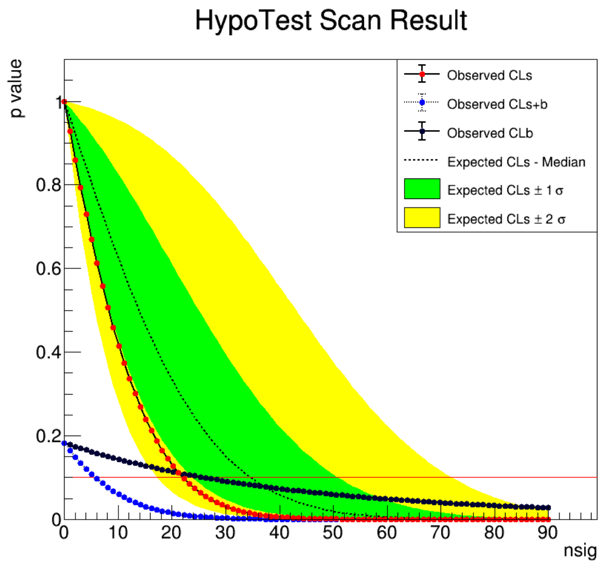

Figure 36: p-Value vs N_{sig} for CLs method

Appendices

A.1 BDT of Charm Tagger result

This section contains the BDT result.

A.1.1 $D^0 \to K^- \pi^+$

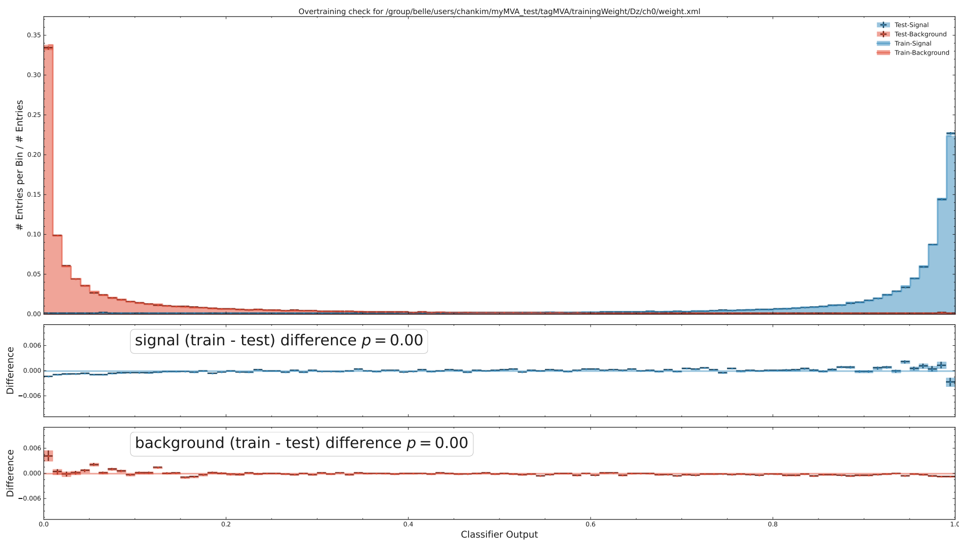

Figure 37: BDT output

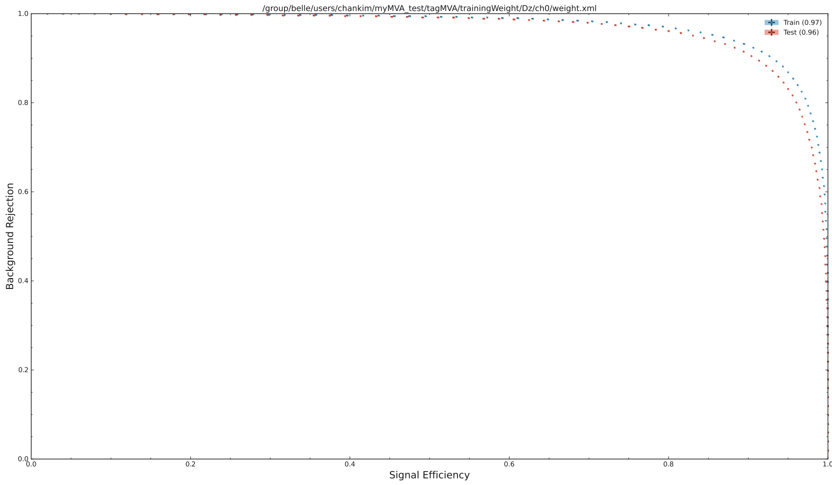

Figure 38: ROC Curve

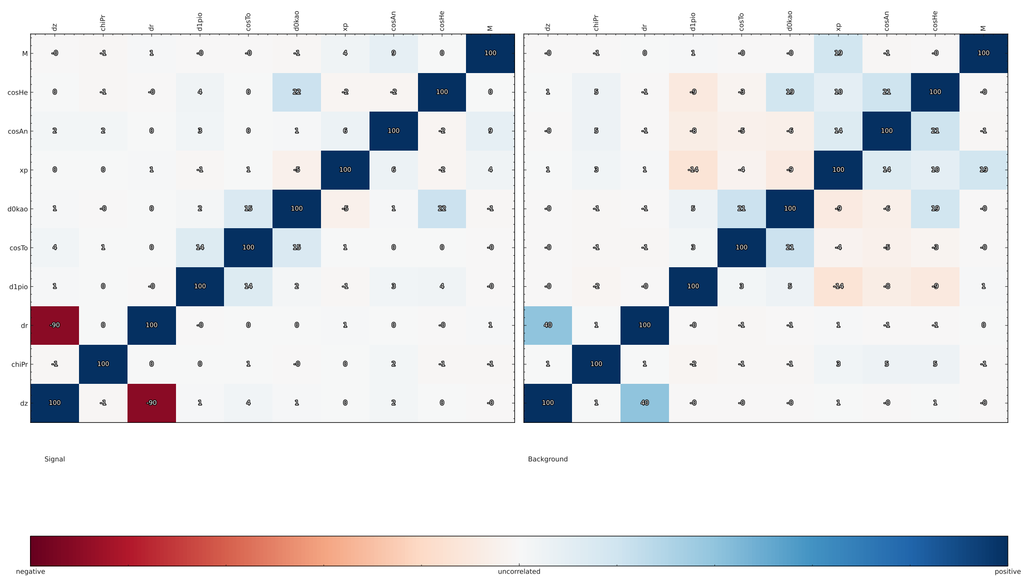

Figure 39: Correlation plot

A.1.2 $D^0 \to K^-\pi^+\pi^0$

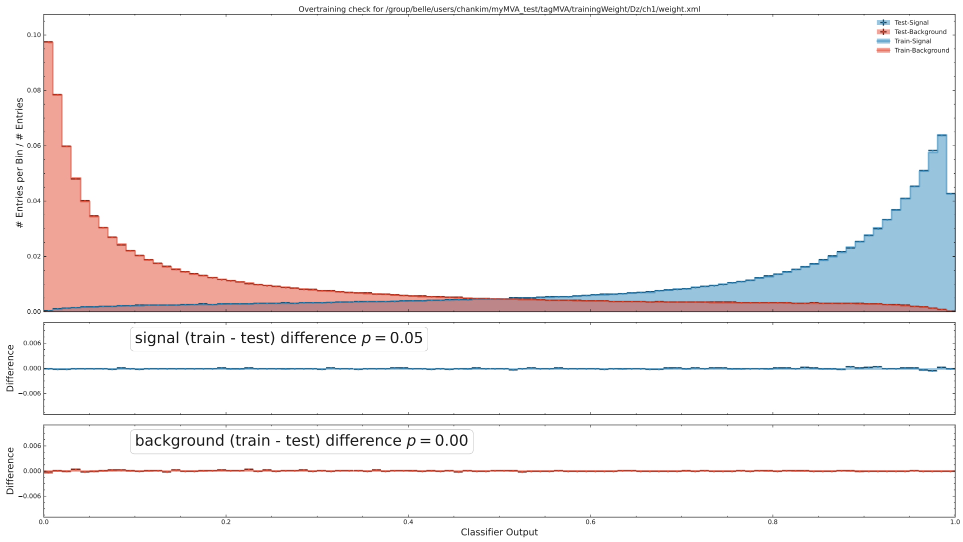

Figure 40: BDT output

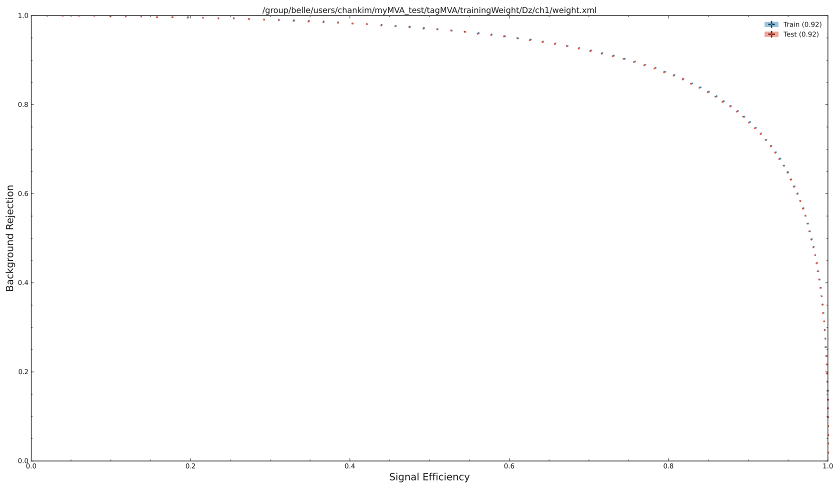

Figure 41: ROC Curve

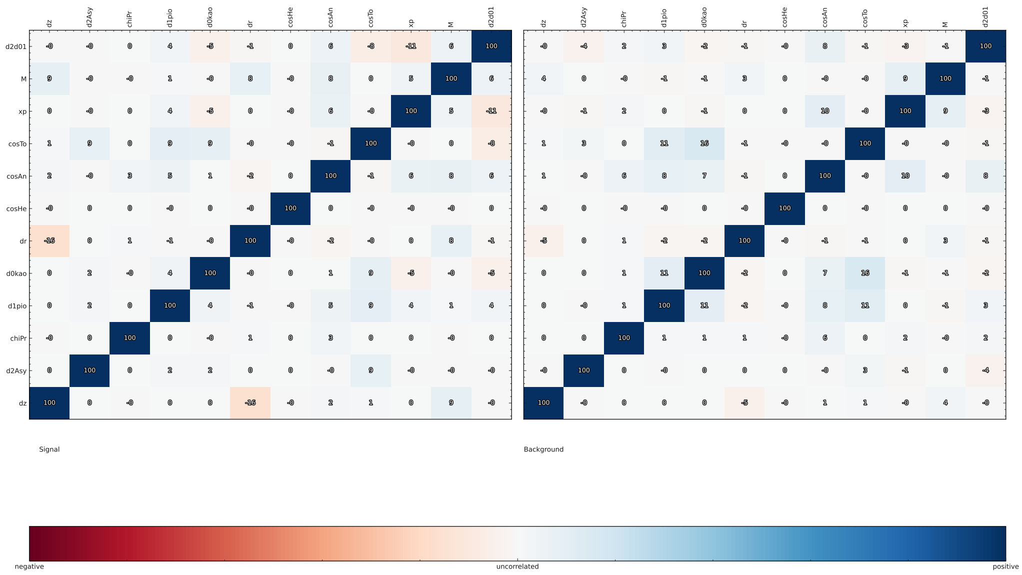

Figure 42: Correlation plot

A.1.3 $D^0 \to K^-\pi^+\pi^0\pi^0$

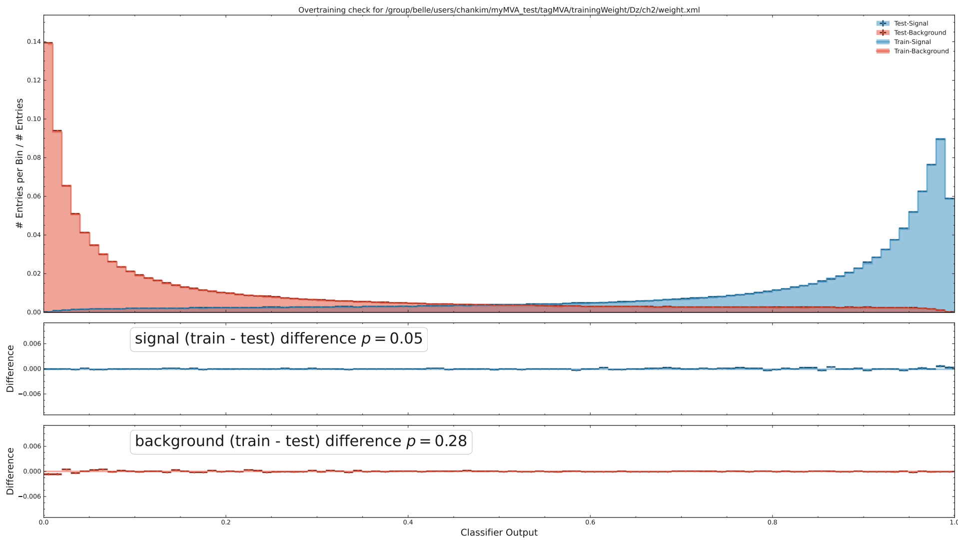

Figure 43: BDT output

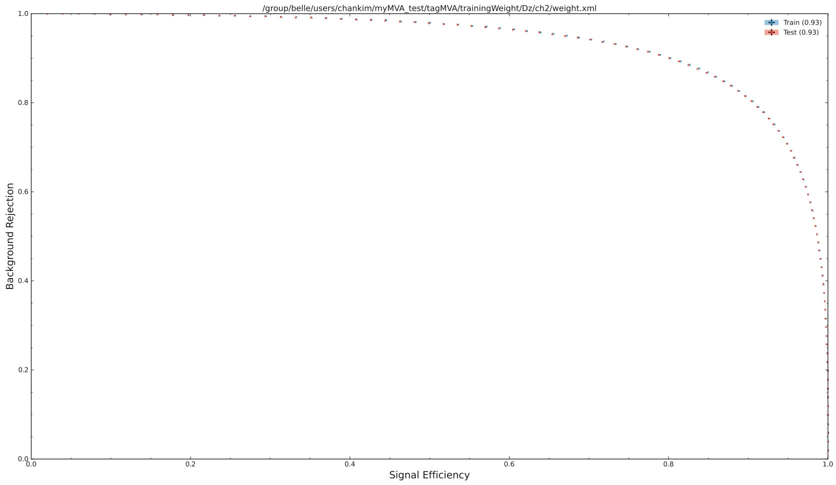

Figure 44: ROC Curve

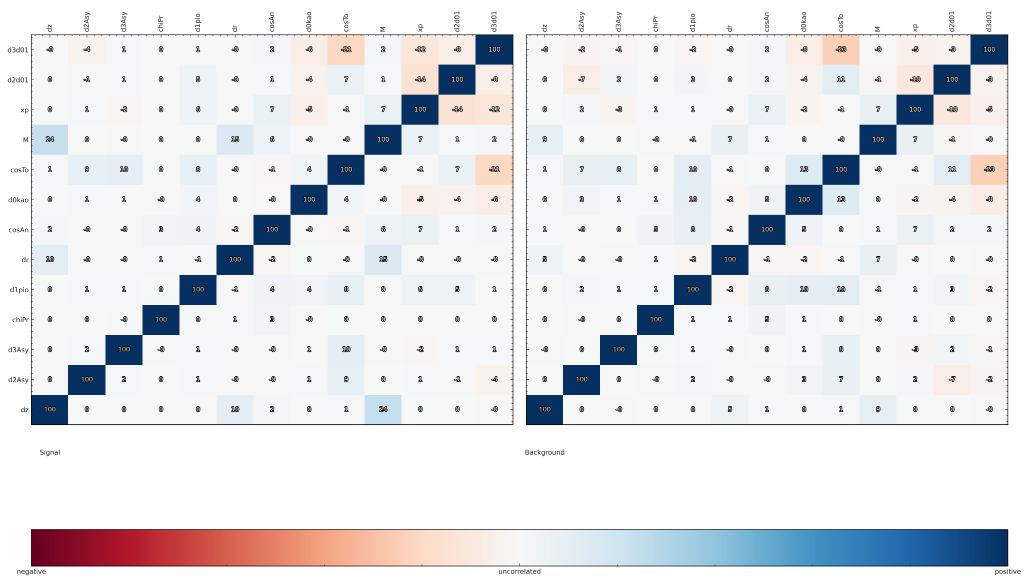

Figure 45: Correlation plot

A.1.4 $D^0 \to K^-\pi^+\pi^-\pi^+$

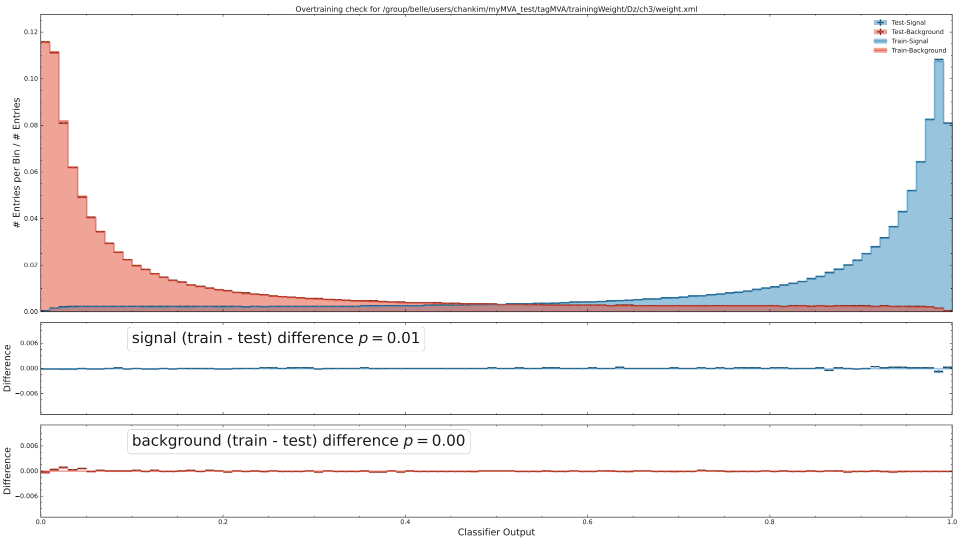

Figure 46: BDT output

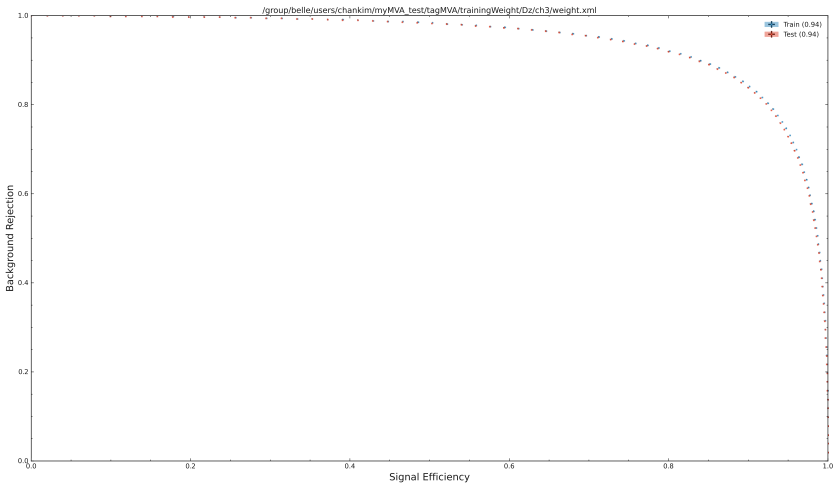

Figure 47: ROC Curve

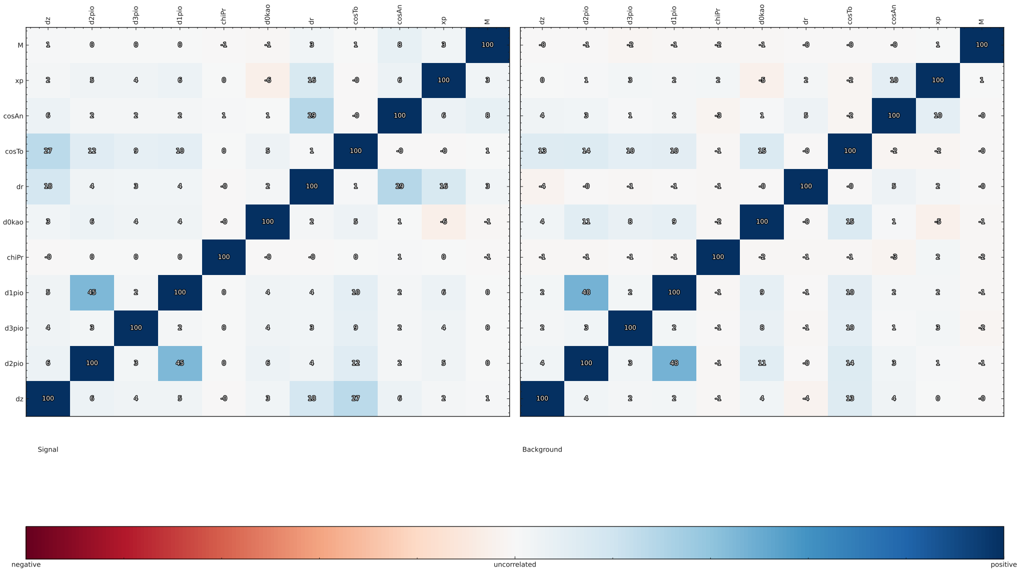

Figure 48: Correlation plot

A.1.5 $D^0 \to K^-\pi^+\pi^-\pi^+\pi^0$

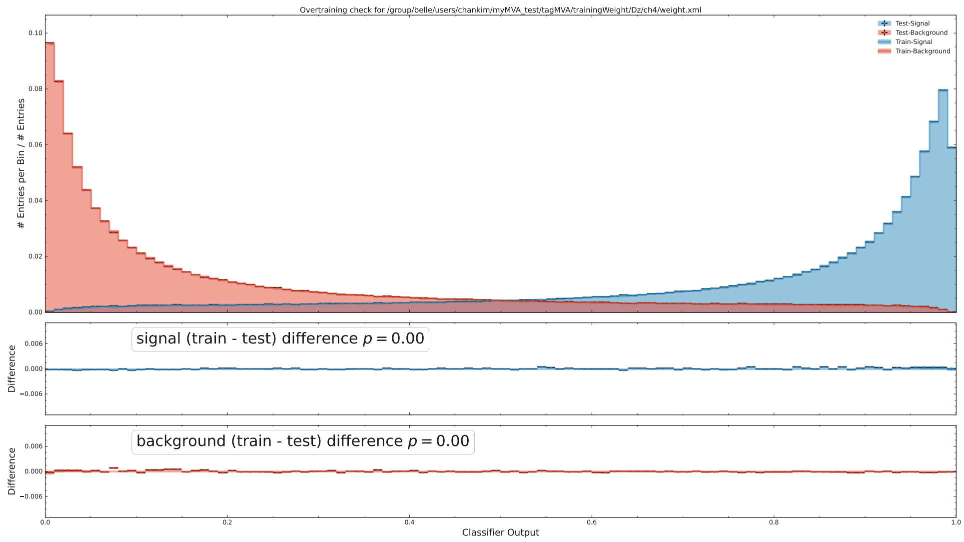

Figure 49: BDT output

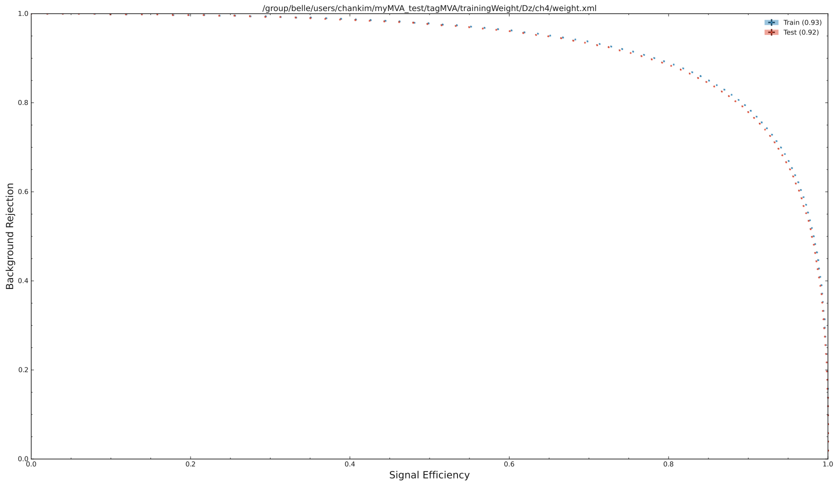

Figure 50: ROC Curve

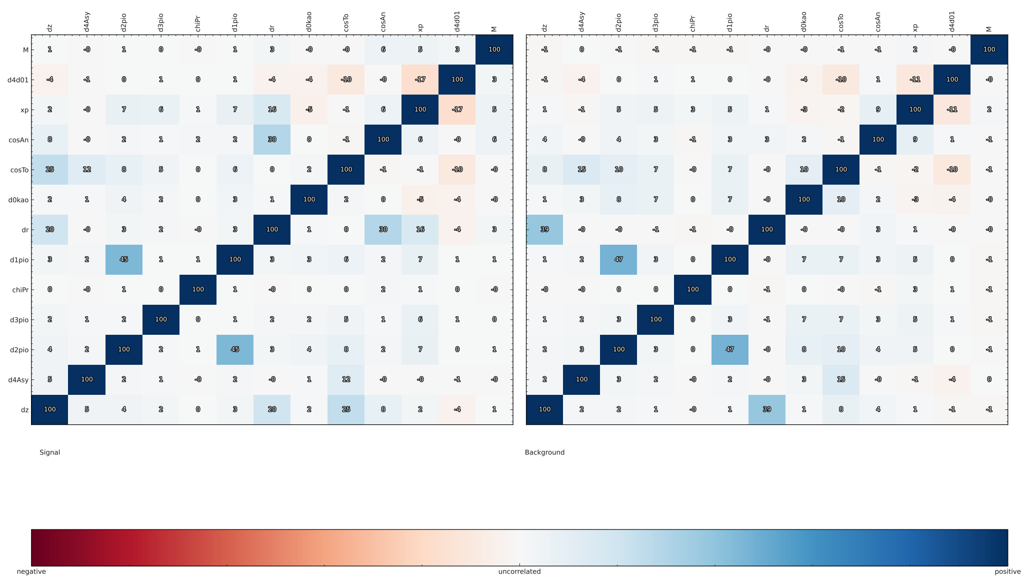

Figure 51: Correlation plot

A.1.6 $D^0 \to \pi^+\pi^-$

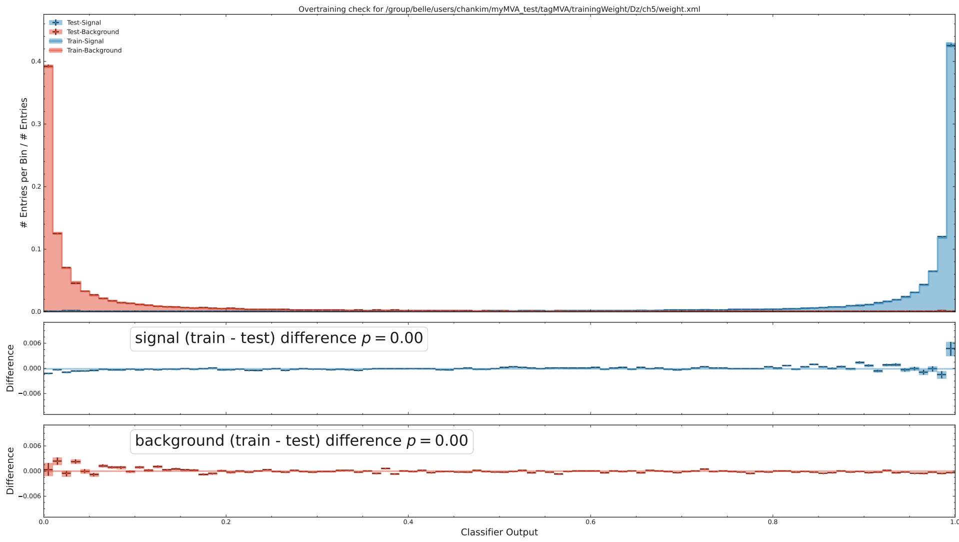

Figure 52: BDT output

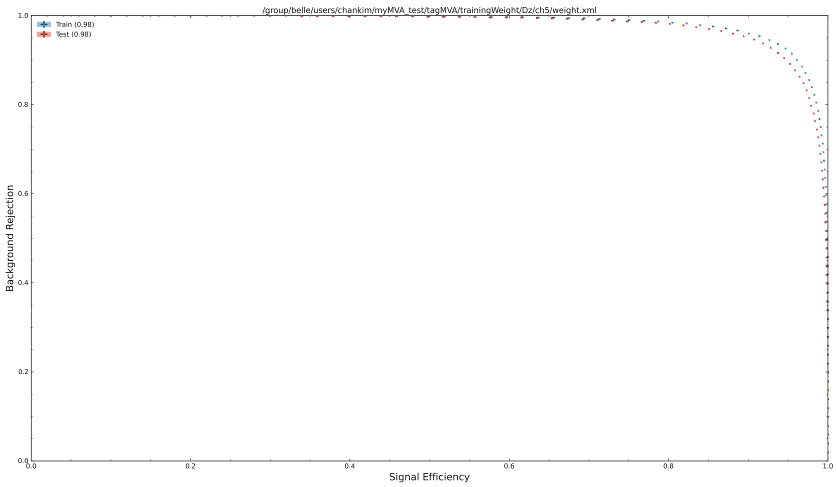

Figure 53: ROC Curve

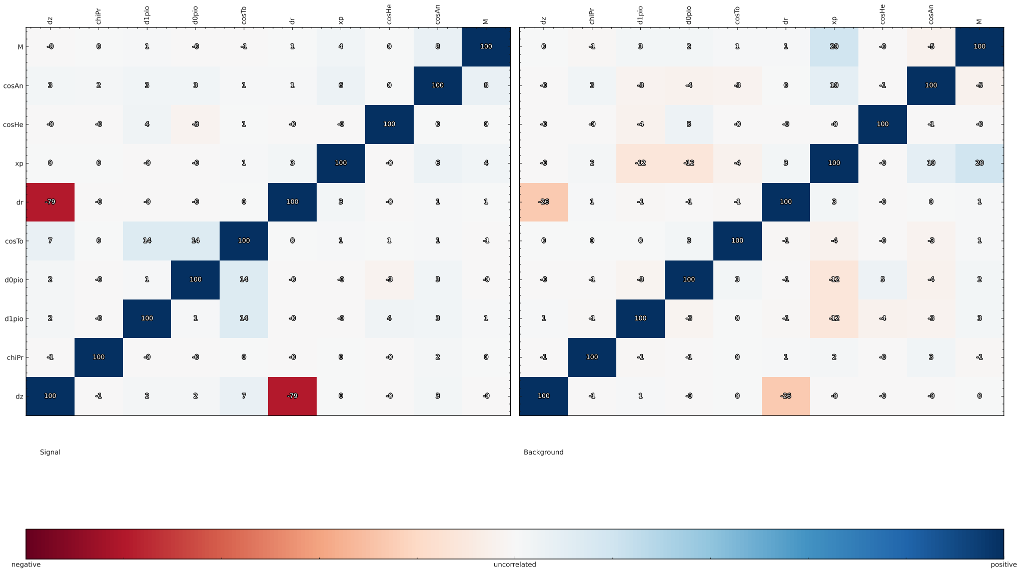

Figure 54: Correlation plot

A.1.7 $D^0 \to \pi^+\pi^-\pi^+\pi^-$

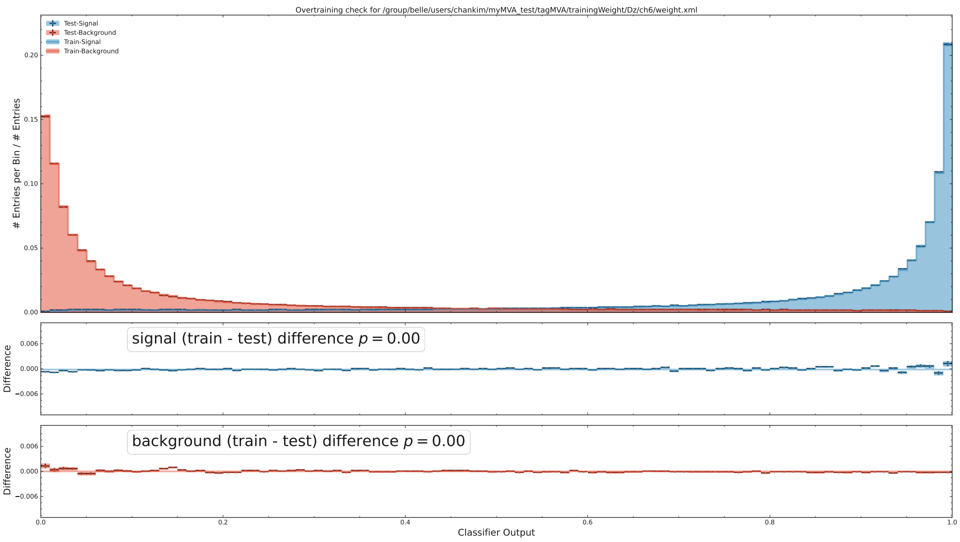

Figure 55: BDT output

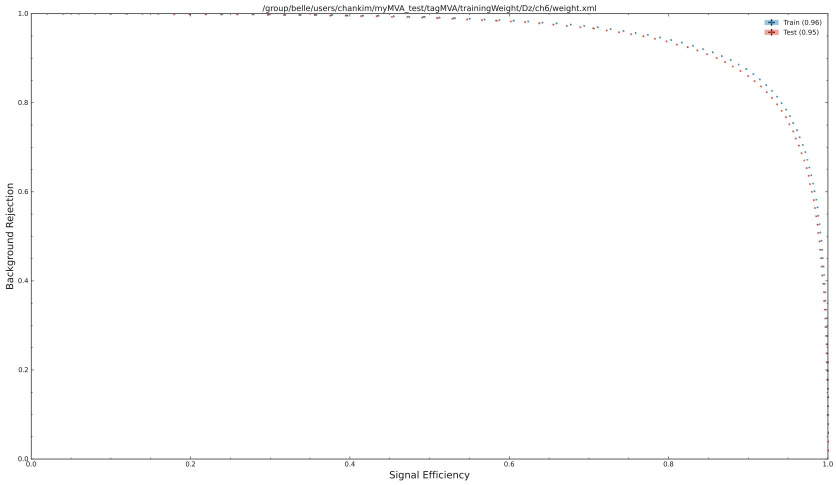

Figure 56: ROC Curve

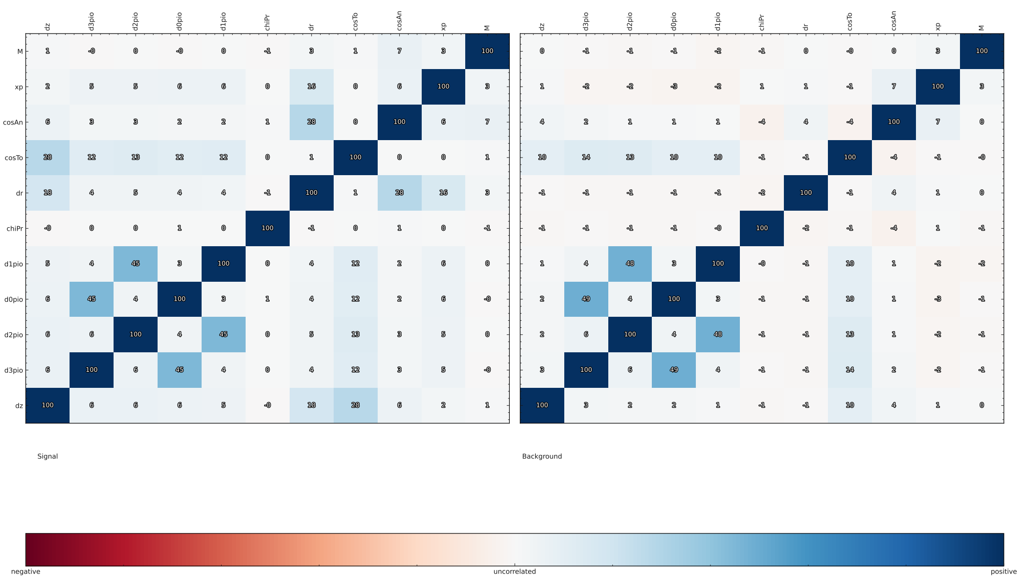

Figure 57: Correlation plot

A.1.8 $D^0 \to \pi^+\pi^-\pi^0$

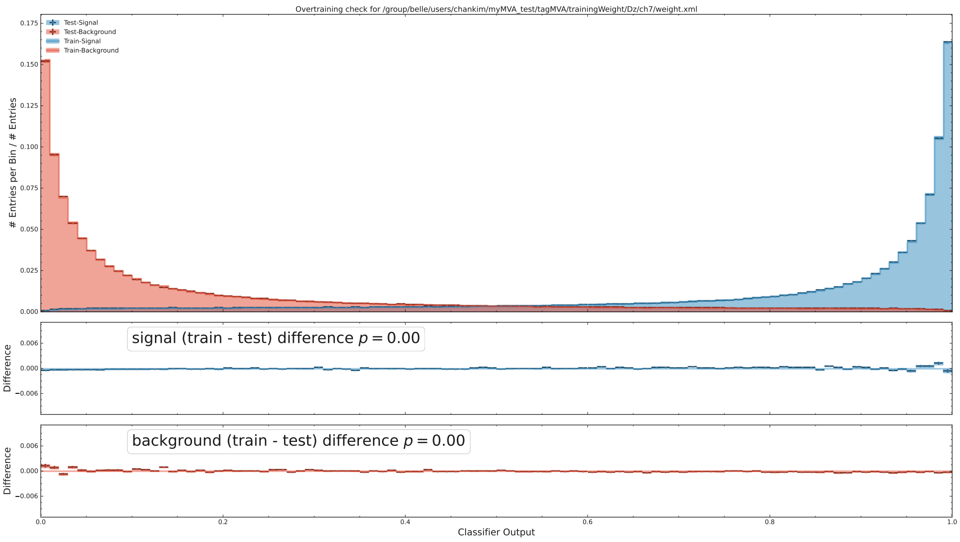

Figure 58: BDT output

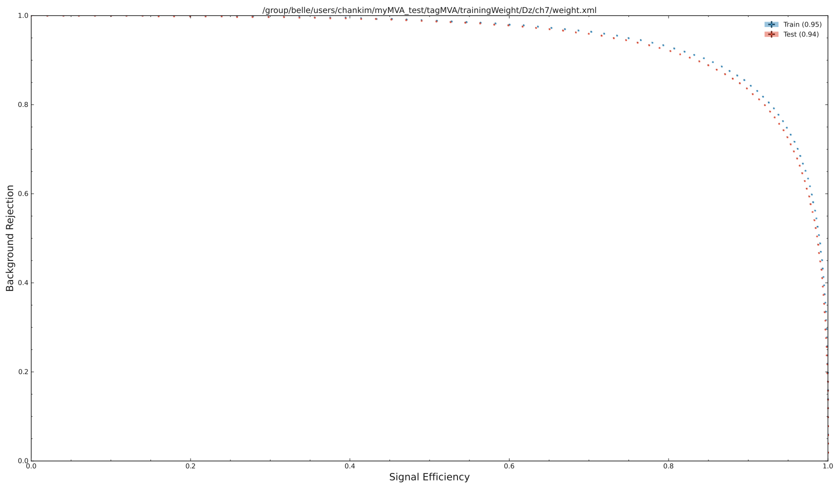

Figure 59: ROC Curve

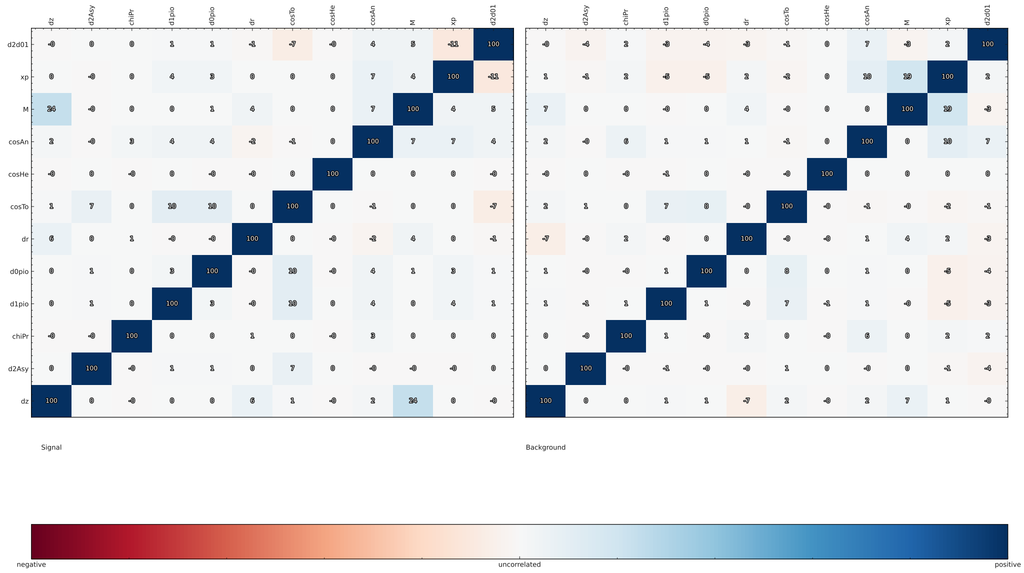

Figure 60: Correlation plot

A.1.9 $D^0 \to \pi^+\pi^-\pi^0\pi^0$

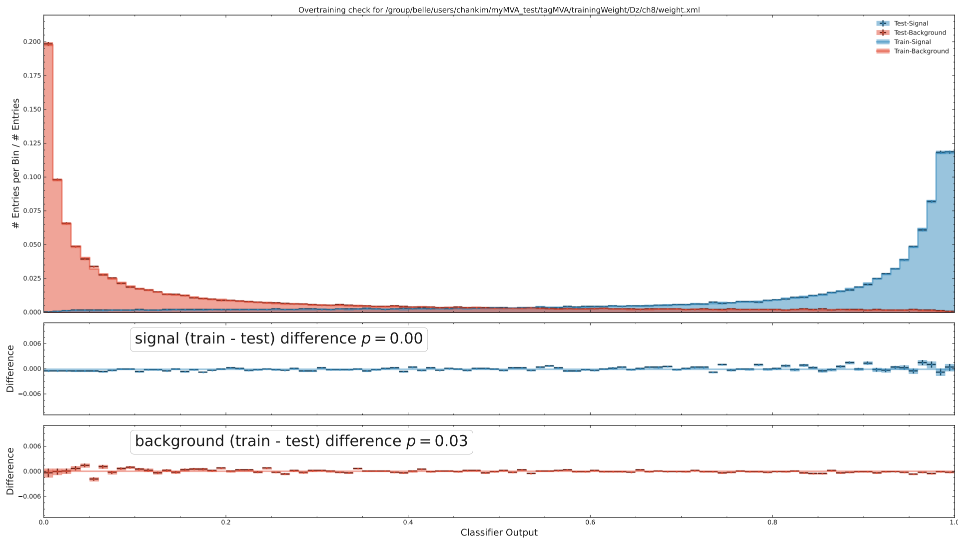

Figure 61: BDT output

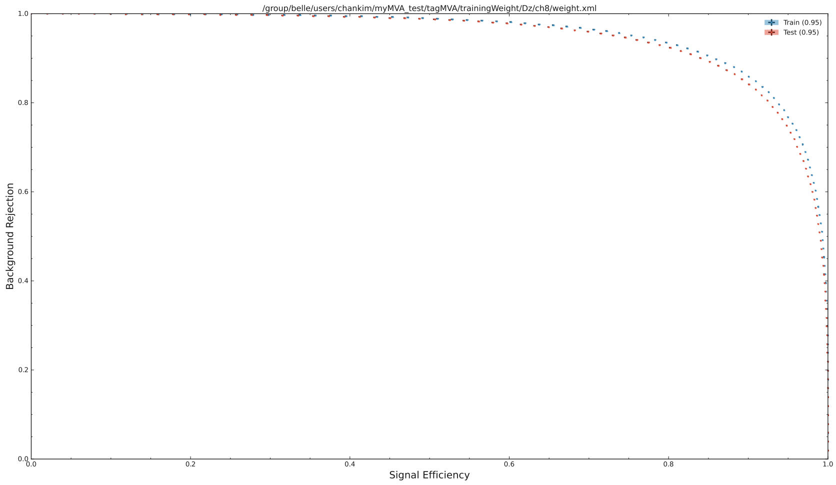

Figure 62: ROC Curve

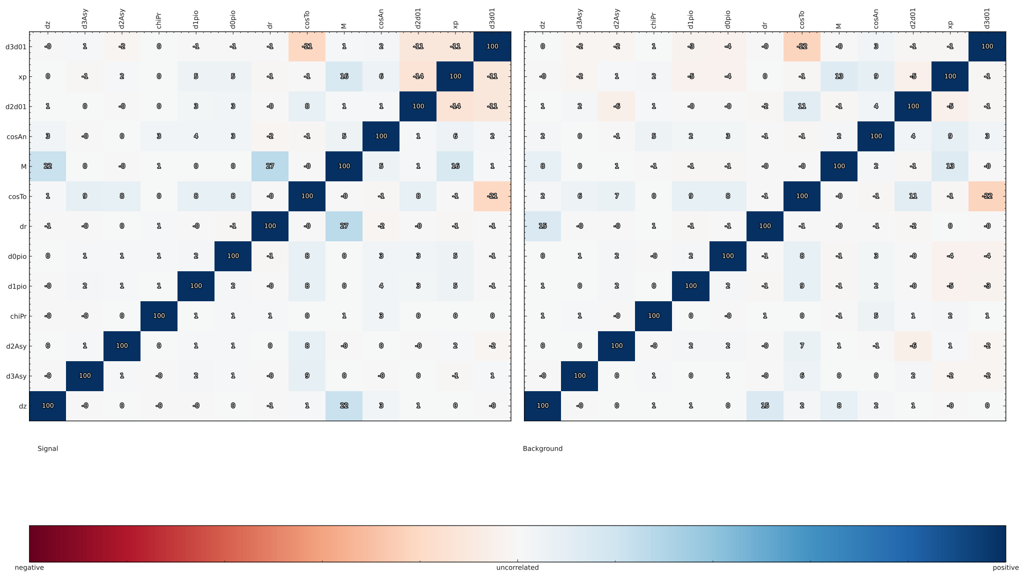

Figure 63: Correlation plot

A.1.10 $D^0 \to \pi^+\pi^- K_S^0$

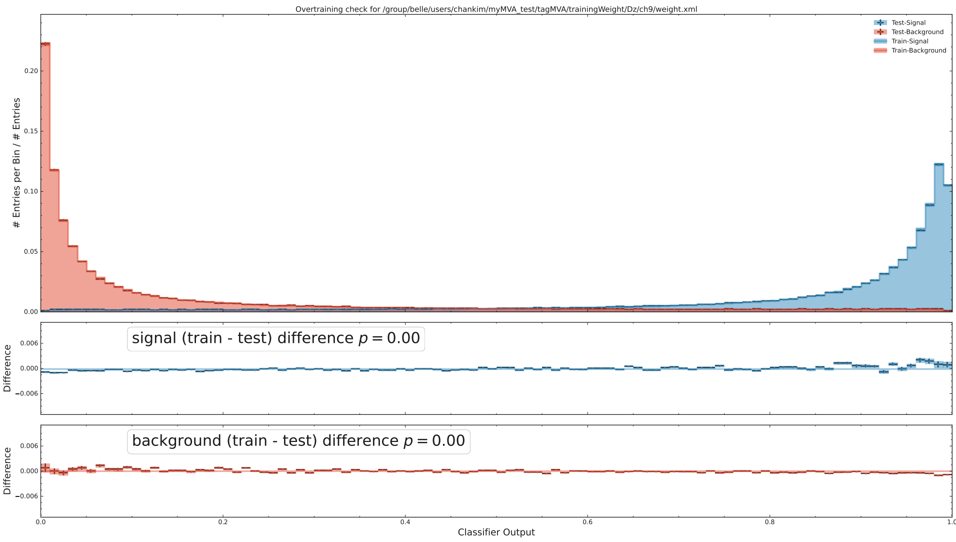

Figure 64: BDT output

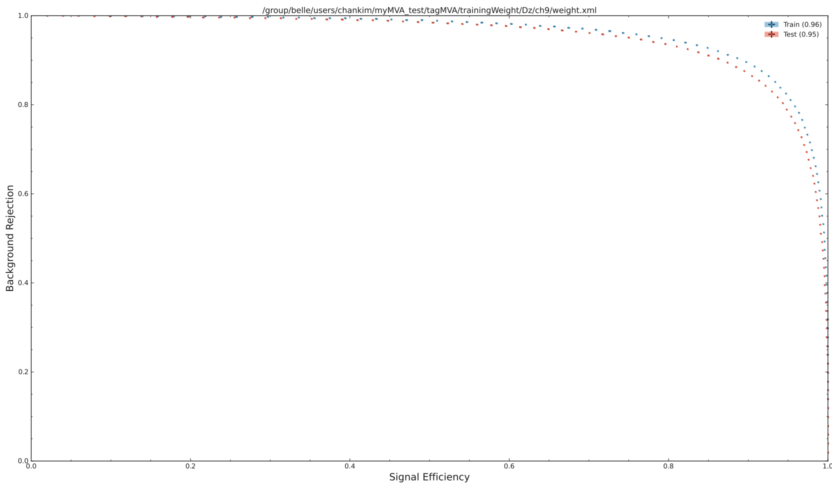

Figure 65: ROC Curve

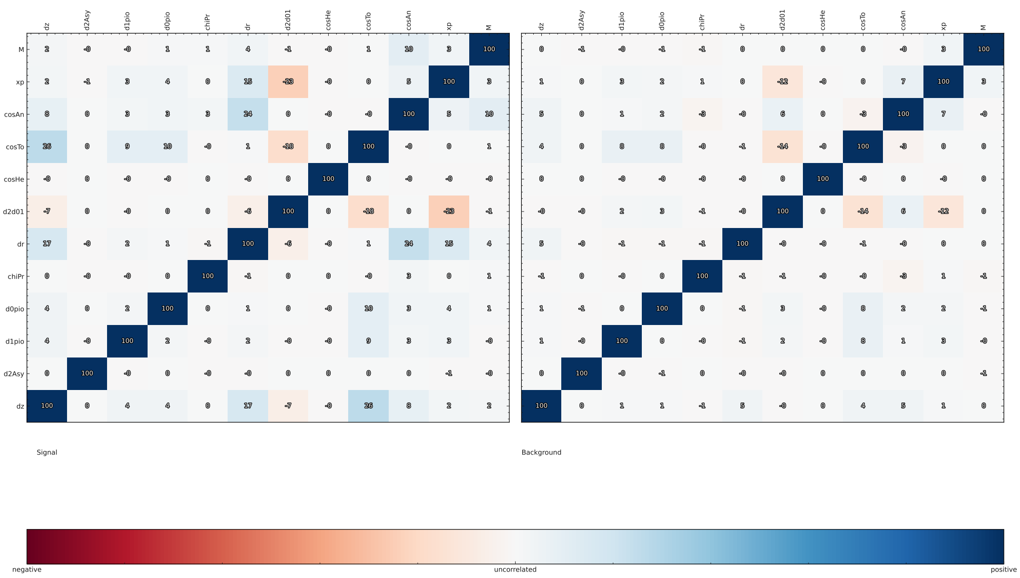

Figure 66: Correlation plot

A.1.11 $D^0 \to \pi^+\pi^-\pi^0 K_S^0$

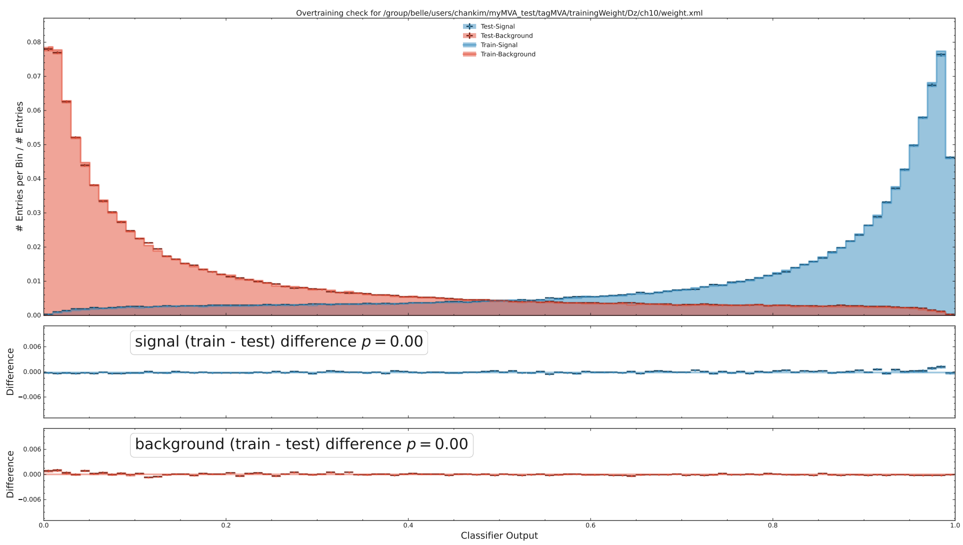

Figure 67: BDT output

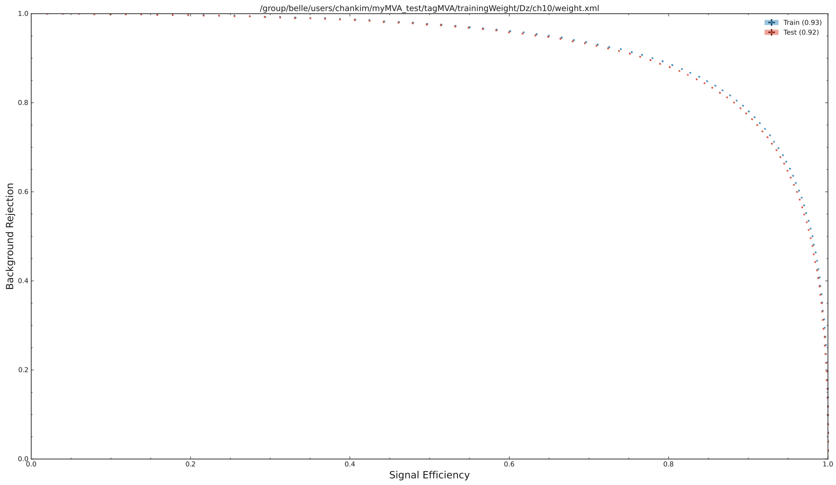

Figure 68: ROC Curve

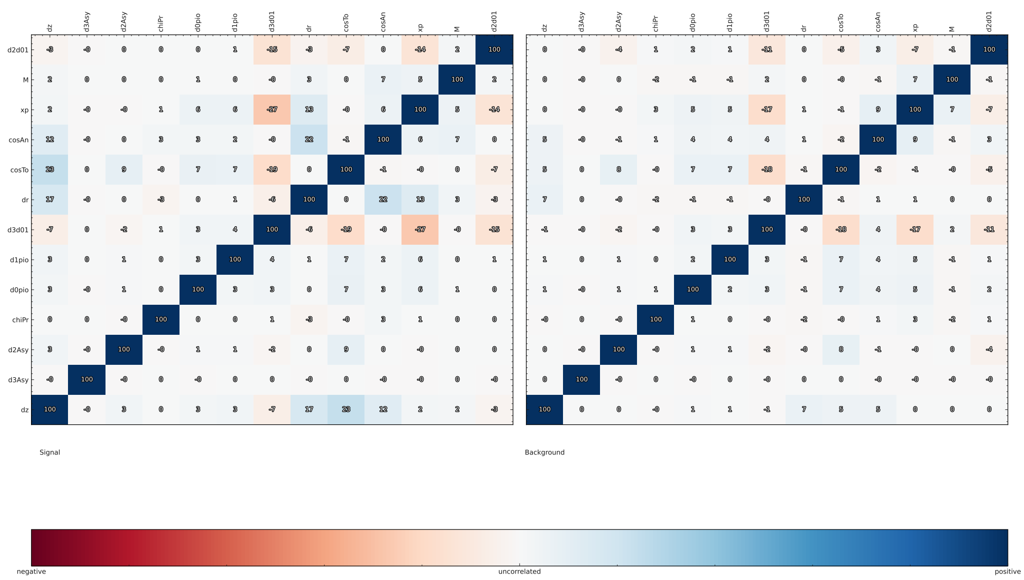

Figure 69: Correlation plot

A.1.12 $D^0 \to \pi^0 K_S^0$

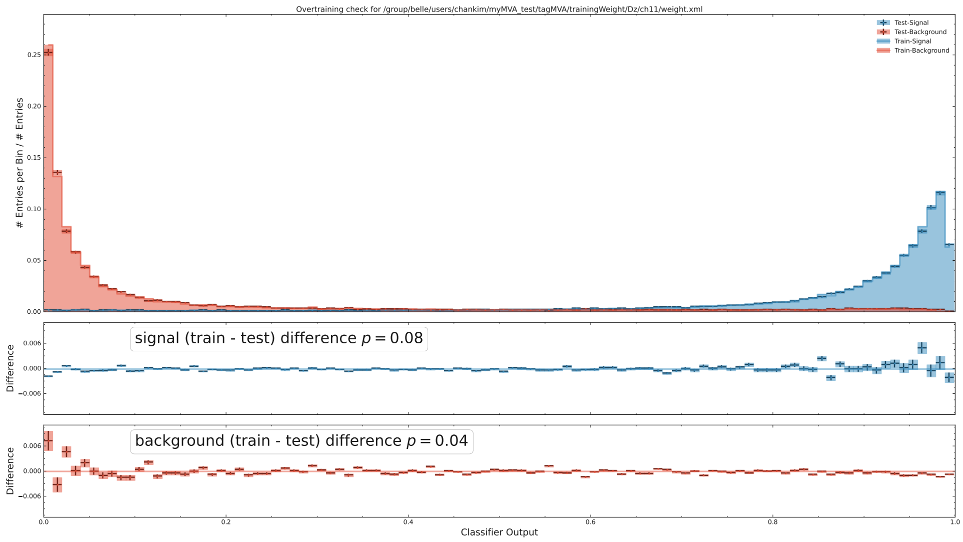

Figure 70: BDT output

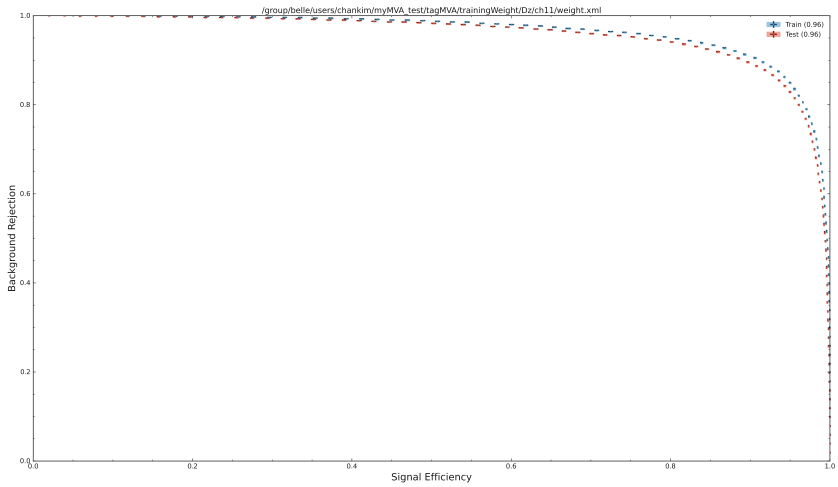

Figure 71: ROC Curve

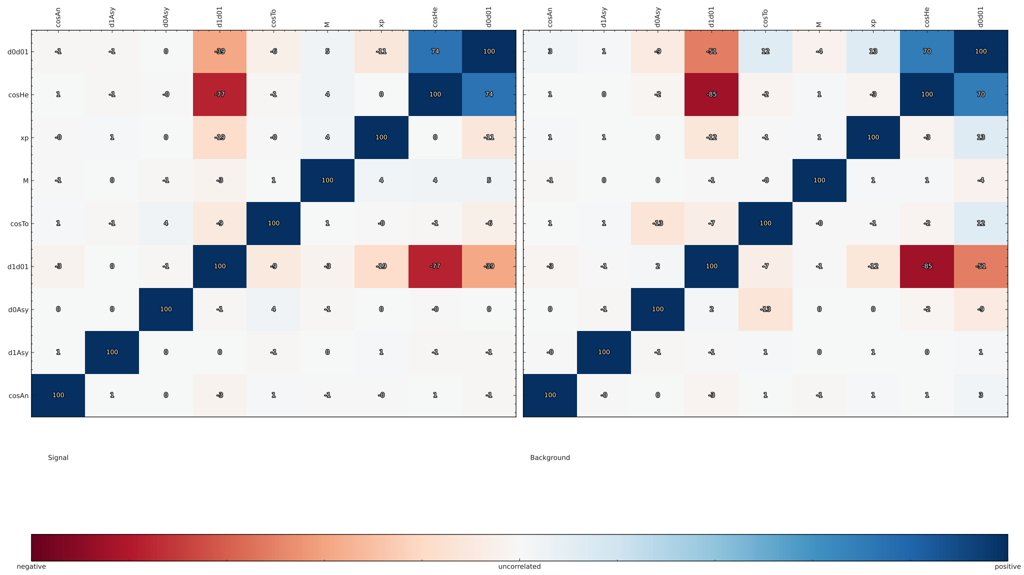

Figure 72: Correlation plot

A.1.13 $D^0 \to K^+K^-$

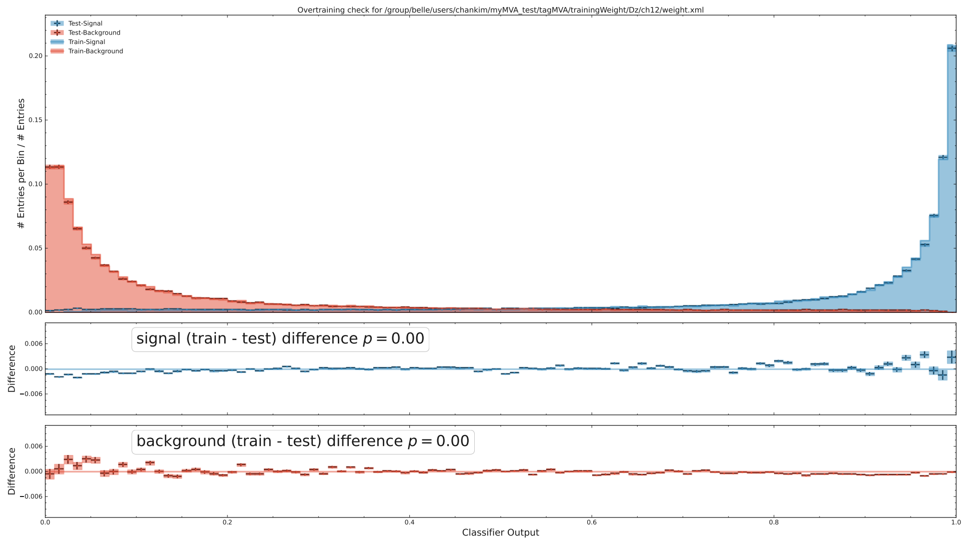

Figure 73: BDT output

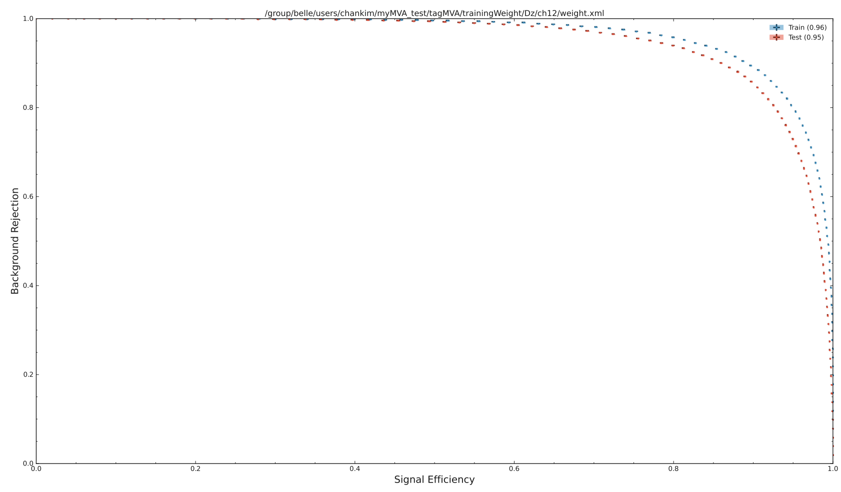

Figure 74: ROC Curve

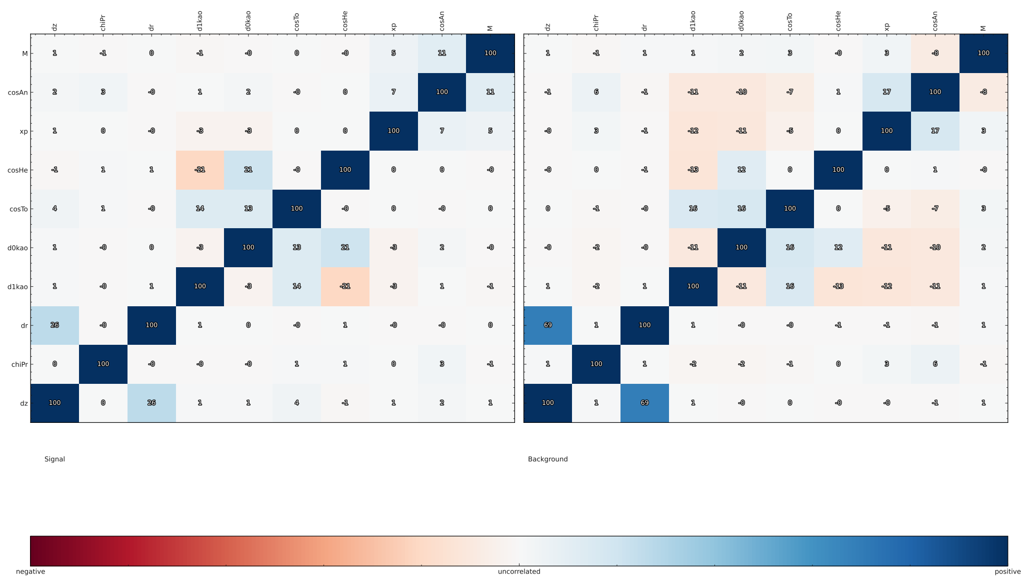

Figure 75: Correlation plot

391 ### A.1.14 $D^0 \to K^+K^-\pi^0$

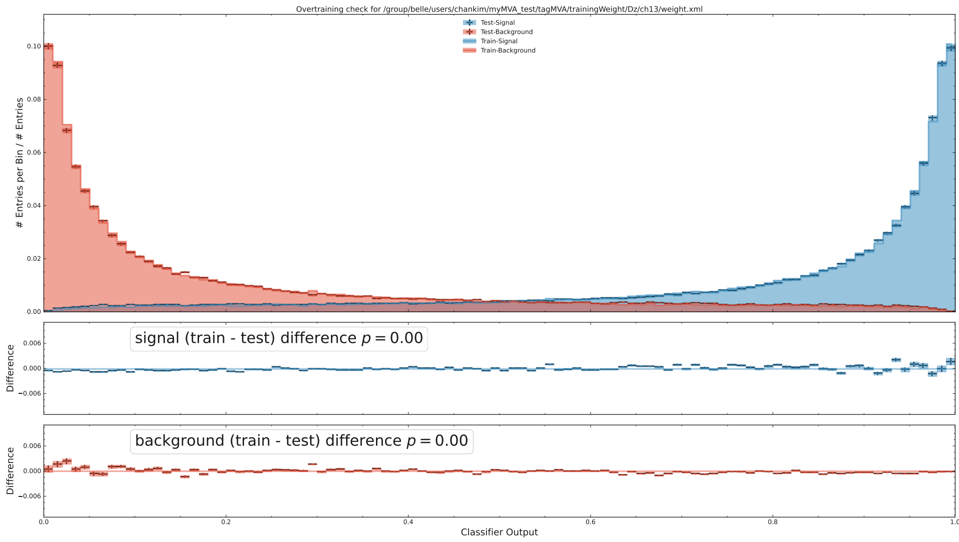

Figure 76: BDT output

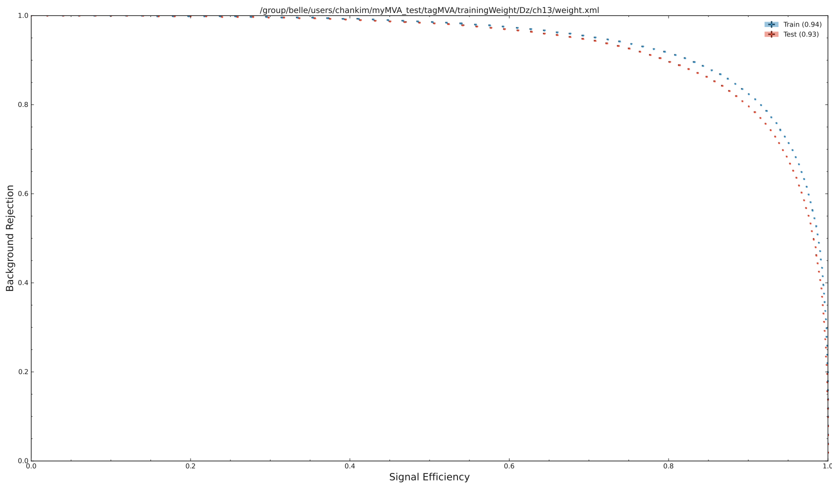

Figure 77: ROC Curve

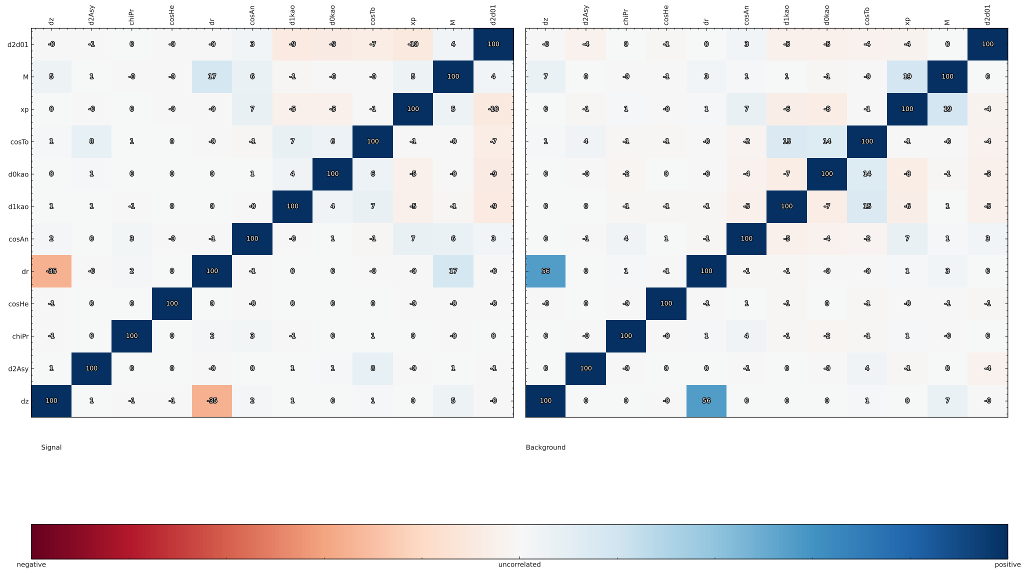

Figure 78: Correlation plot

A.1.15 $D^0 \to K^+K^-K^0_S$

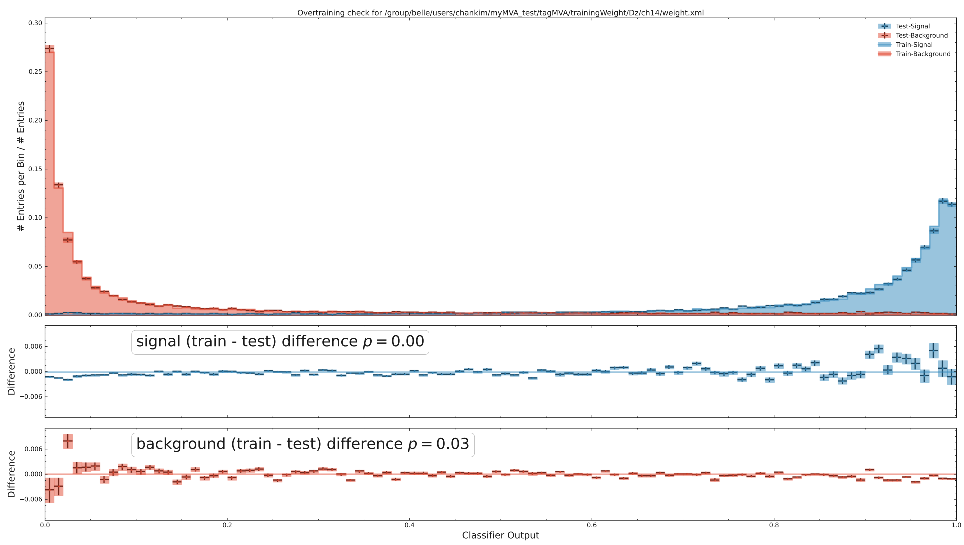

Figure 79: BDT output

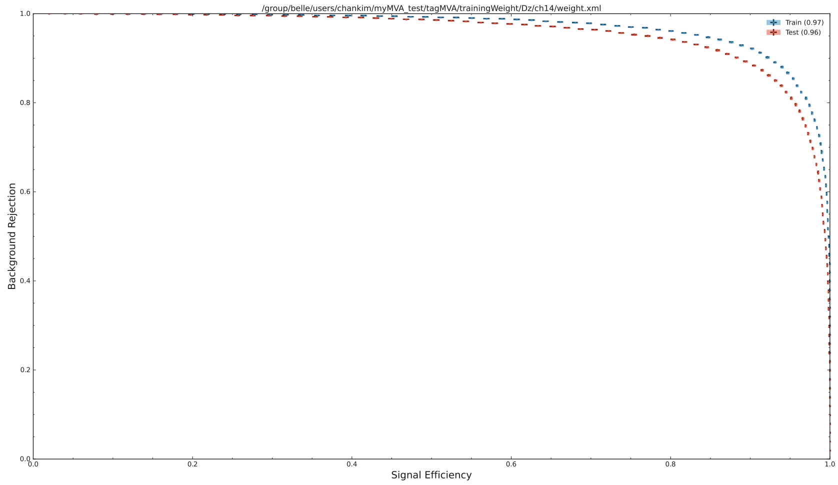

Figure 80: ROC Curve

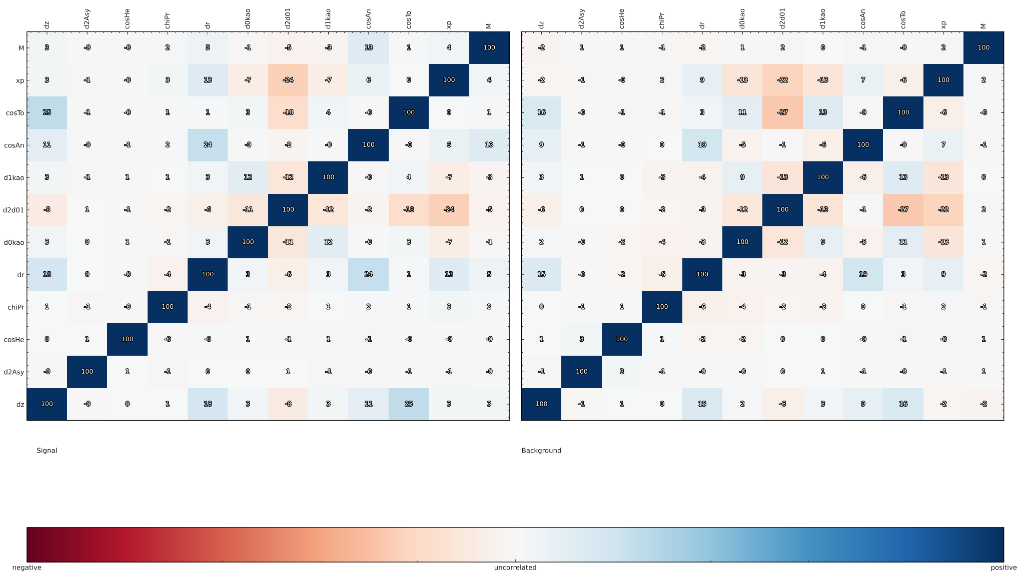

Figure 81: Correlation plot

A.1.16 $D^+ \to K^-\pi^+\pi^+$

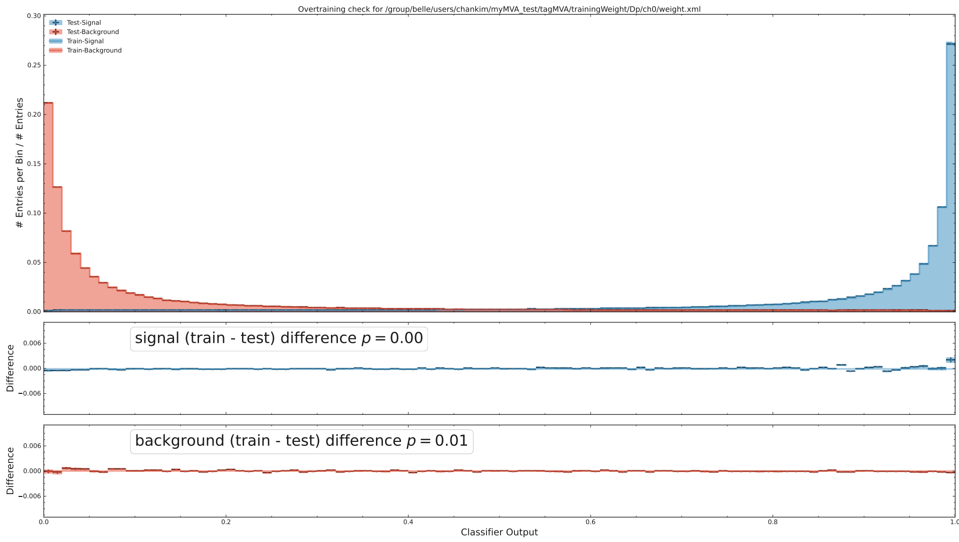

Figure 82: BDT output

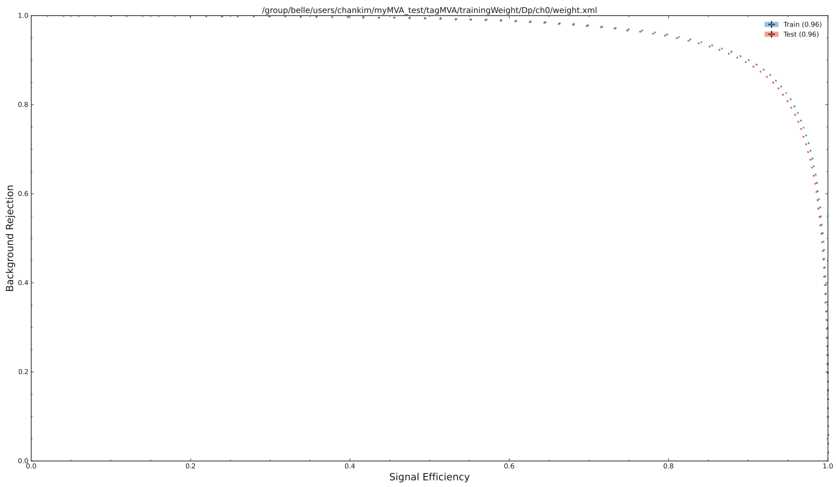

Figure 83: ROC Curve

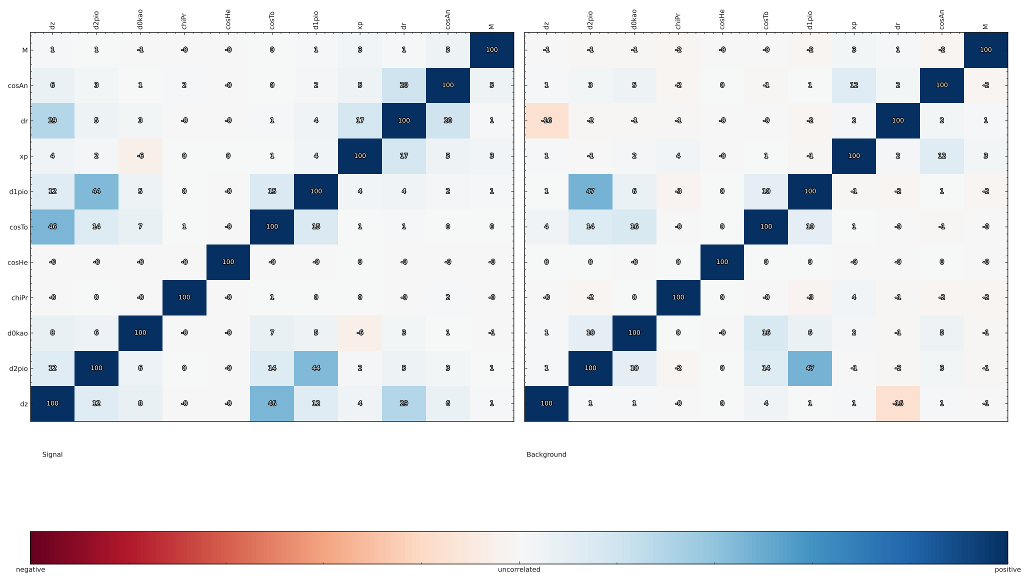

Figure 84: Correlation plot

A.1.17 $D^+ \to K^-\pi^+\pi^+\pi^0$

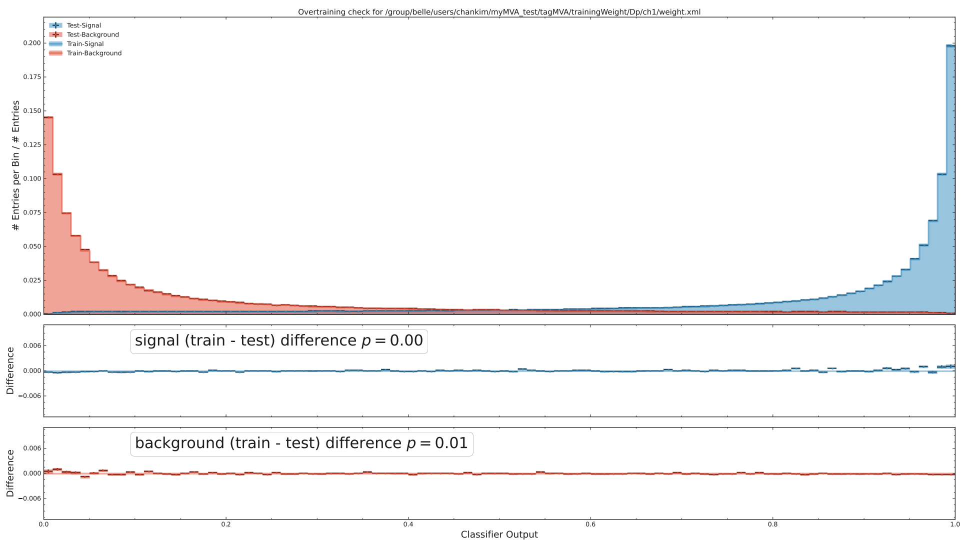

Figure 85: BDT output

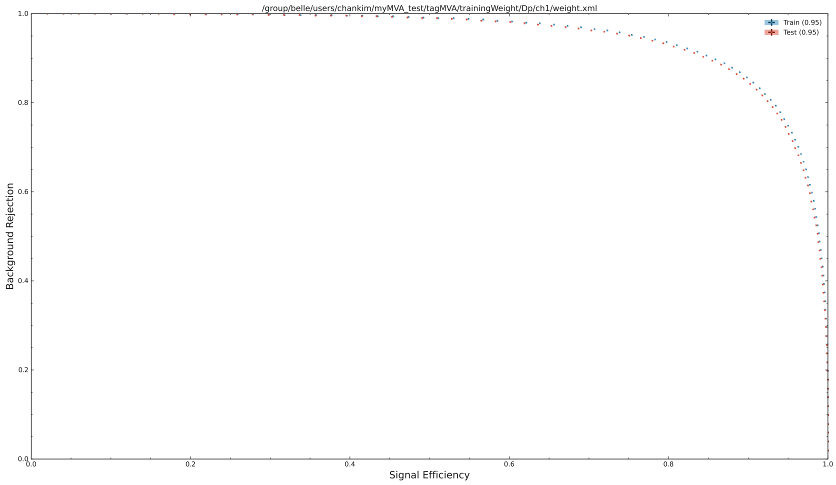

Figure 86: ROC Curve

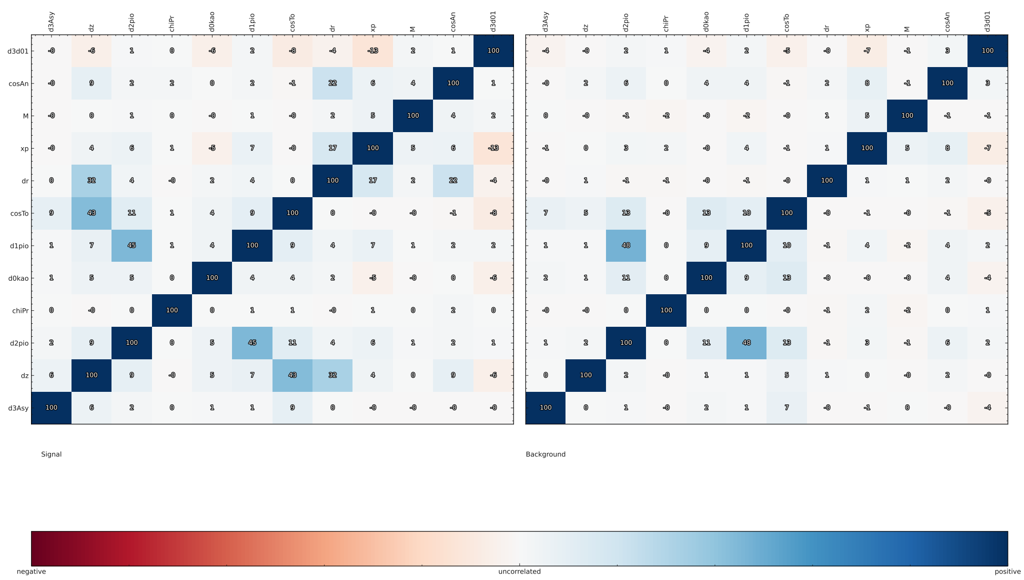

Figure 87: Correlation plot

A.1.18 $D^+ \to K^- K^+ \pi^+$

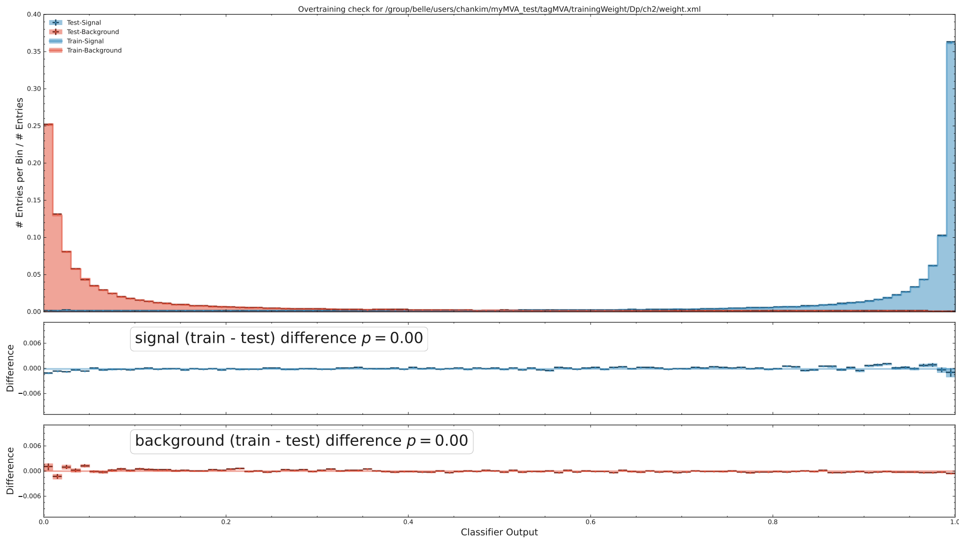

Figure 88: BDT output

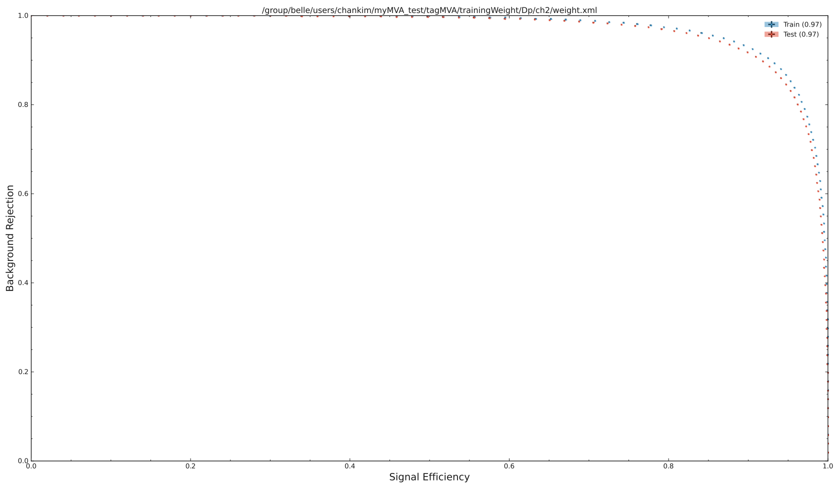

Figure 89: ROC Curve

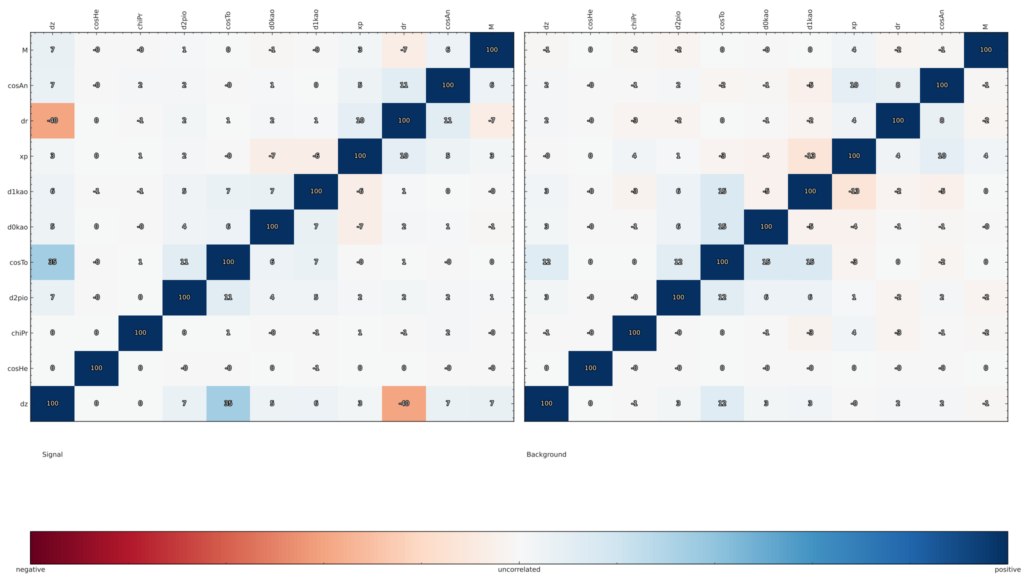

Figure 90: Correlation plot

396 ### A.1.19 $D^+ \to K^- K^+ \pi^+ \pi^0$

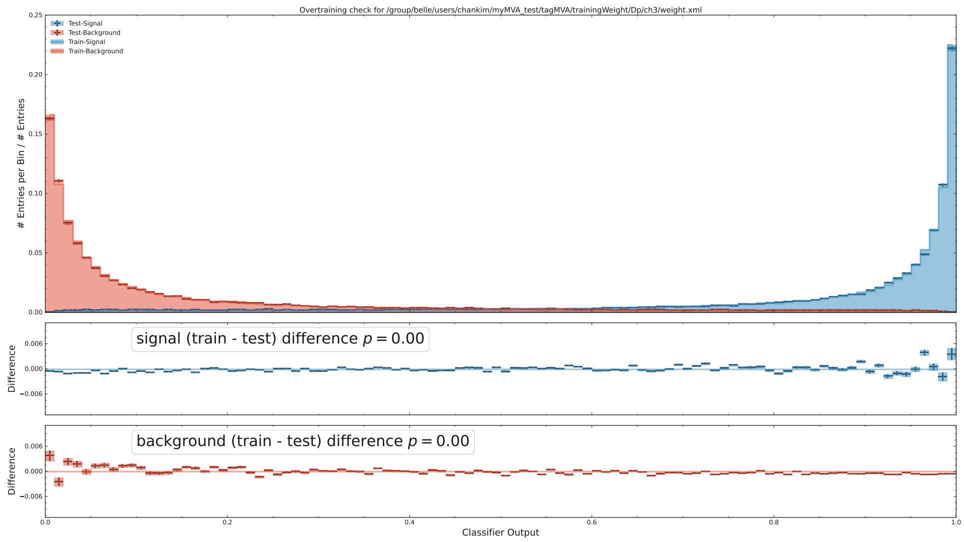

Figure 91: BDT output

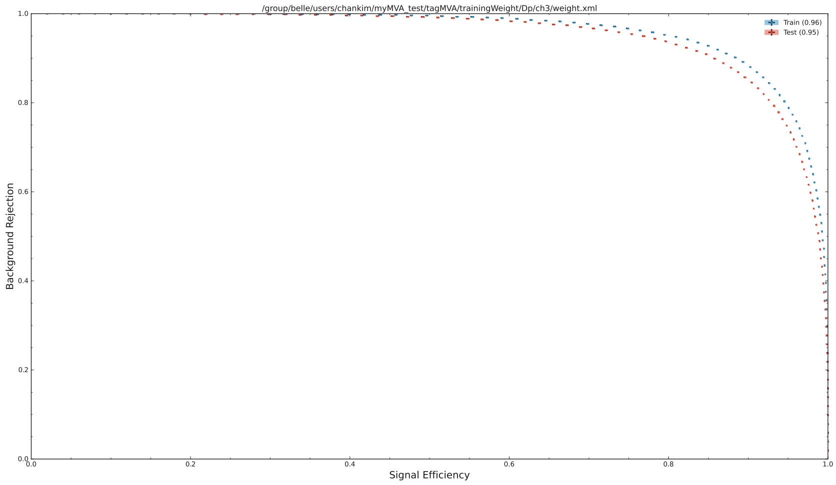

Figure 92: ROC Curve

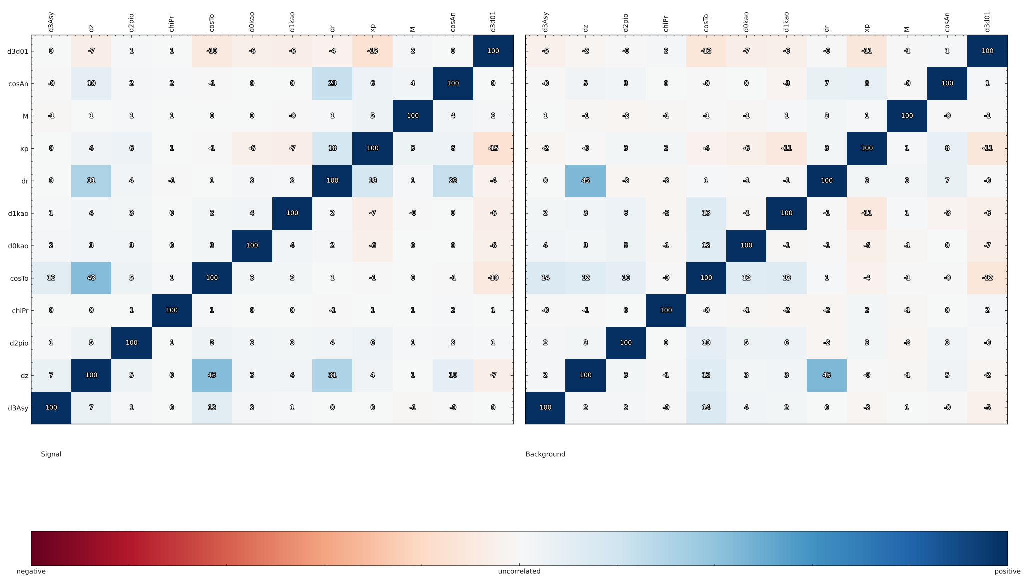

Figure 93: Correlation plot

A.1.20 $D^+ \to \pi^+\pi^0$

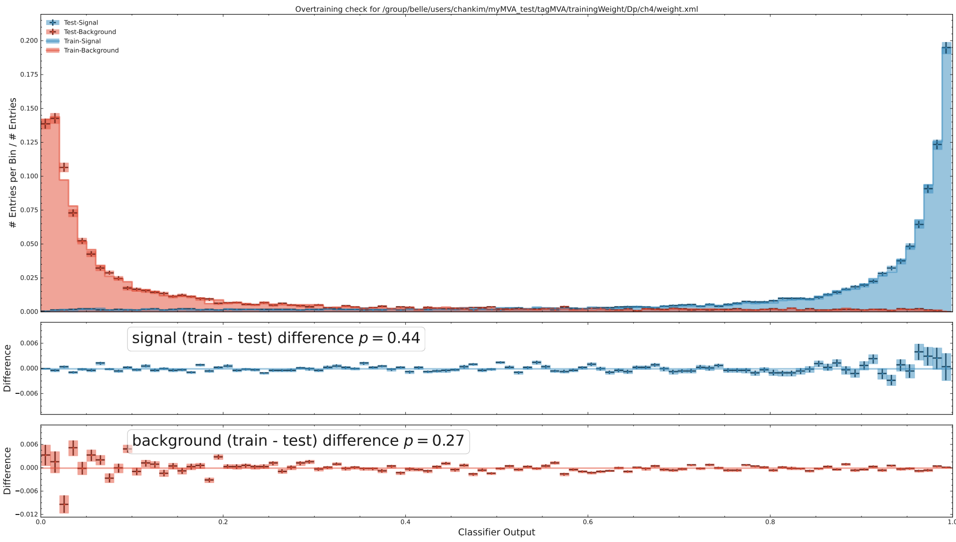

Figure 94: BDT output

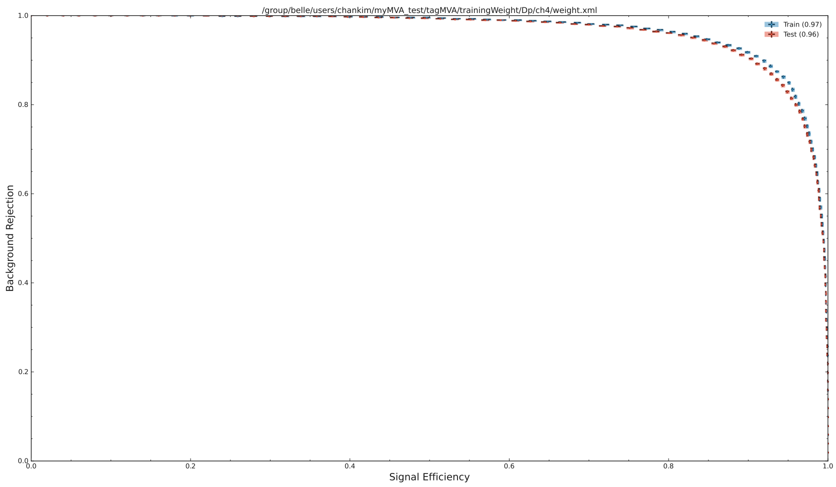

Figure 95: ROC Curve

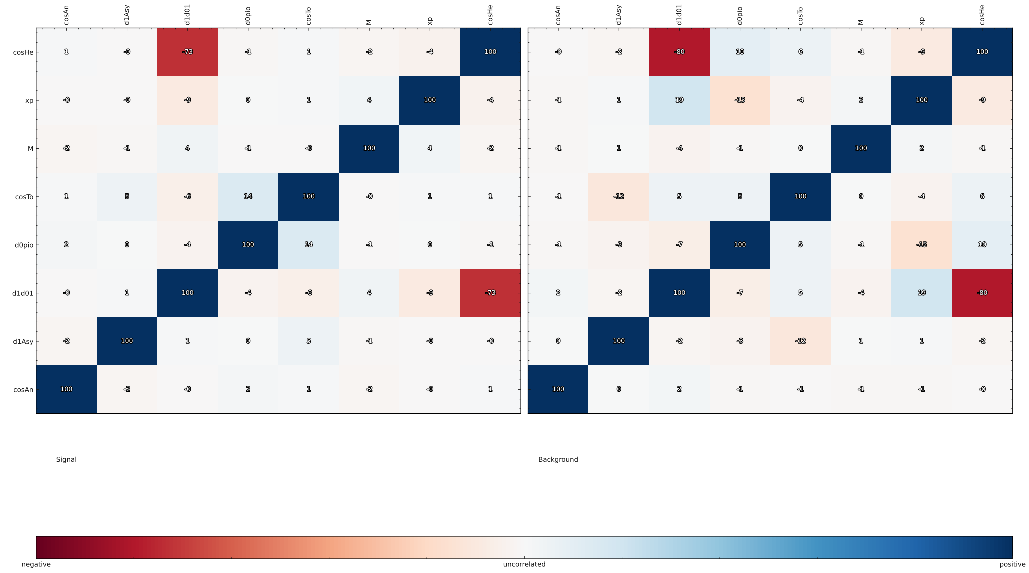

Figure 96: Correlation plot

A.1.21 $D^+ \to \pi^+\pi^-\pi^+$

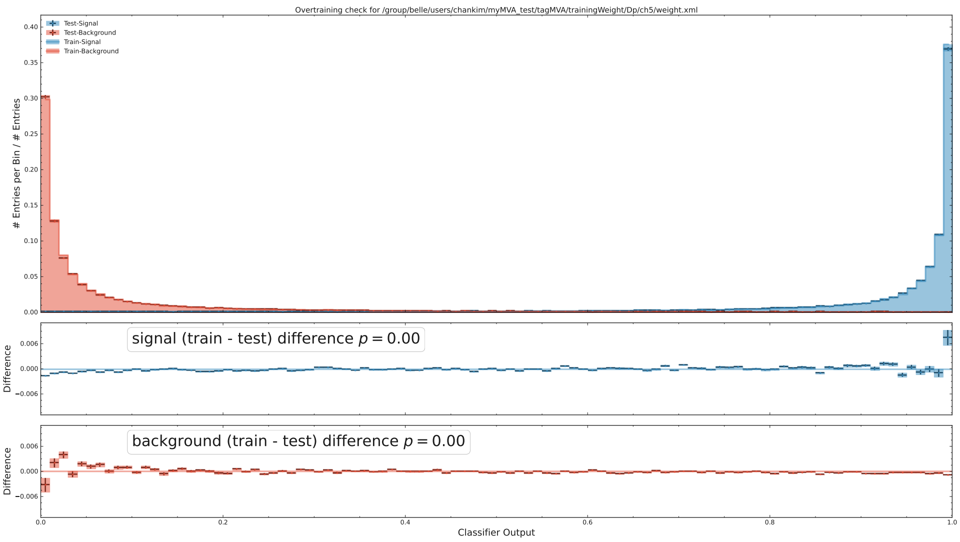

Figure 97: BDT output

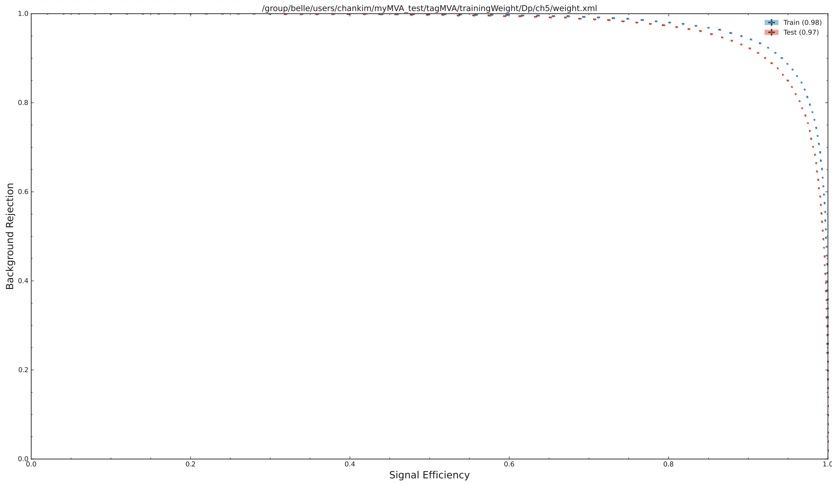

Figure 98: ROC Curve

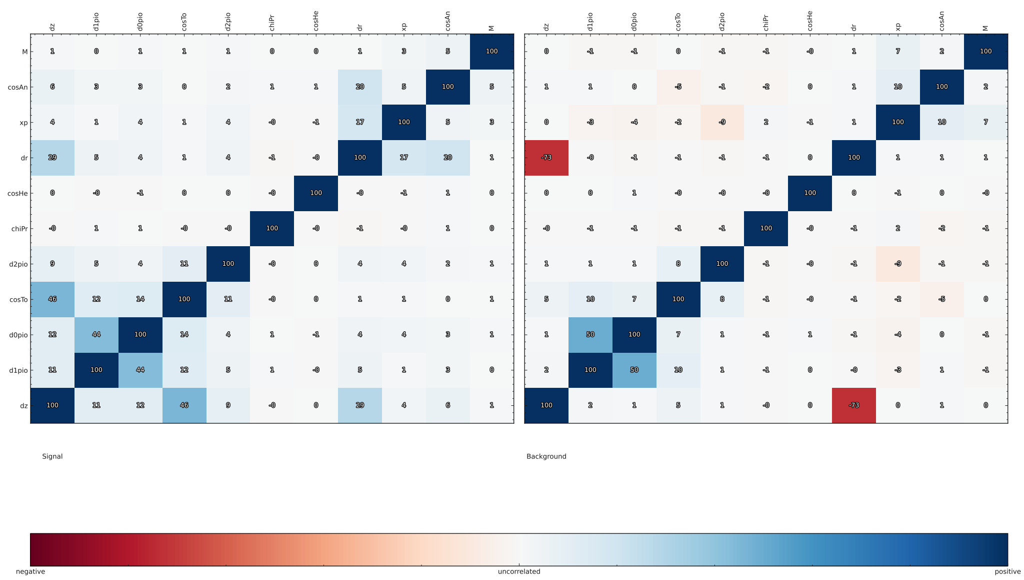

Figure 99: Correlation plot

A.1.22 $D^+ \to \pi^+\pi^-\pi^+\pi^0$

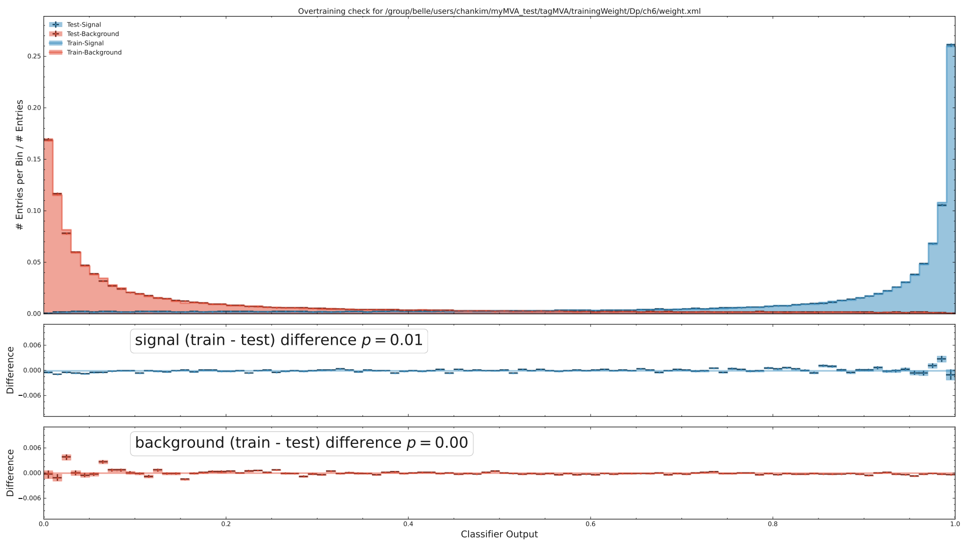

Figure 100: BDT output

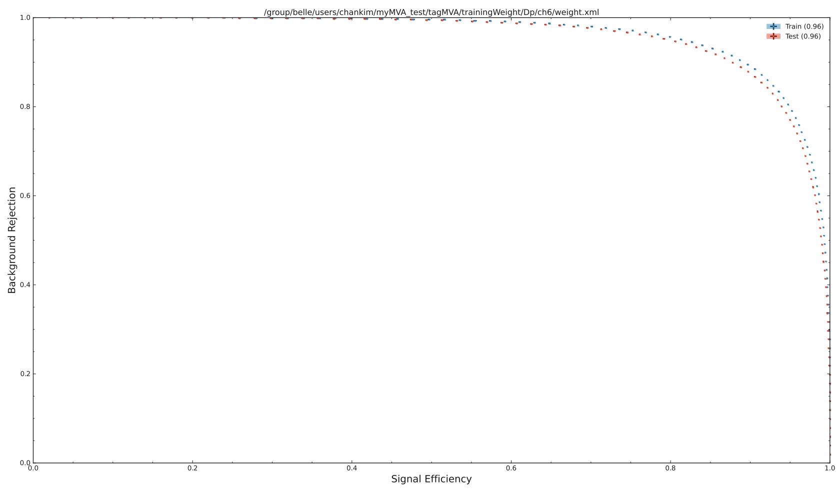

Figure 101: ROC Curve

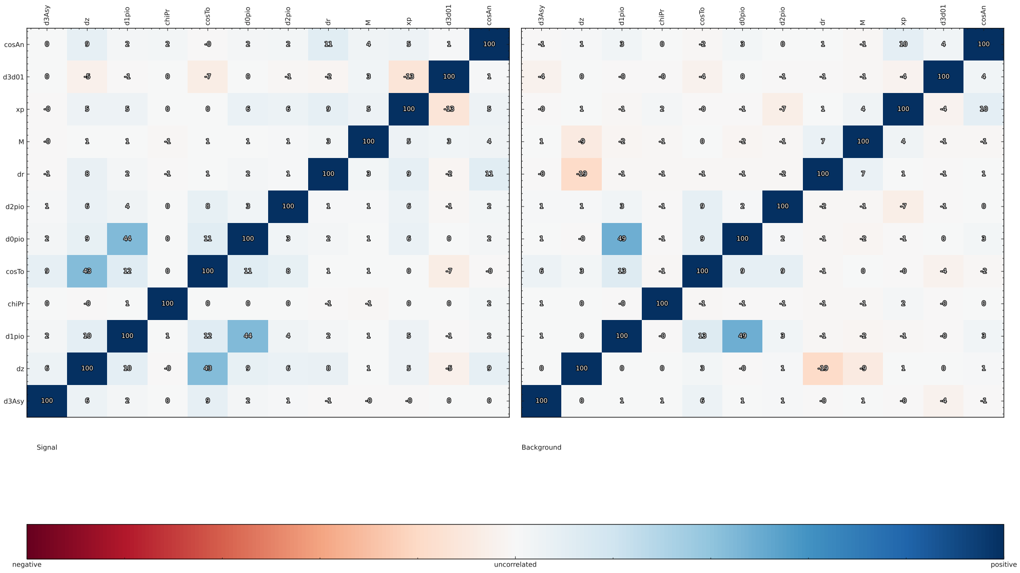

Figure 102: Correlation plot

A.1.23 $D^+ \to \pi^+ K^0_S$

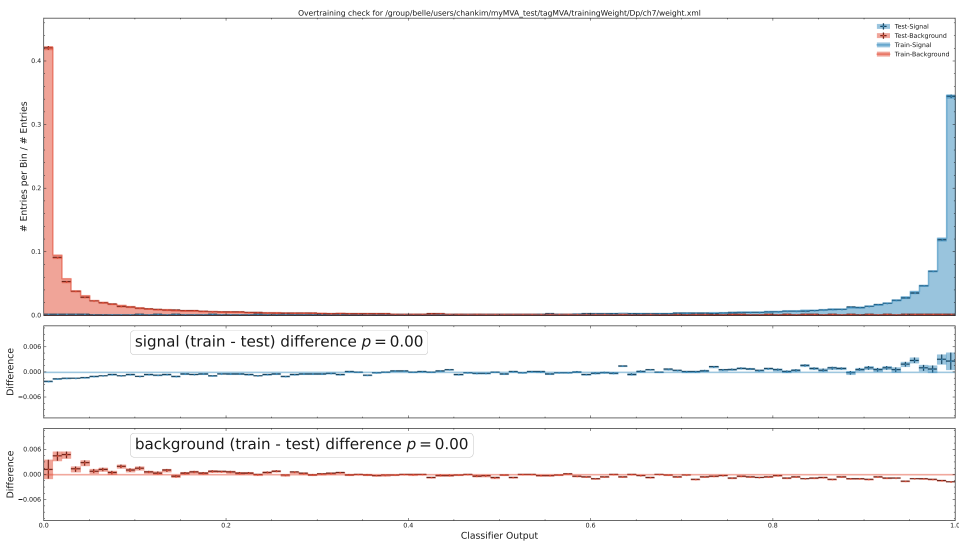

Figure 103: BDT output

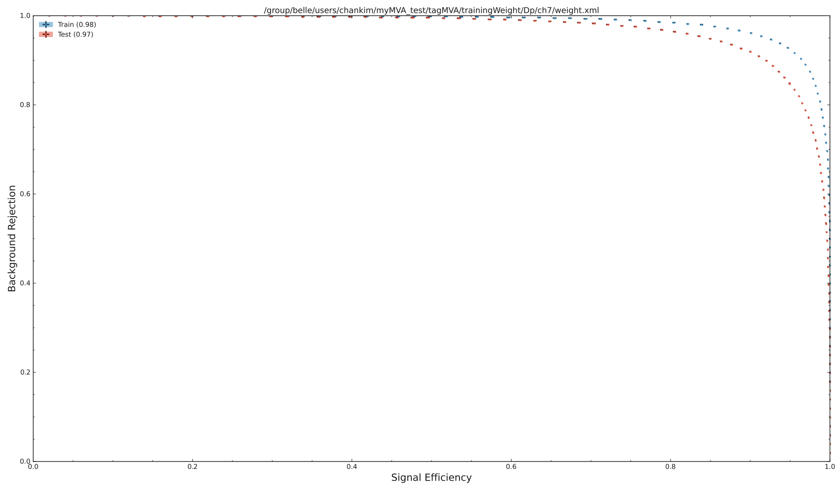

Figure 104: ROC Curve

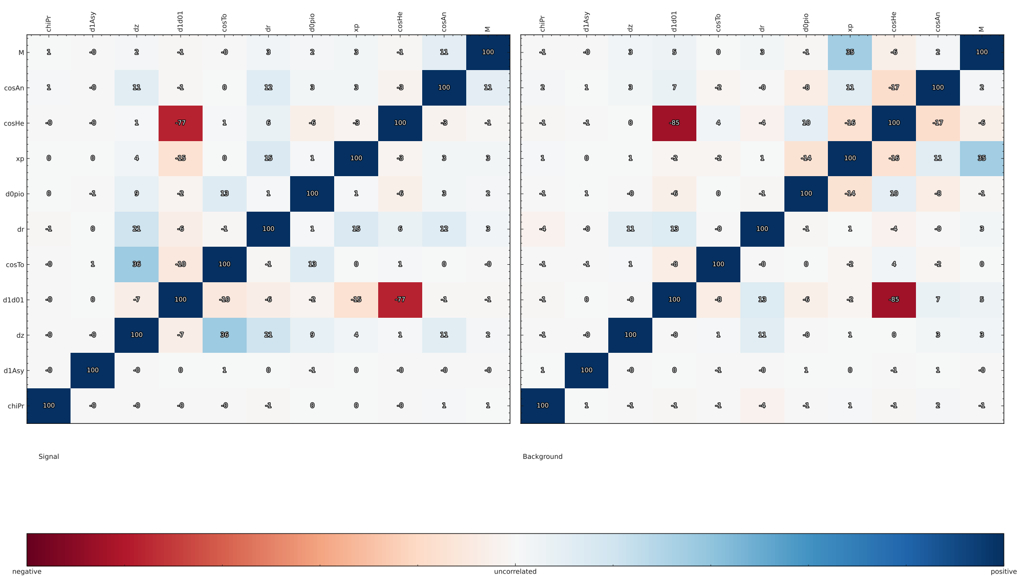

Figure 105: Correlation plot

A.1.24 $D^+ \to \pi^+\pi^0 K_S^0$

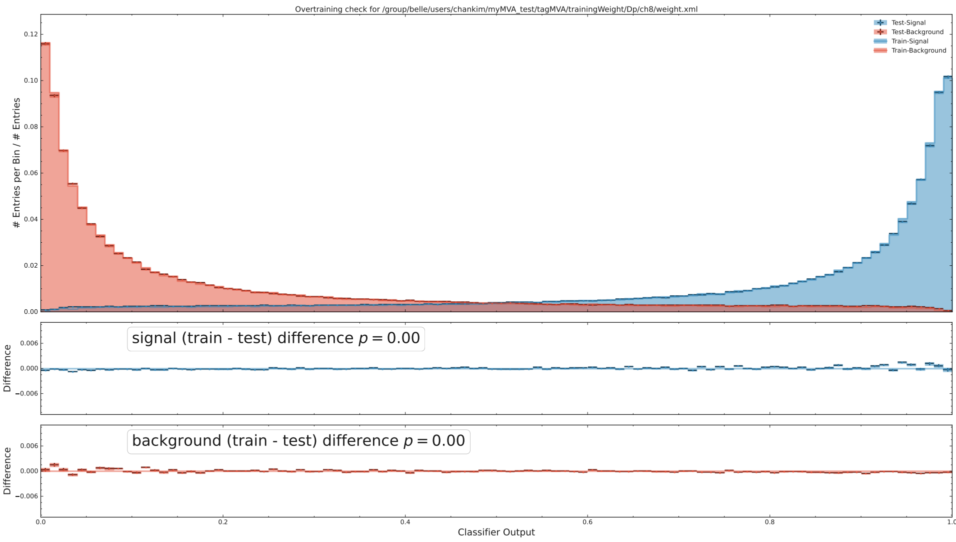

Figure 106: BDT output

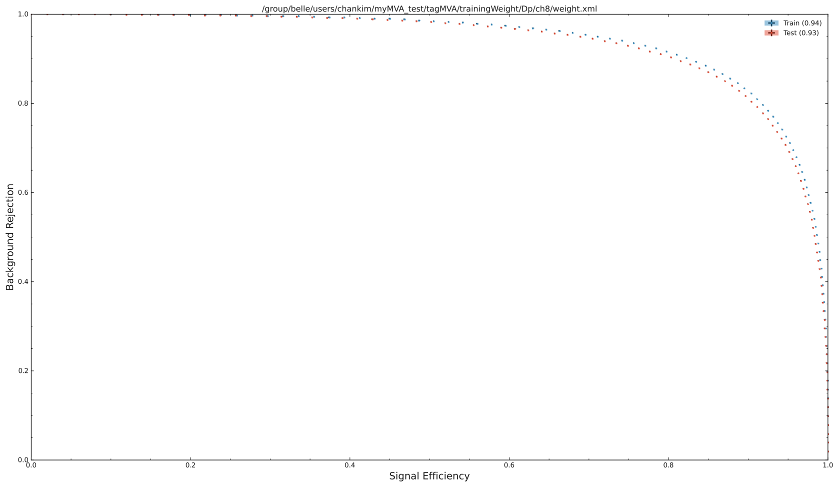

Figure 107: ROC Curve

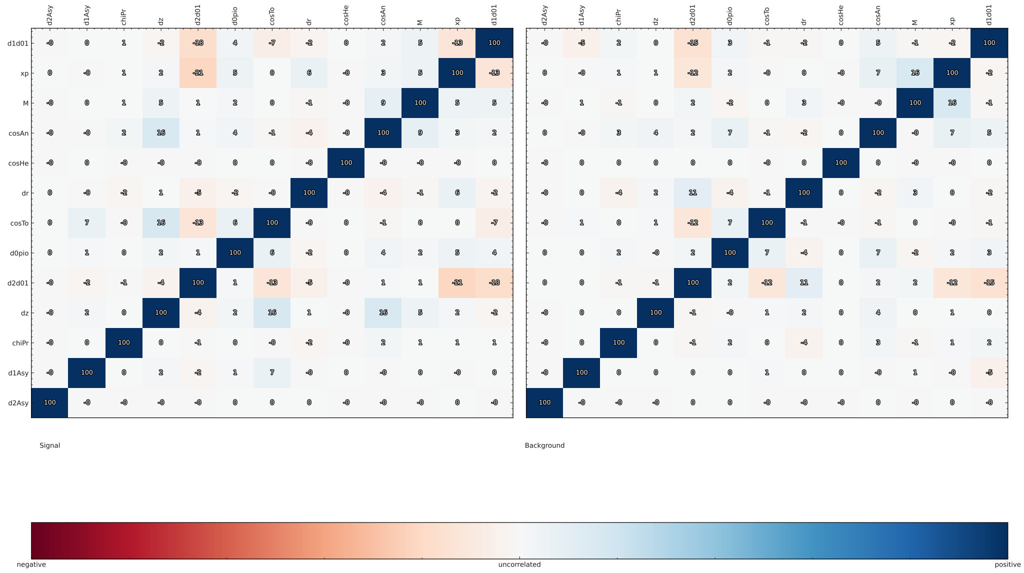

Figure 108: Correlation plot

A.1.25 $D^+ \to \pi^+\pi^-\pi^+K_S^0$

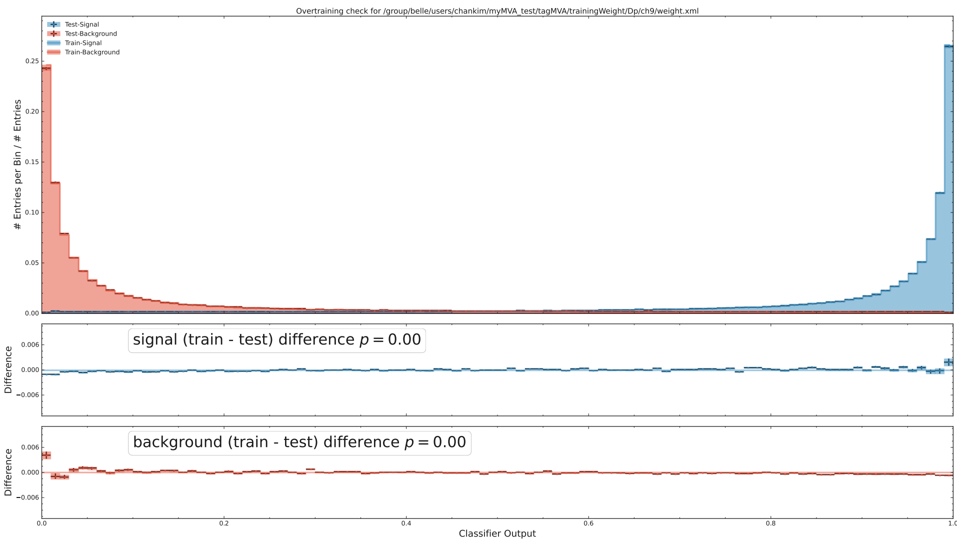

Figure 109: BDT output

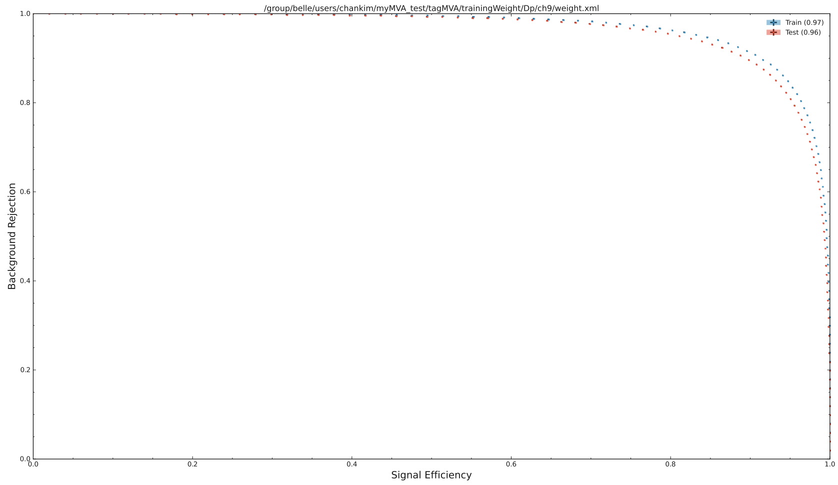

Figure 110: ROC Curve

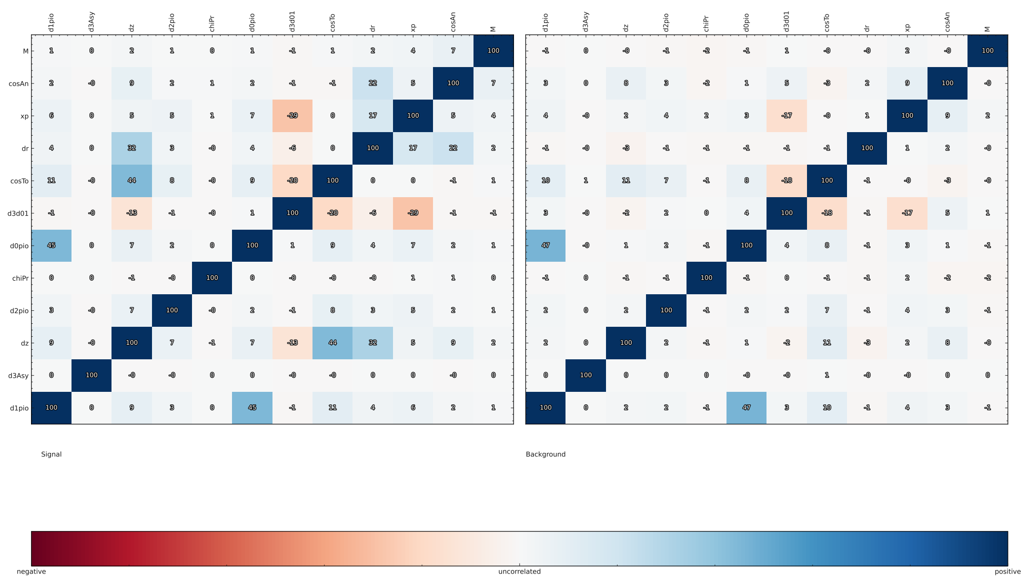

Figure 111: Correlation plot

A.1.26 $D^+ \to K^+ K_S^0 K_S^0$

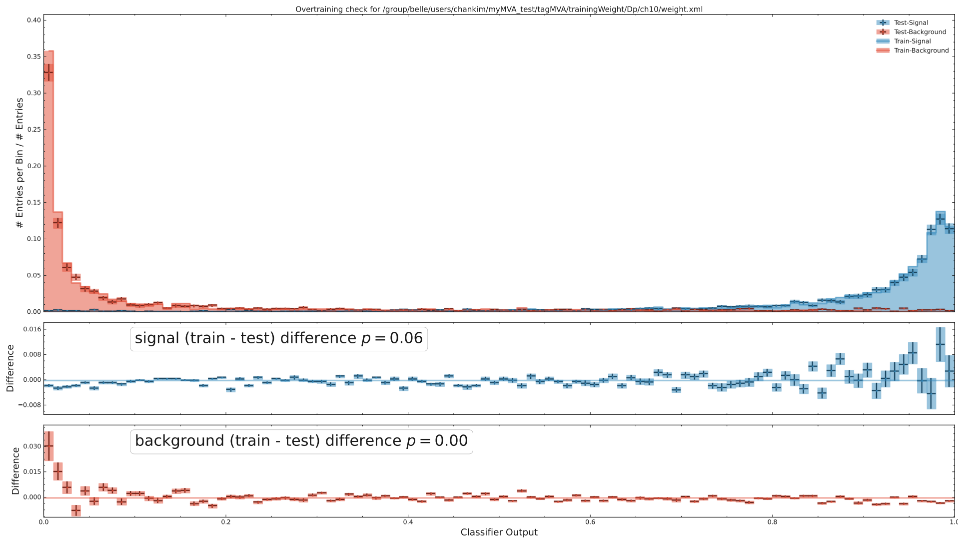

Figure 112: BDT output

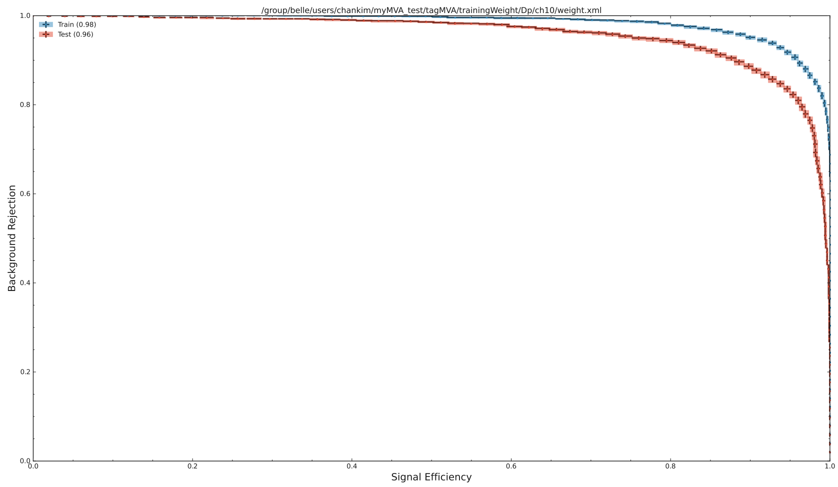

Figure 113: ROC Curve

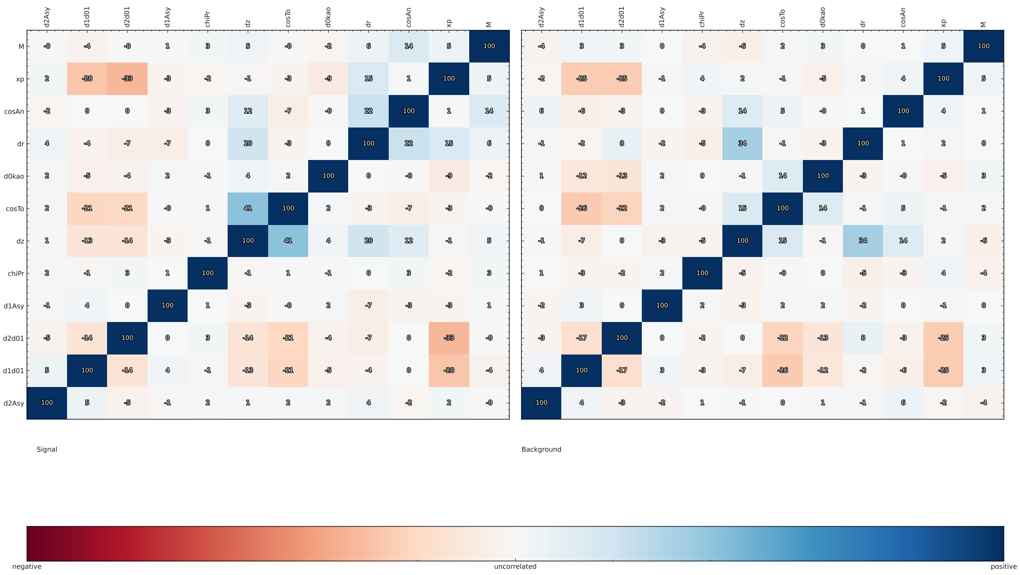

Figure 114: Correlation plot

A.1.27 $D_s^+ \to K^+K^-\pi^+$

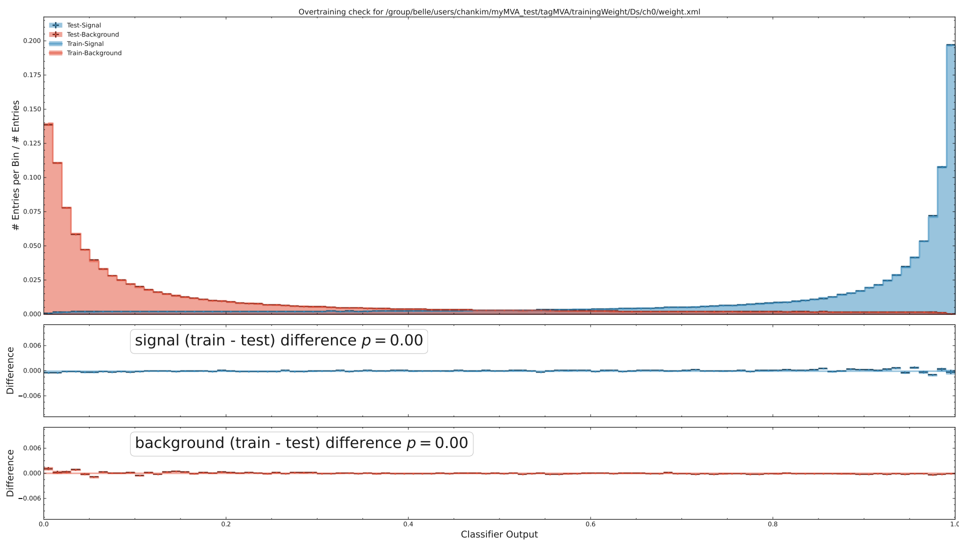

Figure 115: BDT output

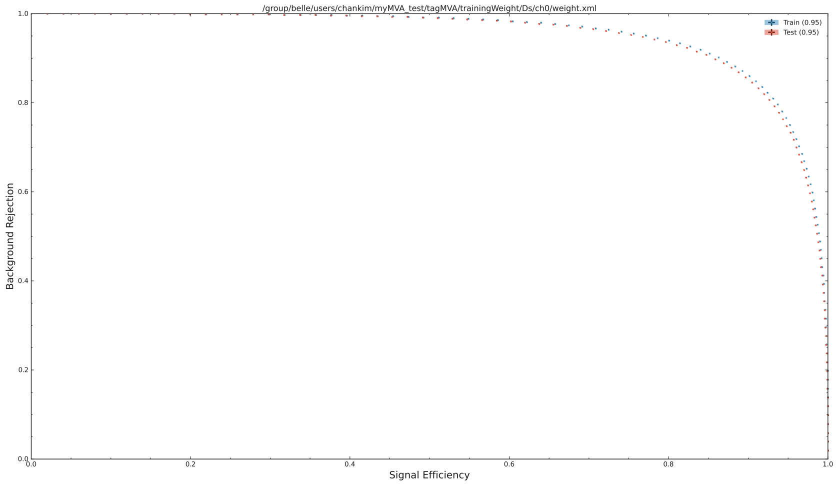

Figure 116: ROC Curve

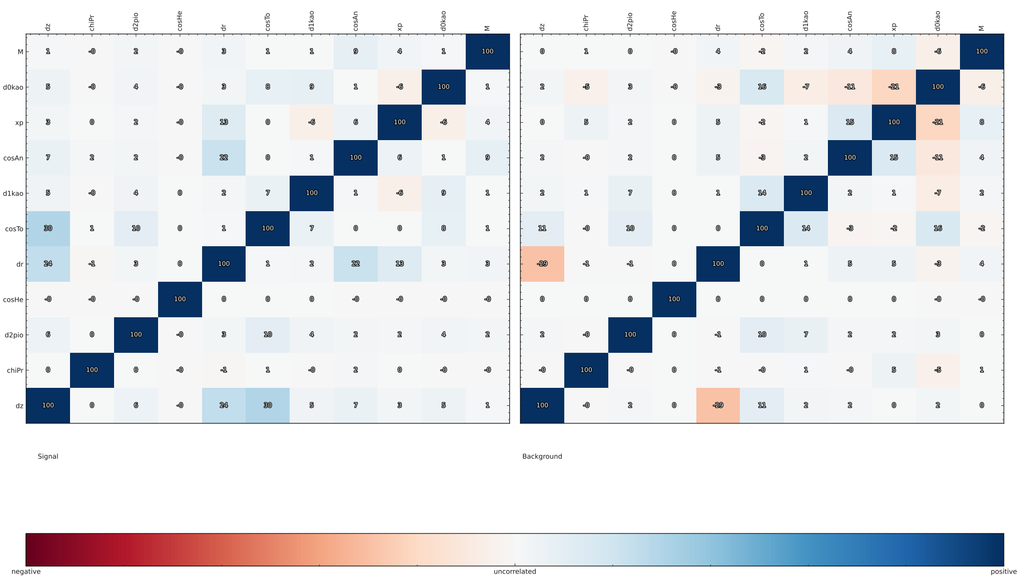

Figure 117: Correlation plot

A.1.28 $D_s^+ \to K^+ K_S^0$

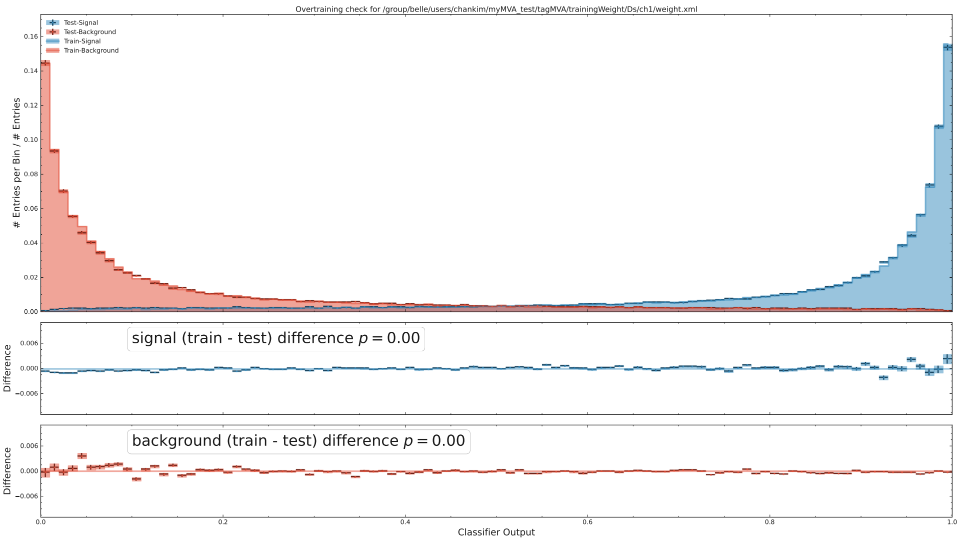

Figure 118: BDT output

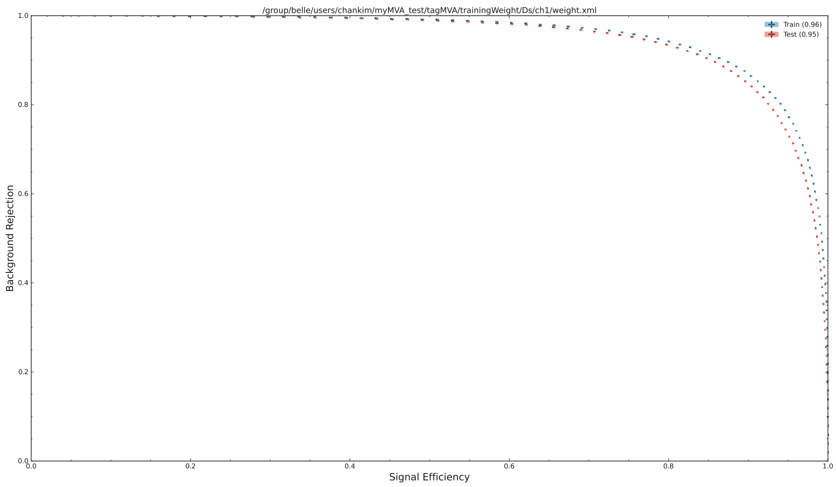

Figure 119: ROC Curve

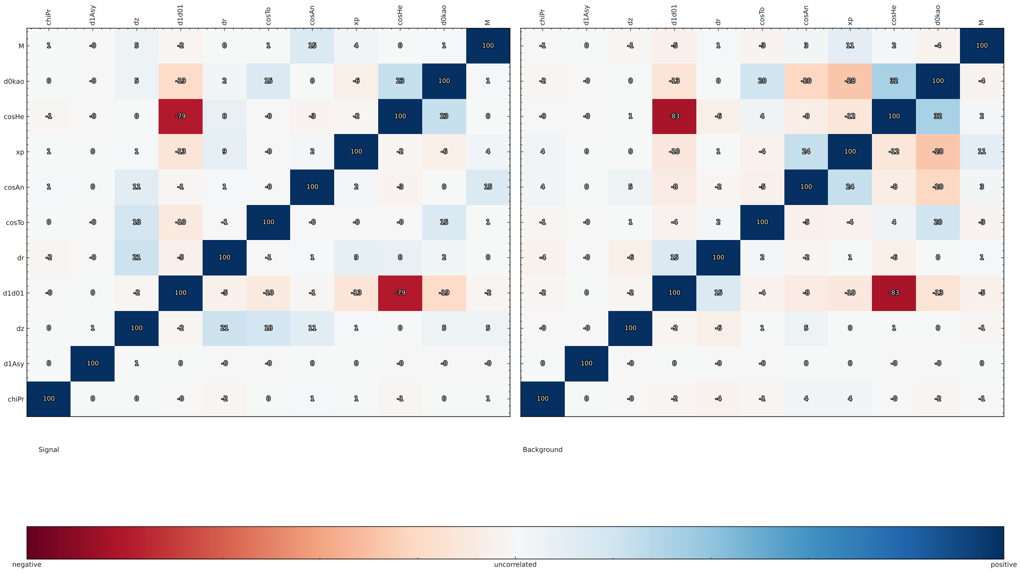

Figure 120: Correlation plot

A.1.29 $D_s^+ \to \pi^+ K_S^0 K_S^0$

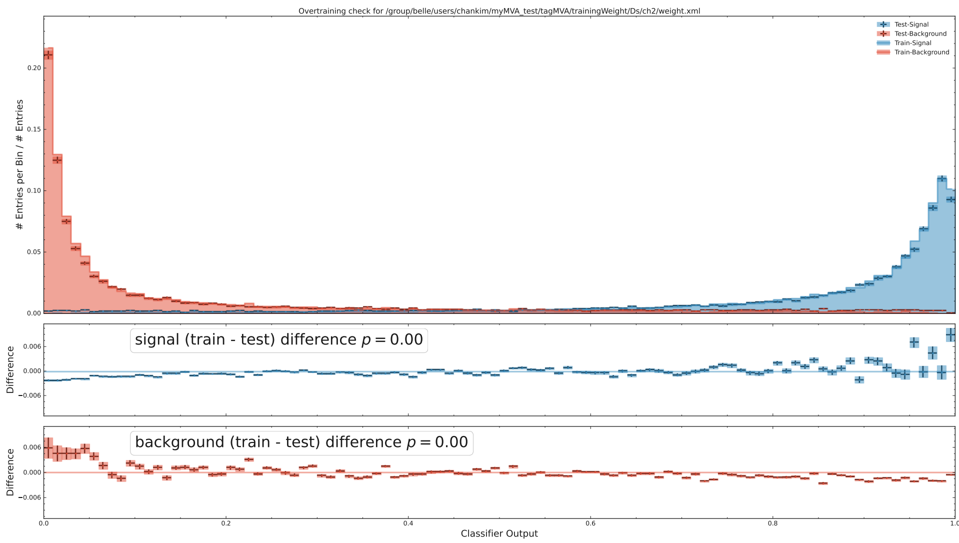

Figure 121: BDT output

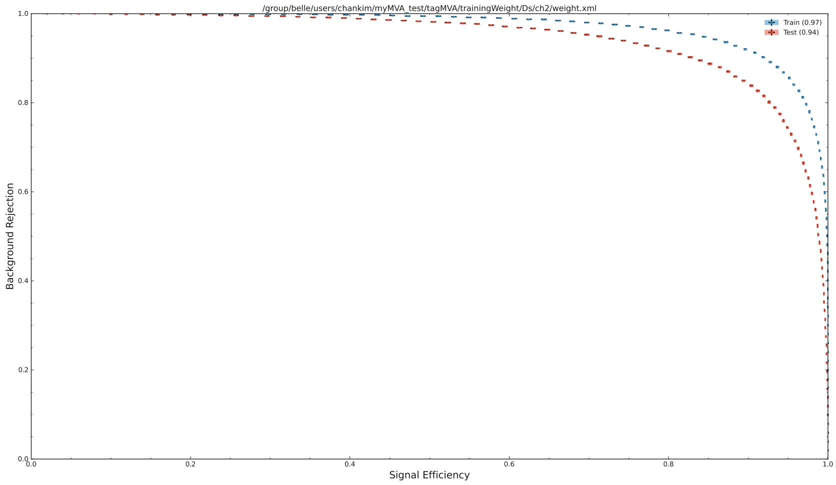

Figure 122: ROC Curve

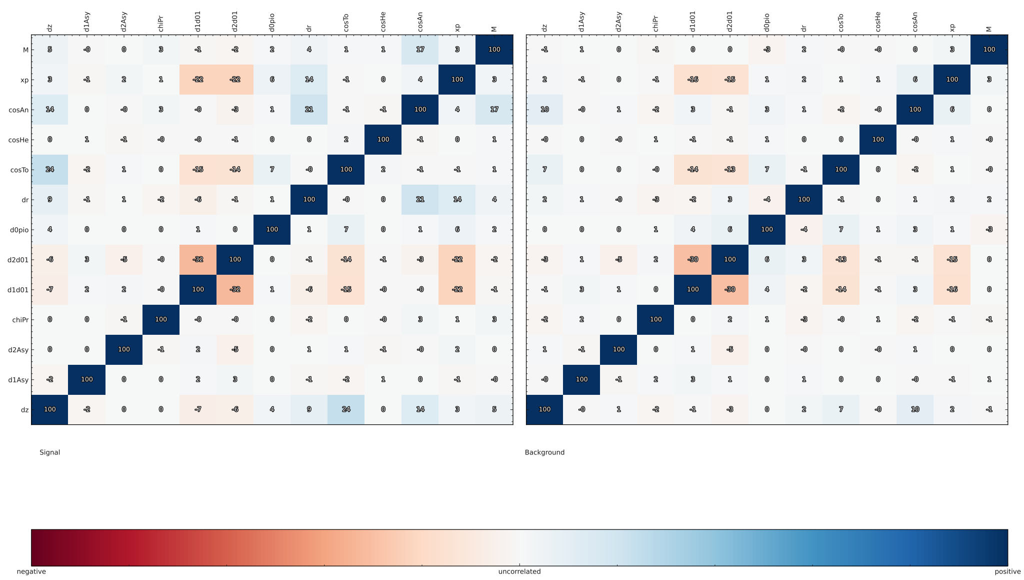

Figure 123: Correlation plot

A.1.30 $D_s^+ \to K^+K^-\pi^+\pi^0$

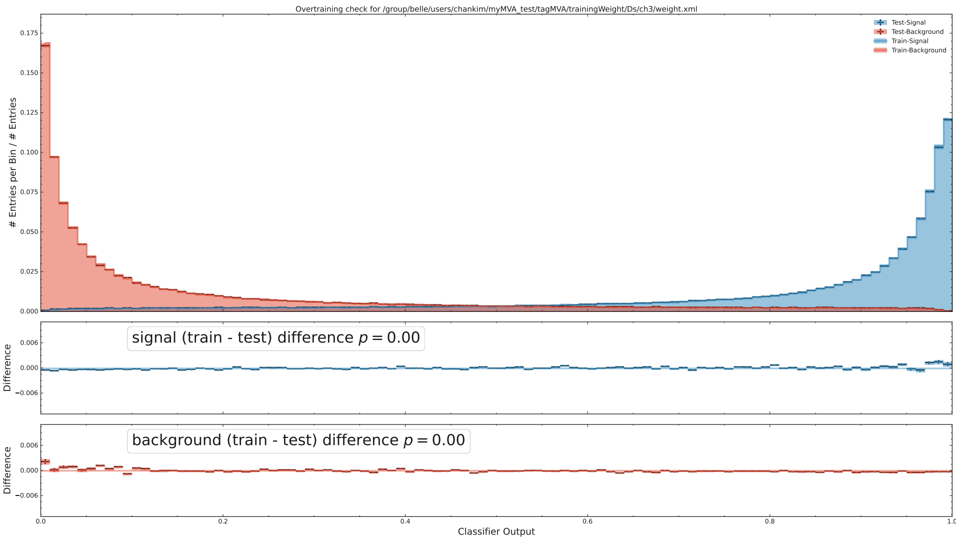

Figure 124: BDT output

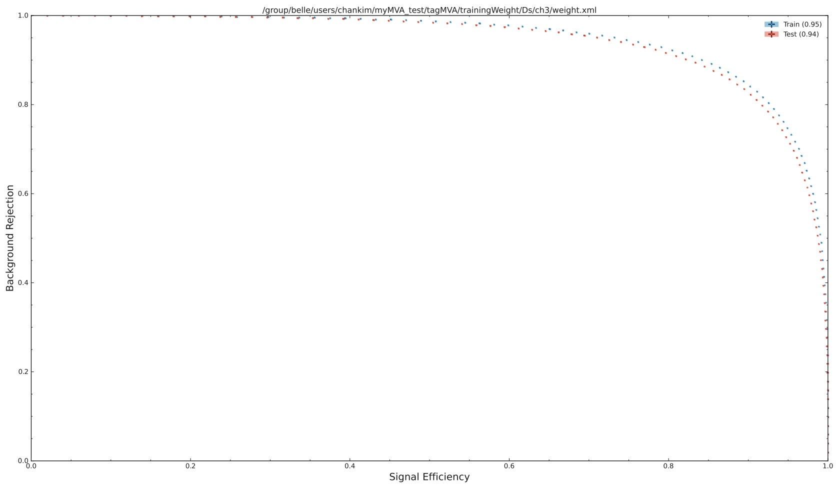

Figure 125: ROC Curve

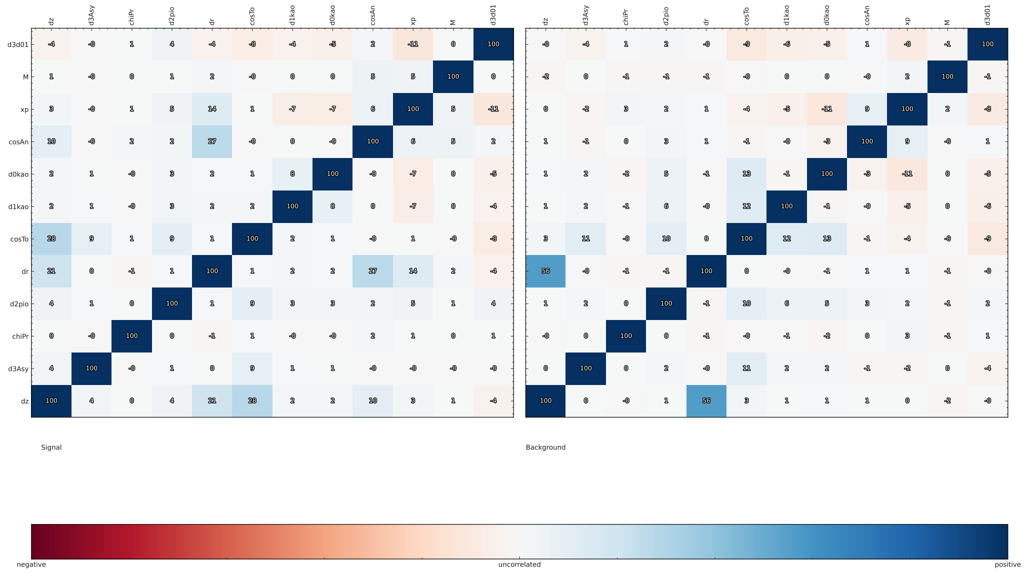

Figure 126: Correlation plot

A.1.31 $D_s^+ \to K^- \pi^+ \pi^+ K_S^0$

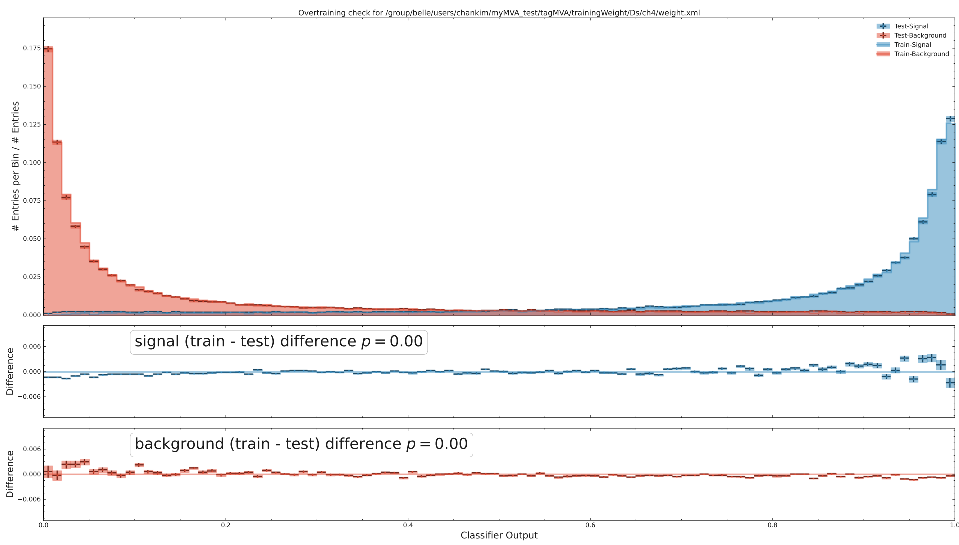

Figure 127: BDT output

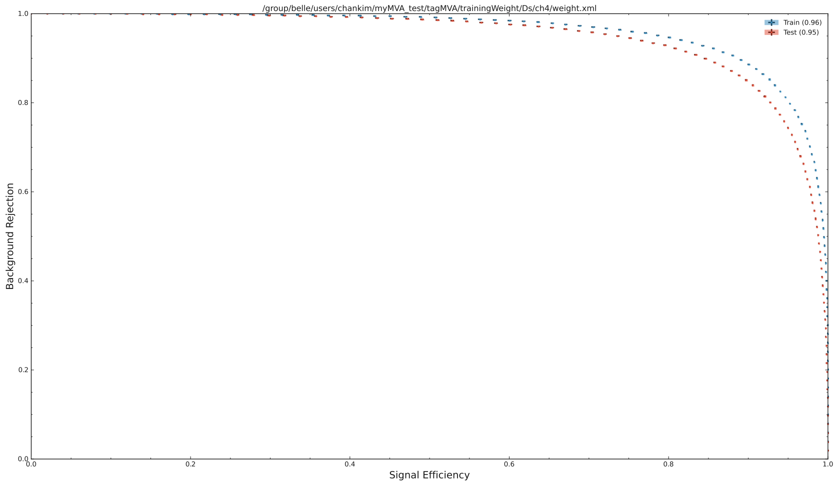

Figure 128: ROC Curve

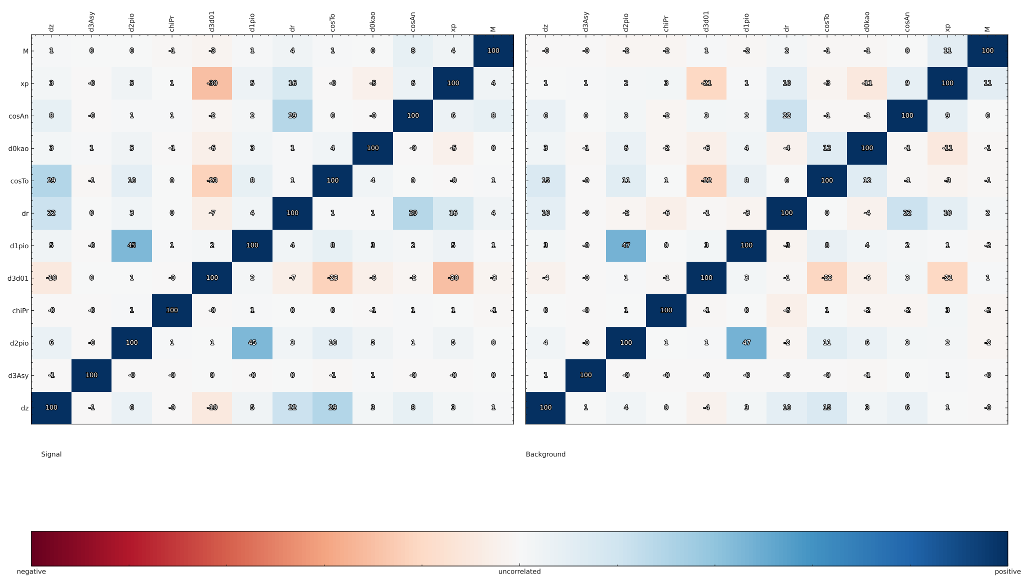

Figure 129: Correlation plot

A.1.32 $D_s^+ \to K^+\pi^+\pi^- K_S^0$

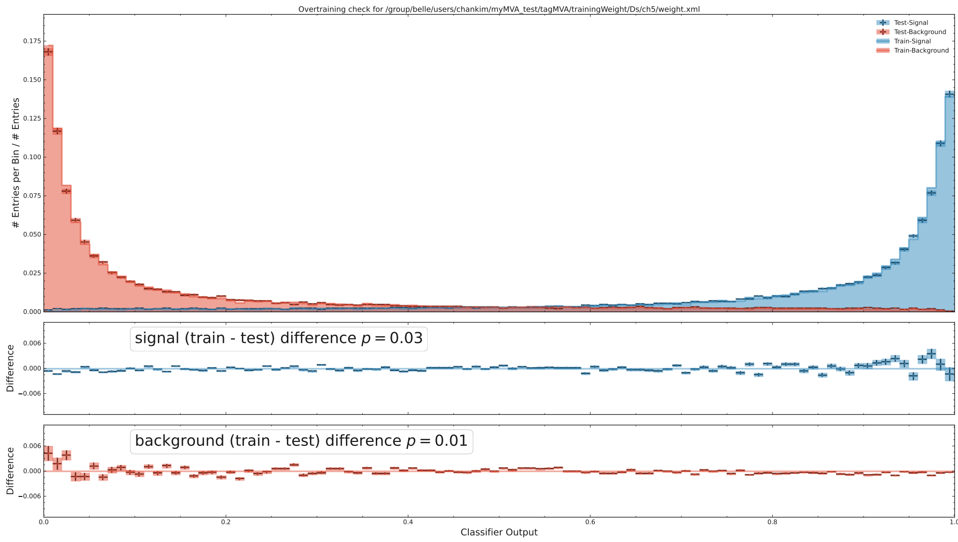

Figure 130: BDT output

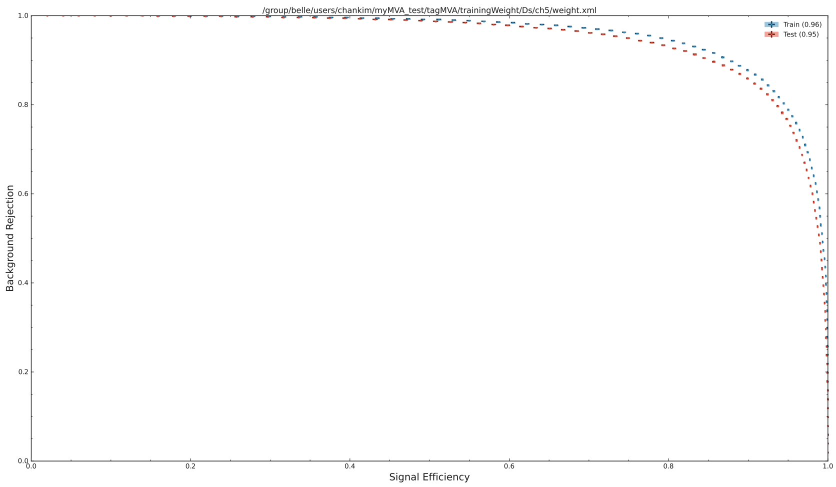

Figure 131: ROC Curve

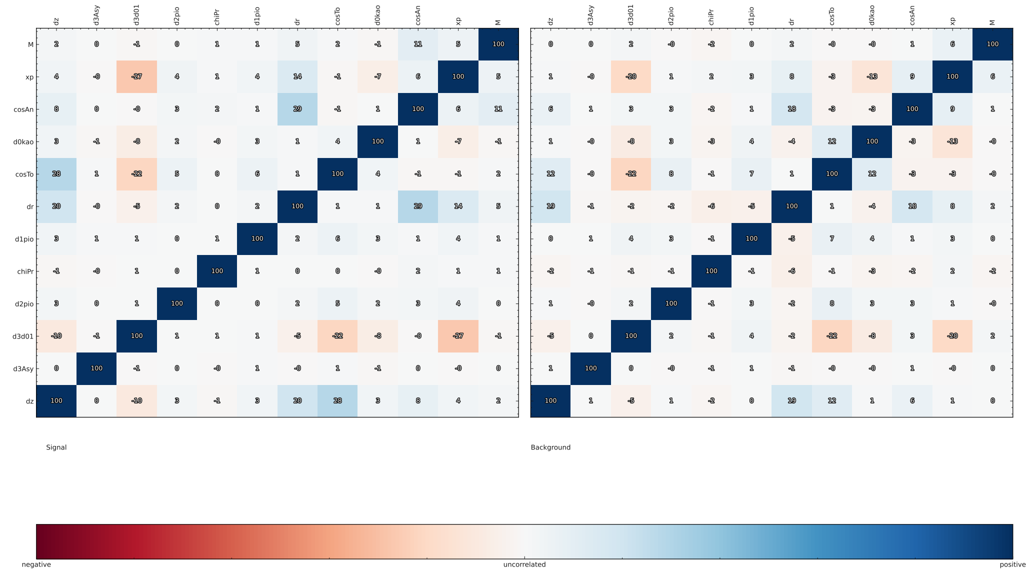

Figure 132: Correlation plot

A.1.33 $D_s^+ \to \pi^+\pi^-\pi^+$

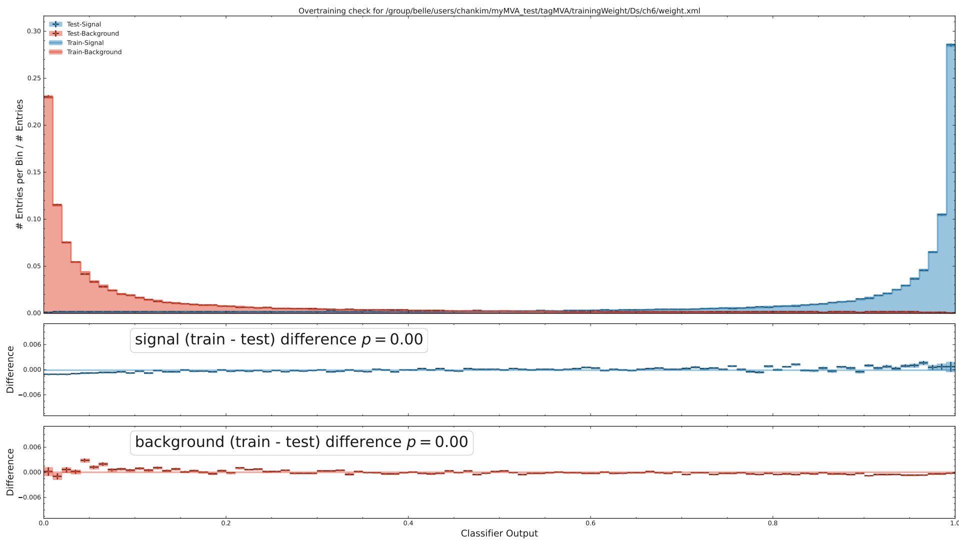

Figure 133: BDT output

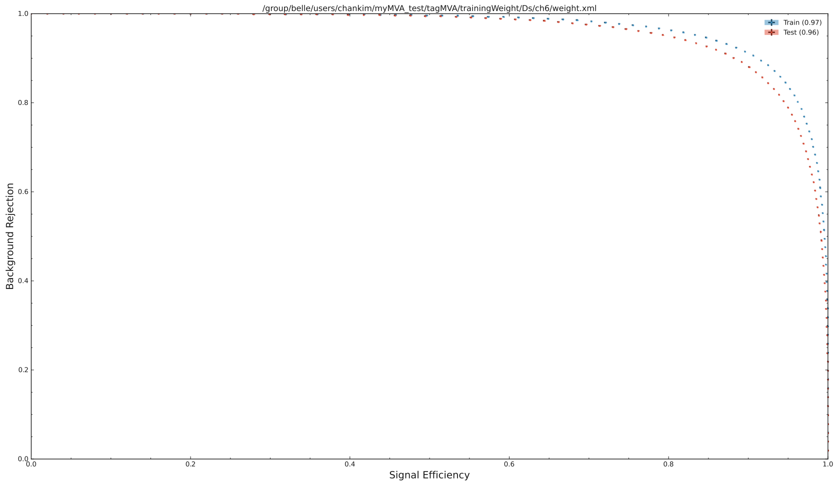

Figure 134: ROC Curve

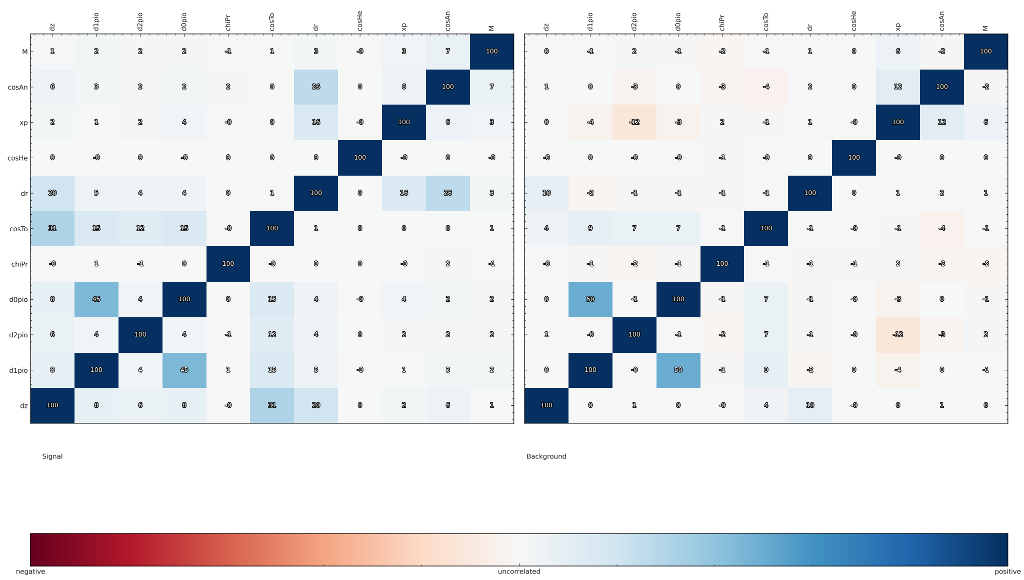

Figure 135: Correlation plot

A.1.34 $D_s^+ \to \pi^+ K_S^0$

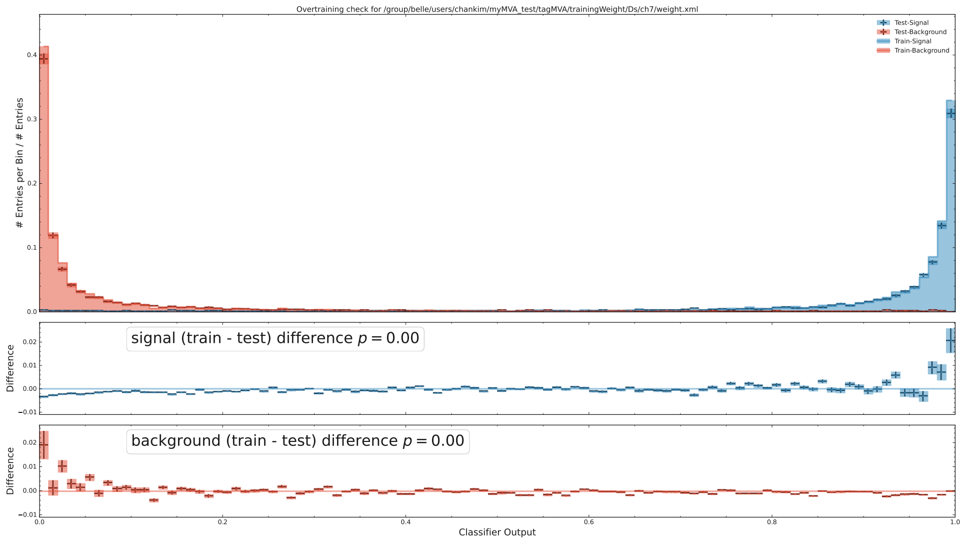

Figure 136: BDT output

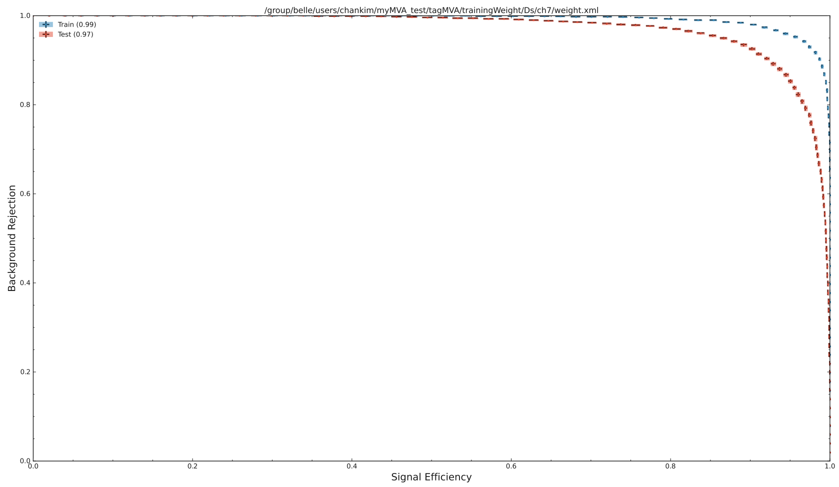

Figure 137: ROC Curve

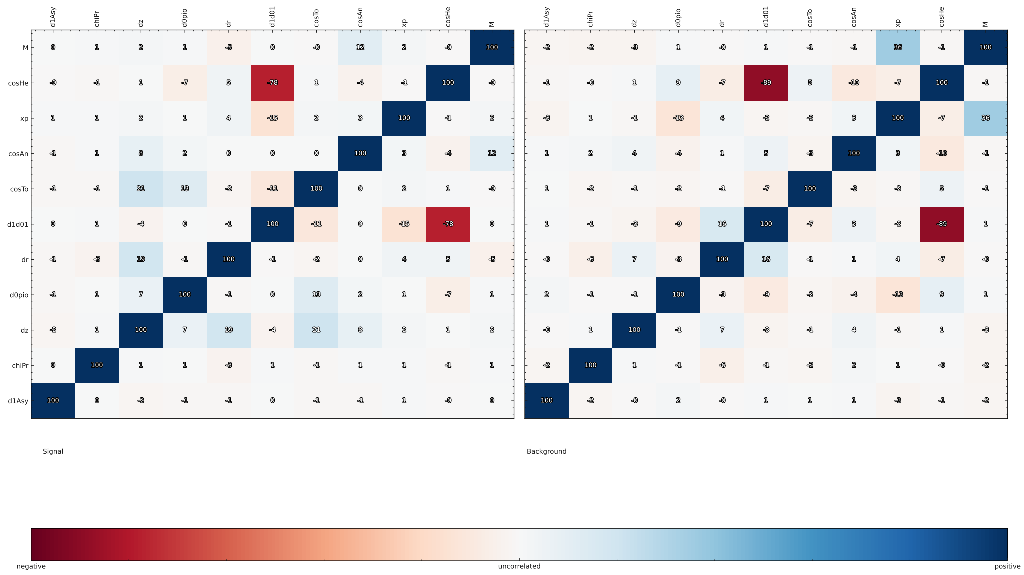

Figure 138: Correlation plot

A.1.35 $D_s^+ \to \pi^+ \pi^0 K_S^0$

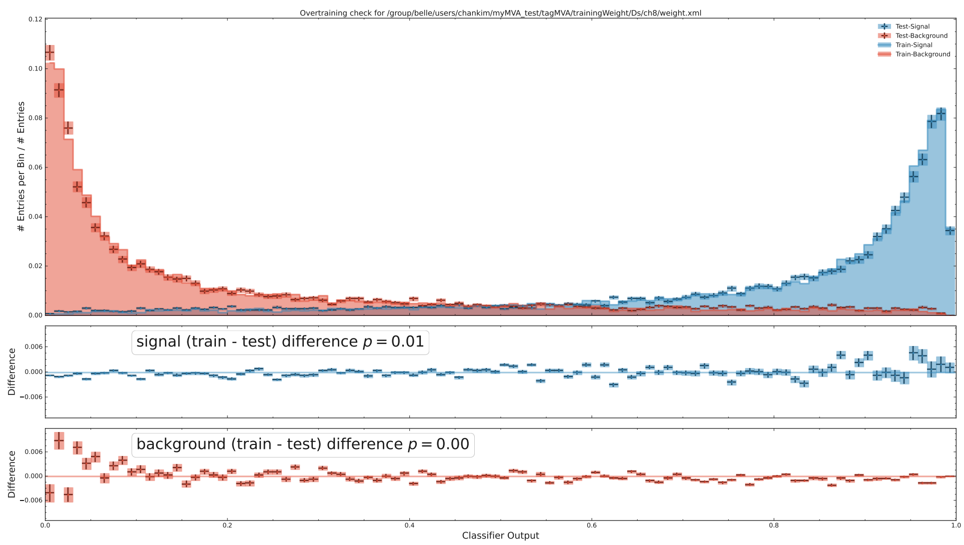

Figure 139: BDT output

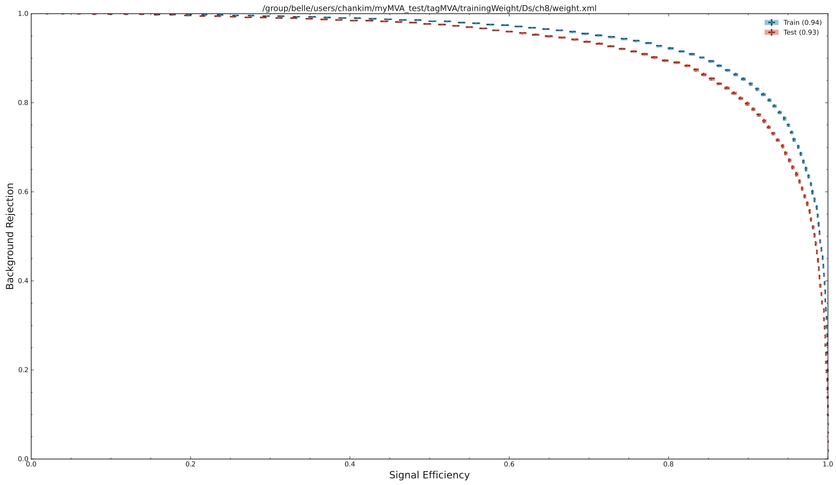

Figure 140: ROC Curve

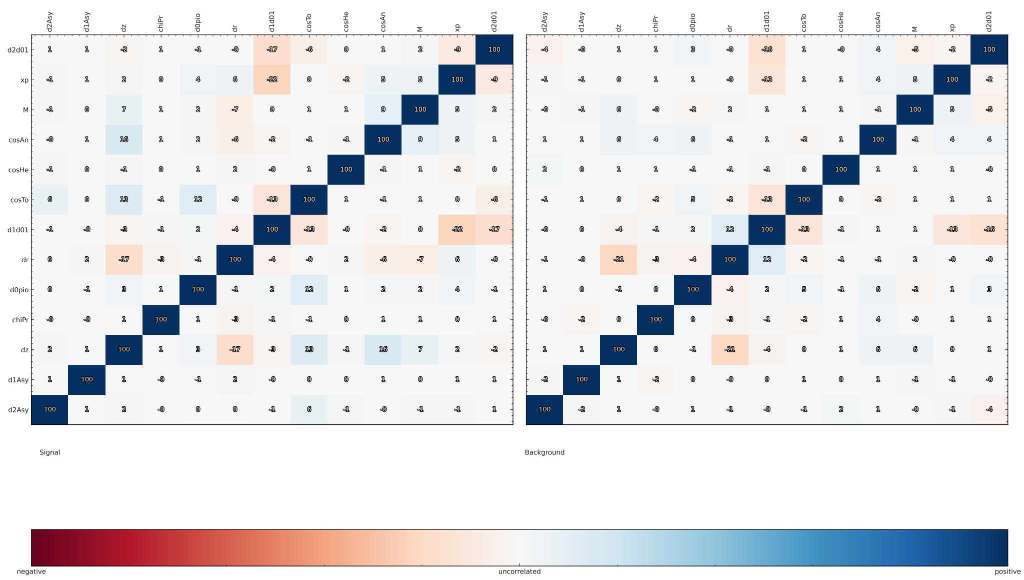

Figure 141: Correlation plot

A.1.36 $D_s^+ \to K^+ K^- \pi^+ \pi^- \pi^+$

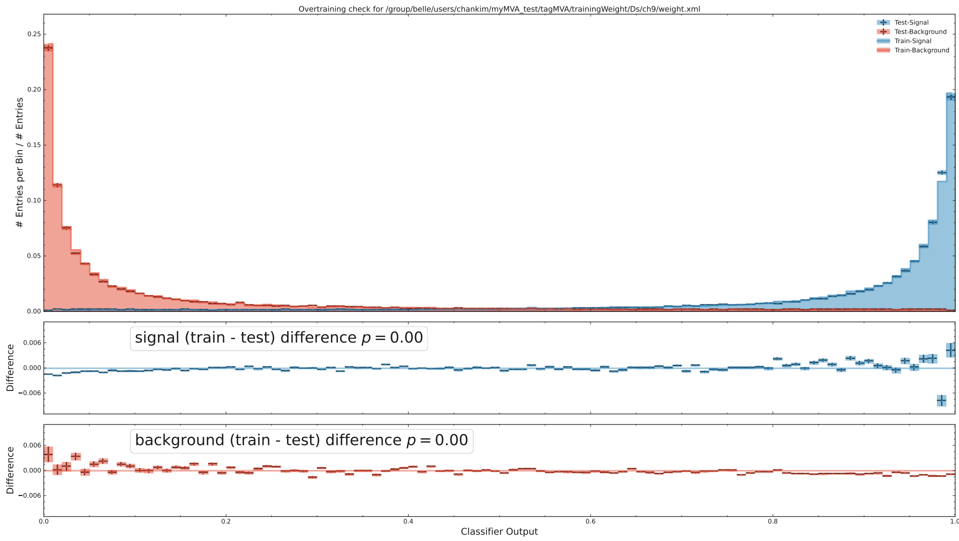

Figure 142: BDT output

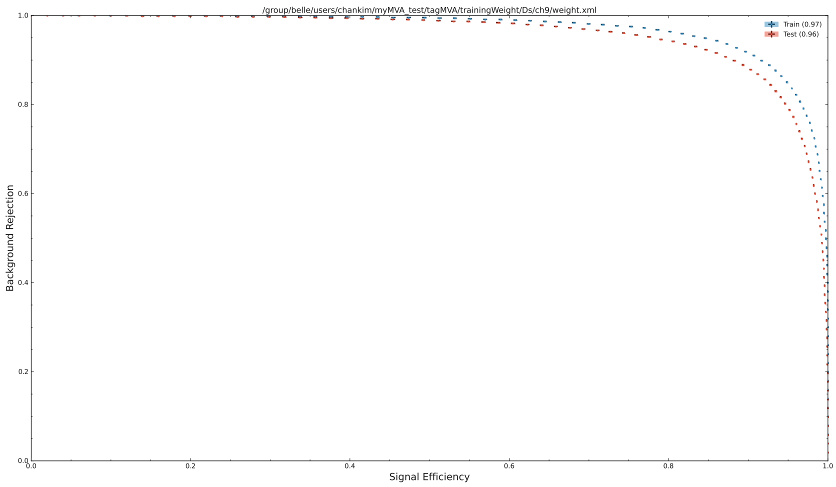

Figure 143: ROC Curve

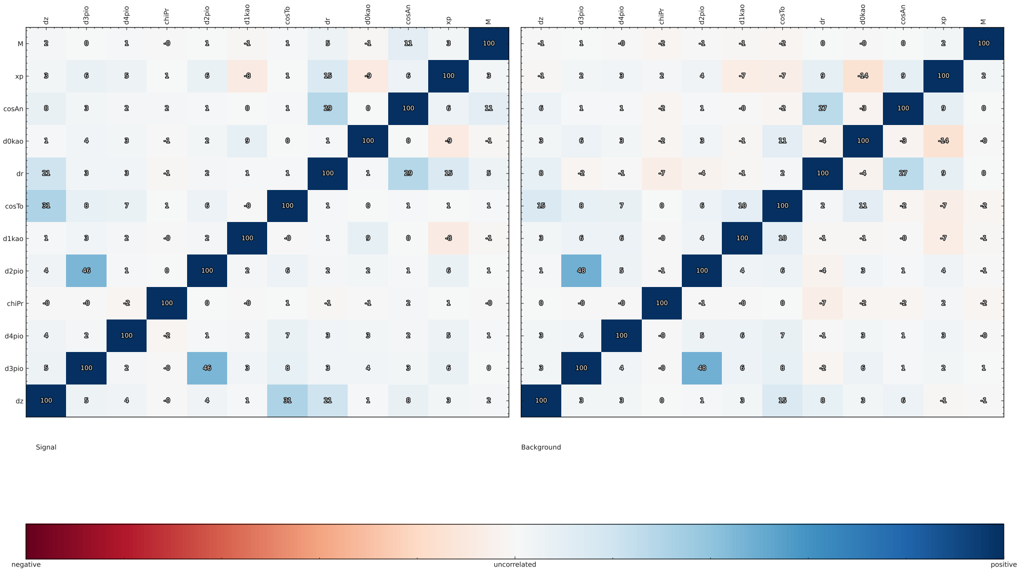

Figure 144: Correlation plot

A.1.37 $\Lambda_c^+ \to p^+ K^- \pi^+$

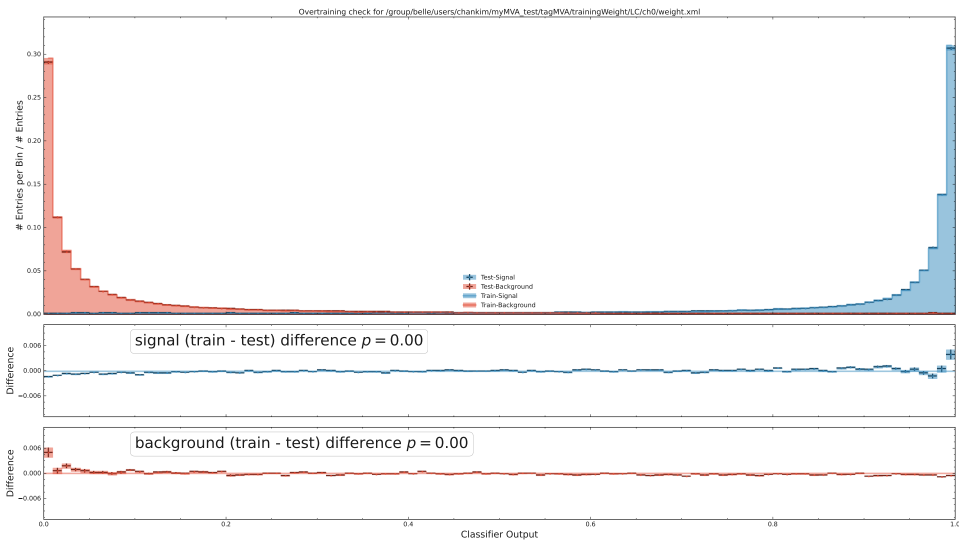

Figure 145: BDT output

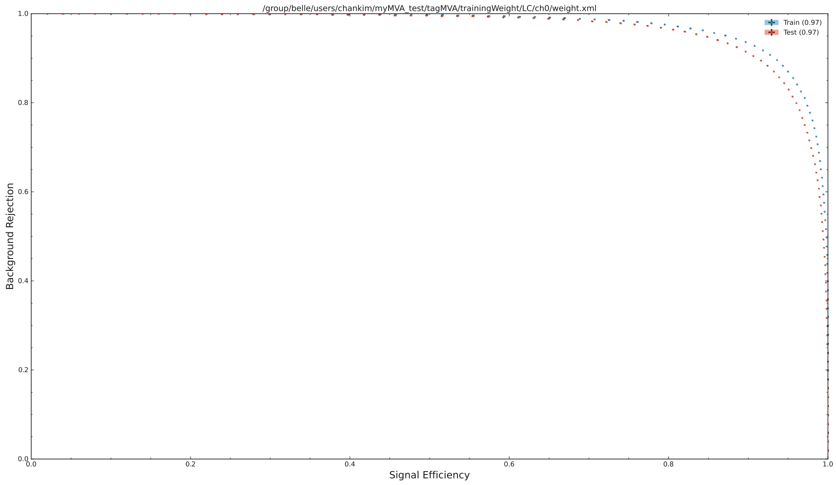

Figure 146: ROC Curve

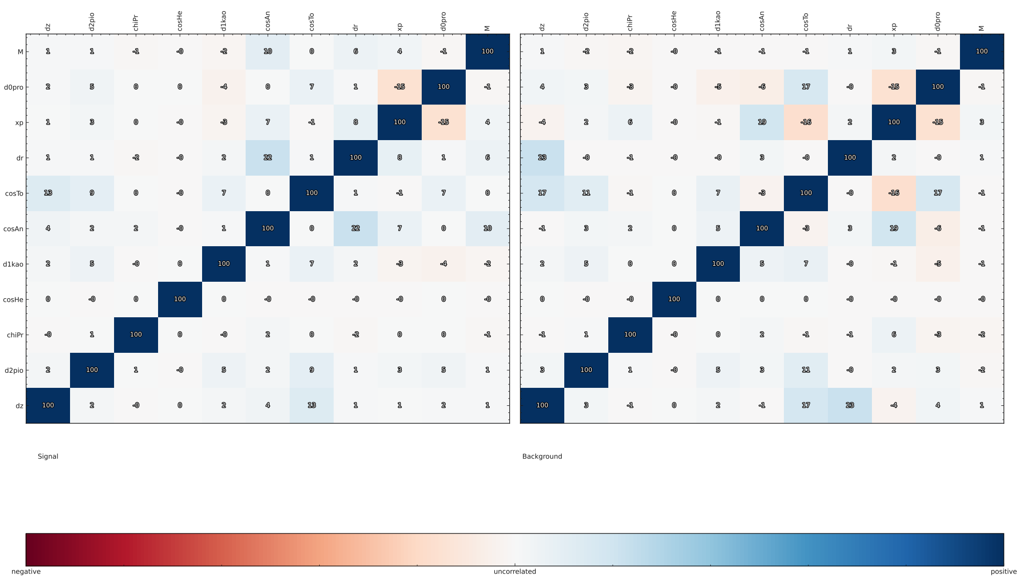

Figure 147: Correlation plot

A.1.38 $\Lambda_c^+ \to p^+\pi^-\pi^+$

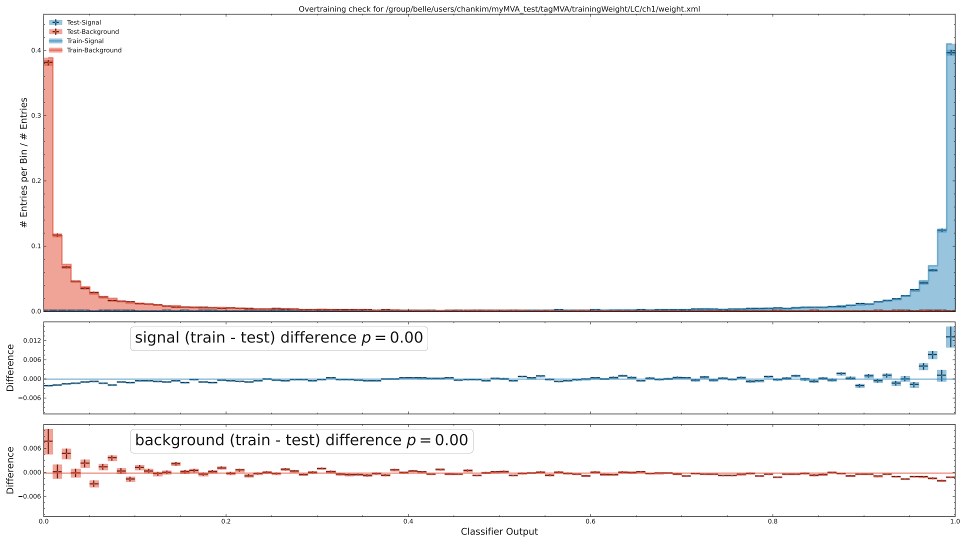

Figure 148: BDT output

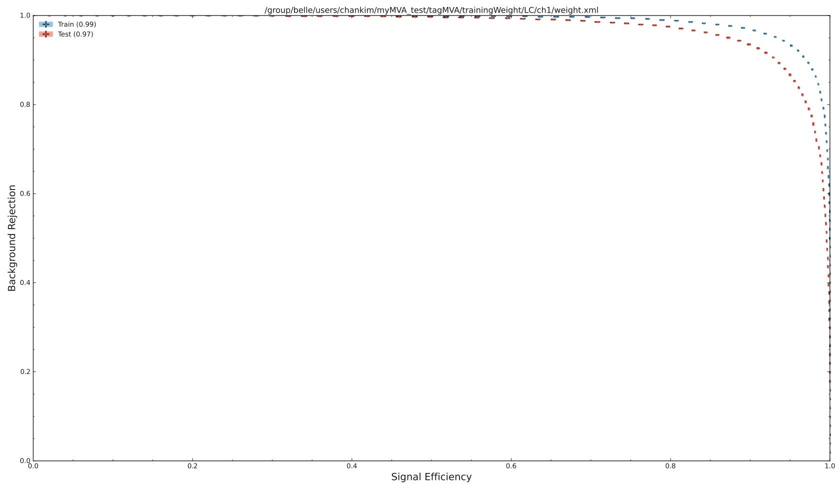

Figure 149: ROC Curve

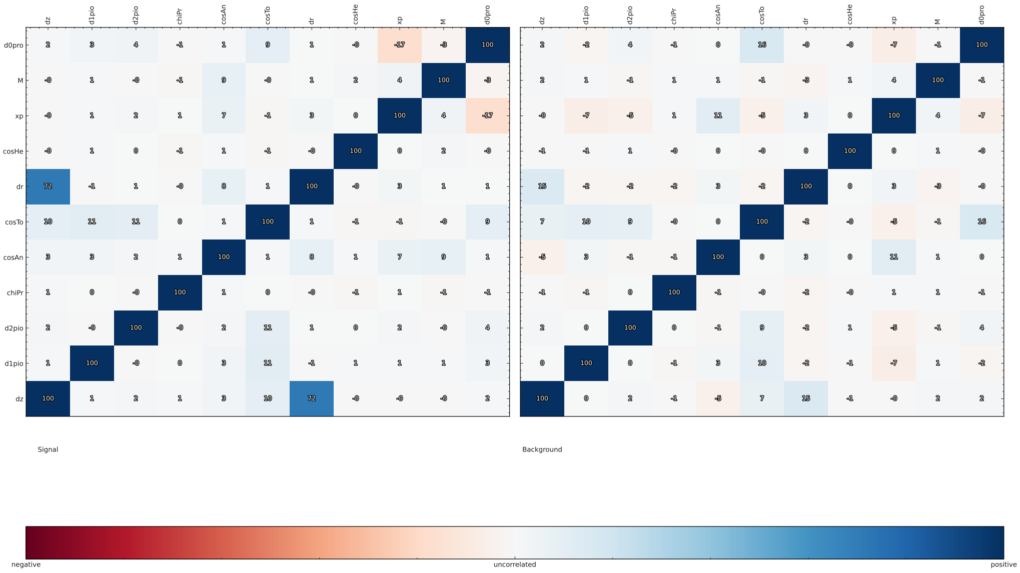

Figure 150: Correlation plot

A.1.39 $\Lambda_c^+ \to p^+ K^- K^+$

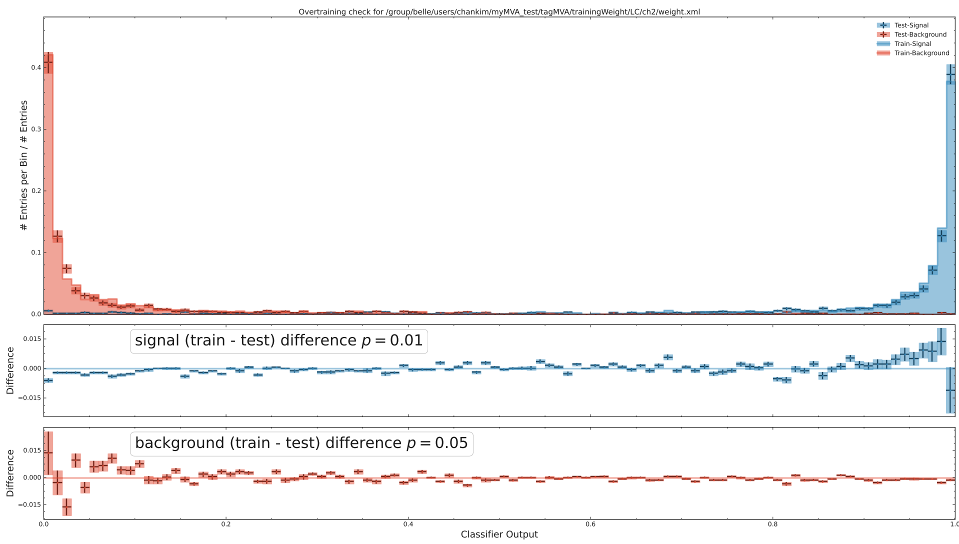

Figure 151: BDT output

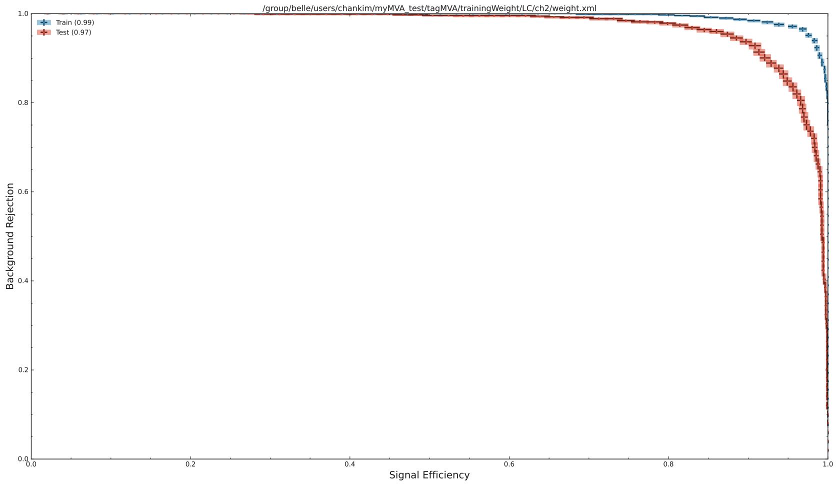

Figure 152: ROC Curve

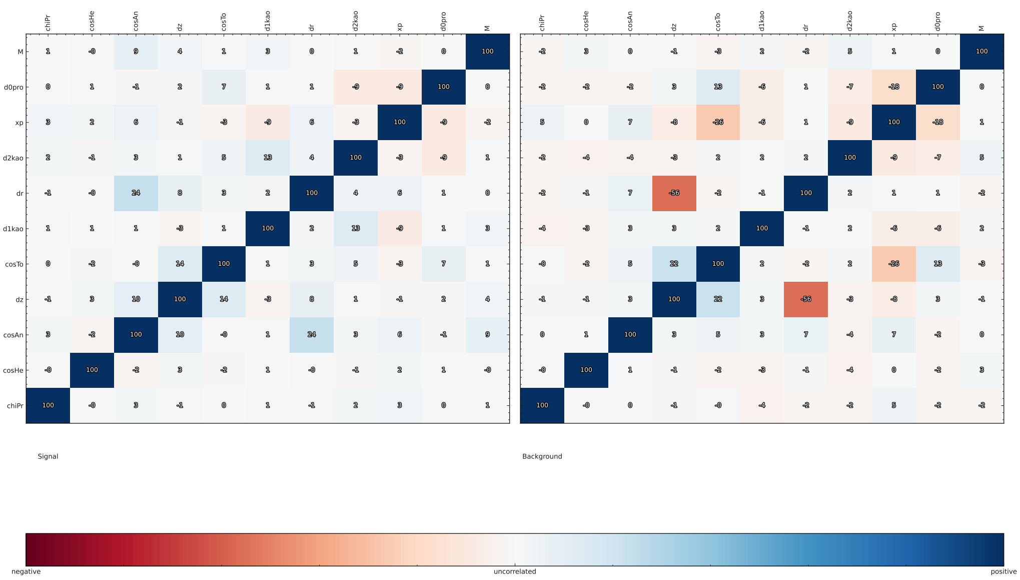

Figure 153: Correlation plot

A.1.40 $\Lambda_c^+ \to p^+ K^- \pi^+ \pi^0$

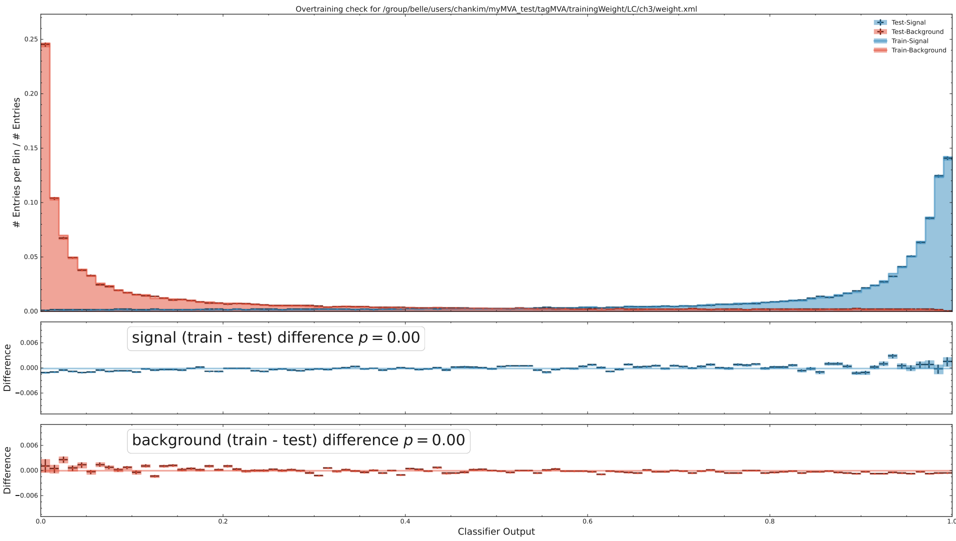

Figure 154: BDT output

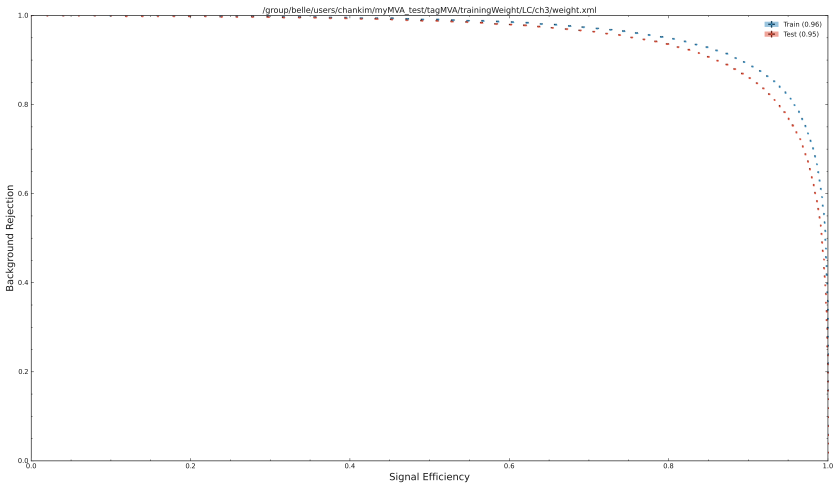

Figure 155: ROC Curve

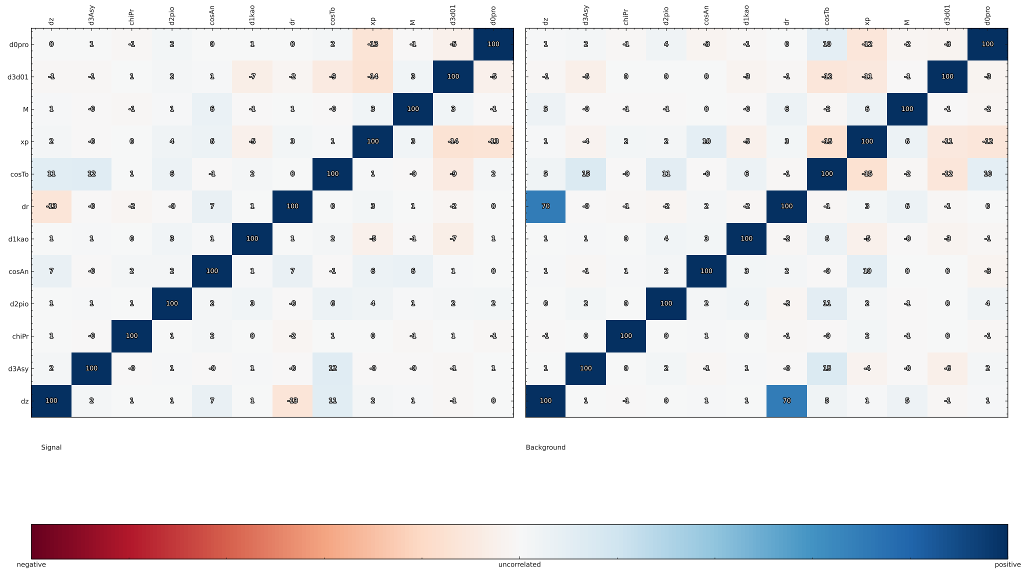

Figure 156: Correlation plot

A.1.41 $\Lambda_c^+ \to p^+ K^- \pi^+ \pi^0 \pi^0$

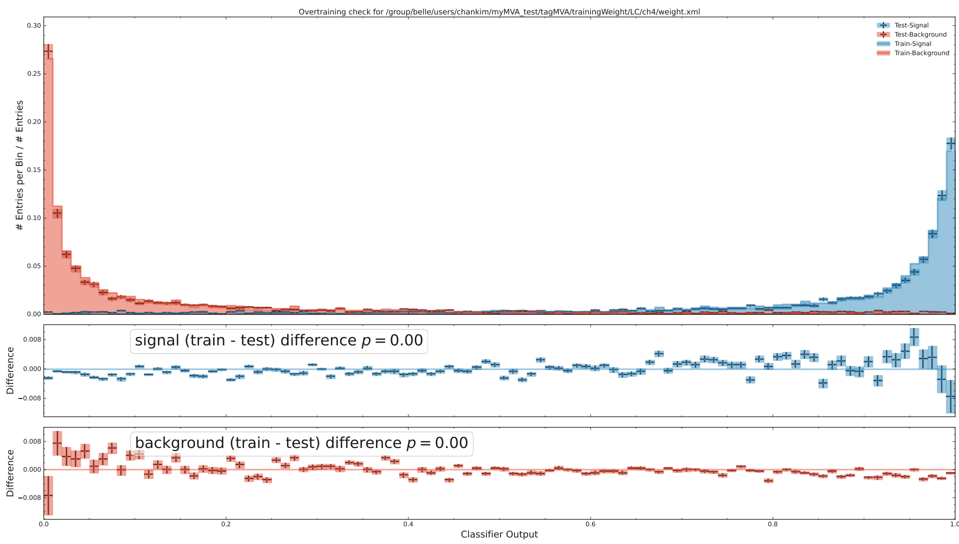

Figure 157: BDT output

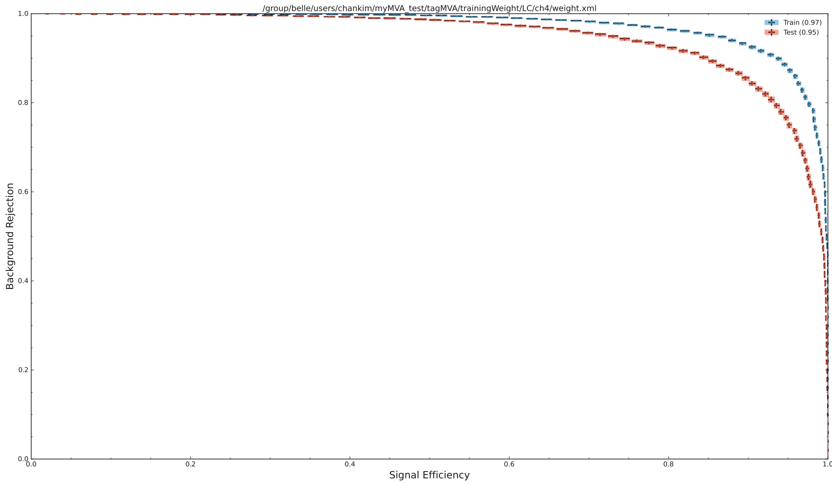

Figure 158: ROC Curve

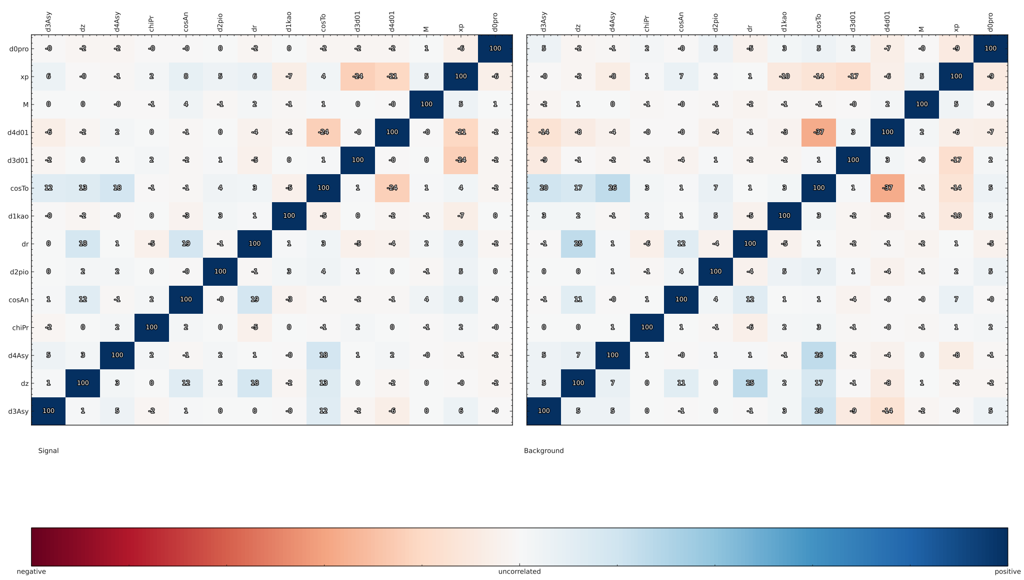

Figure 159: Correlation plot

A.1.42 $\Lambda_c^+ \to p^+\pi^-\pi^+\pi^-\pi^+$

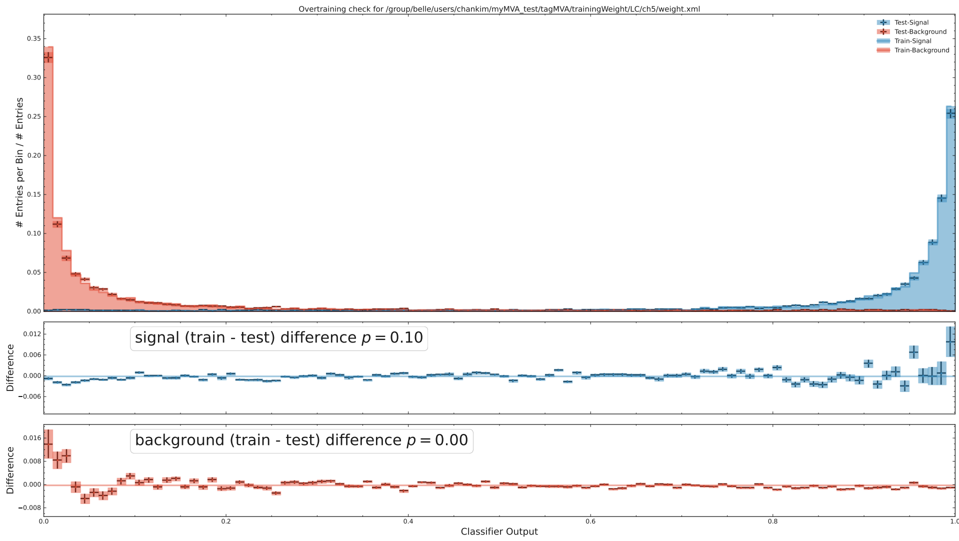

Figure 160: BDT output

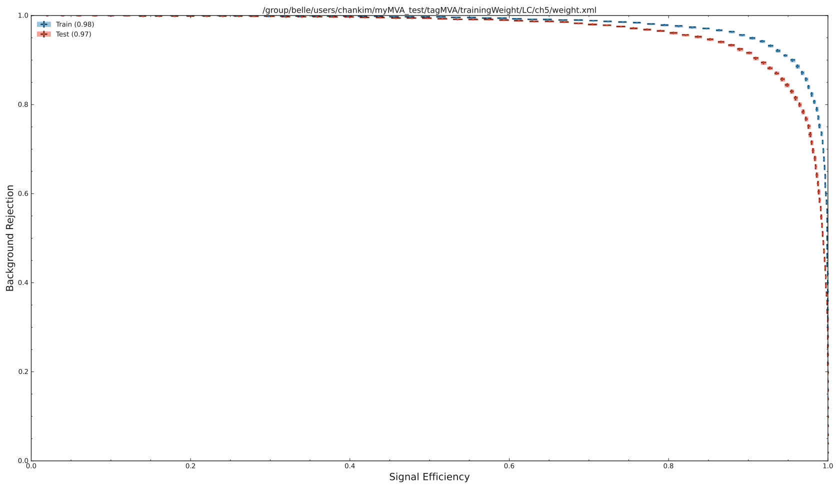

Figure 161: ROC Curve

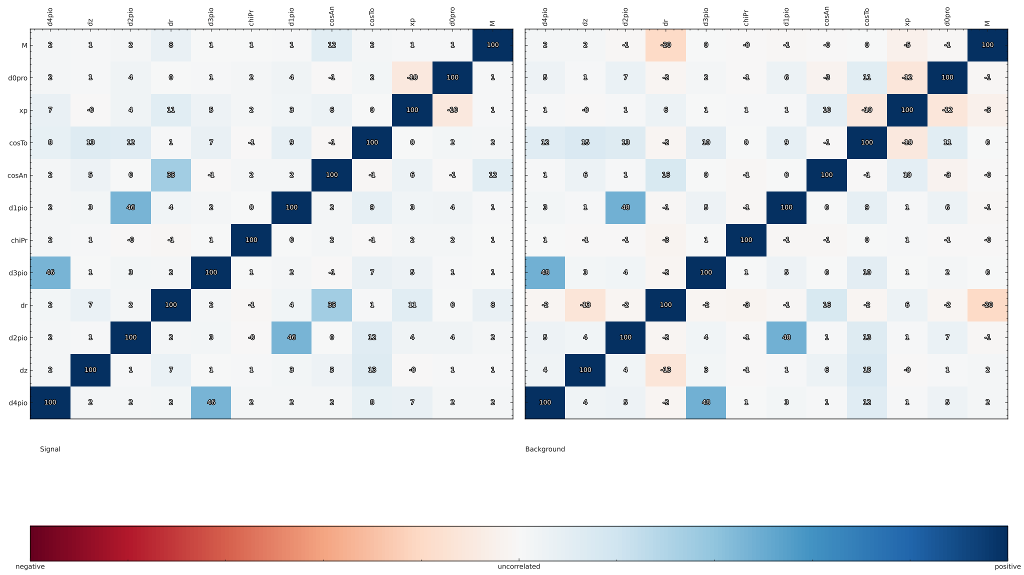

Figure 162: Correlation plot

A.1.43 $\Lambda_c^+ \to p^+ K_S^0$

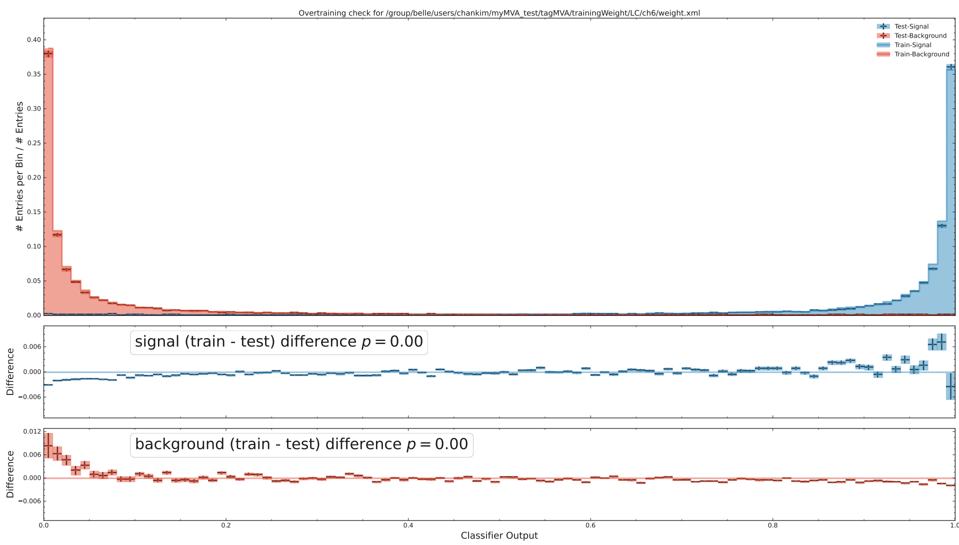

Figure 163: BDT output

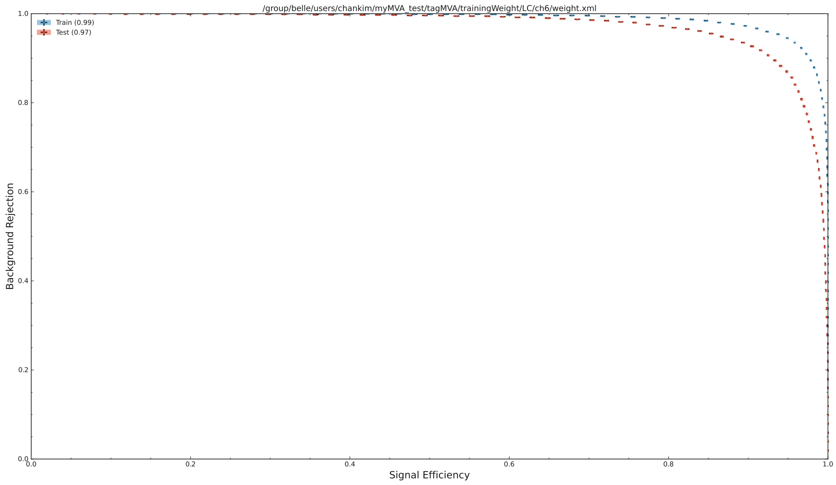

Figure 164: ROC Curve

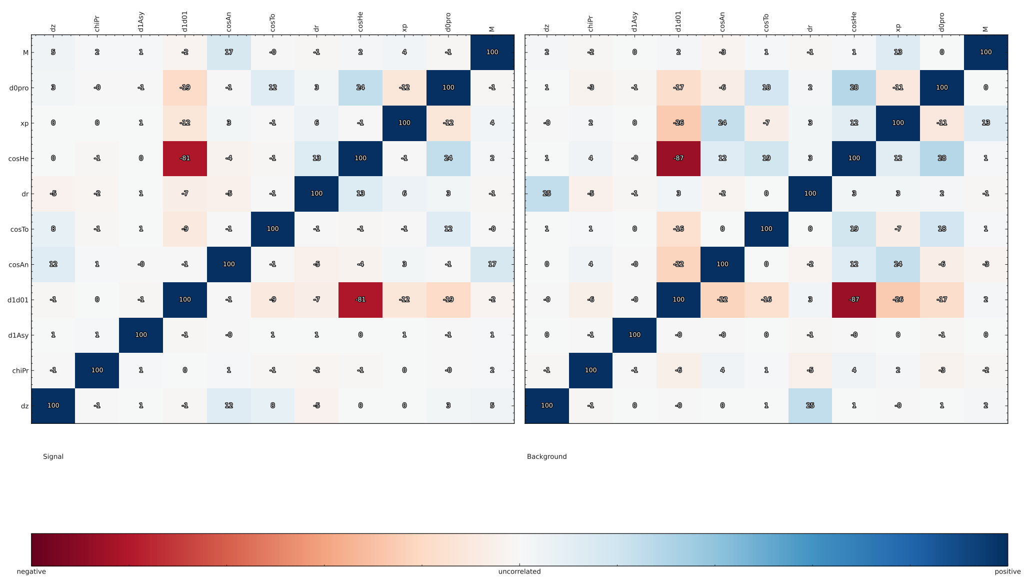

Figure 165: Correlation plot

A.1.44 $\Lambda_c^+ \to p^+ K_S^0 \pi^0$

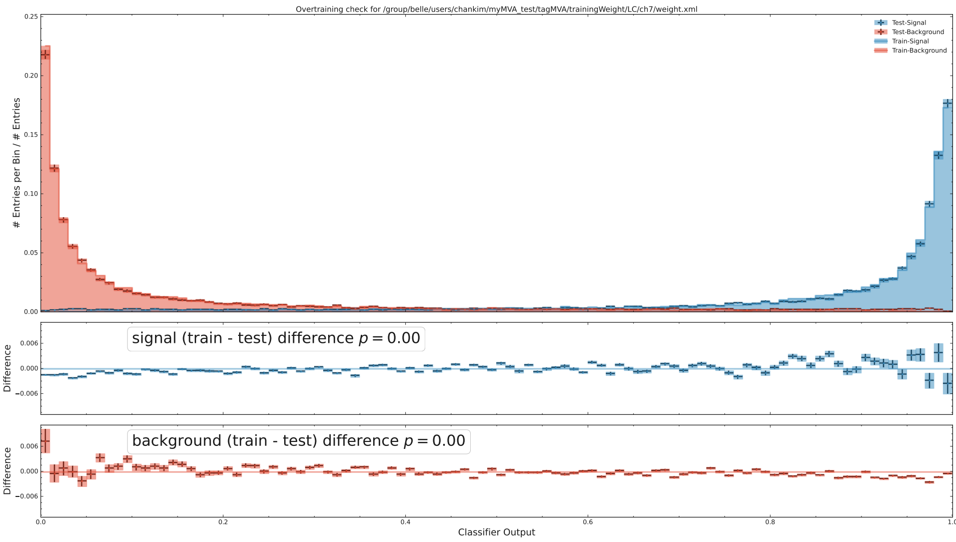

Figure 166: BDT output

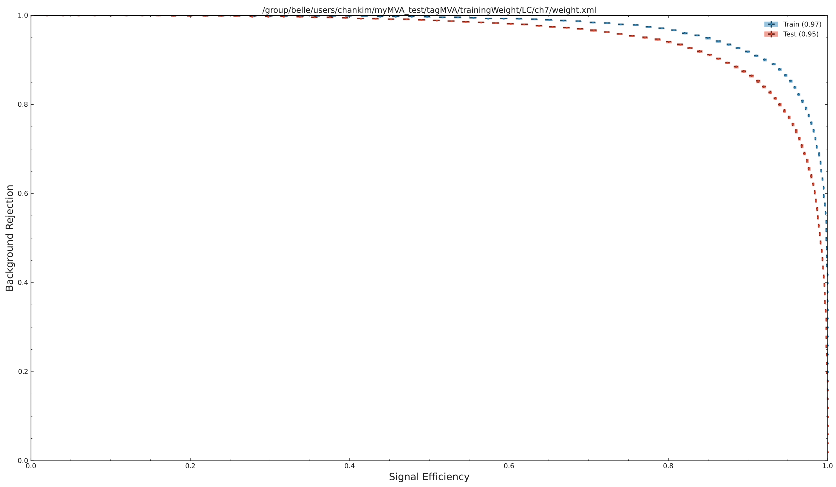

Figure 167: ROC Curve

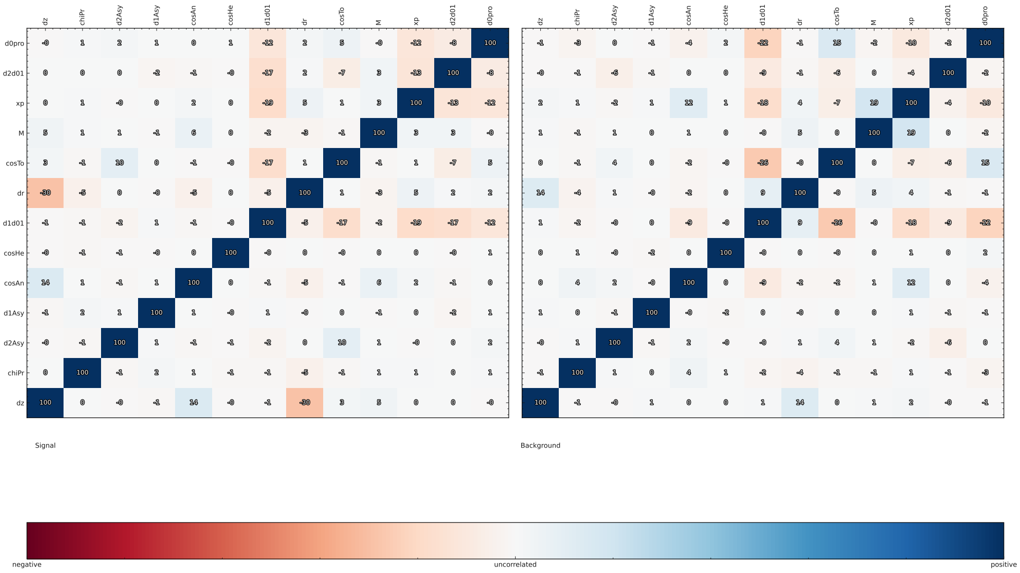

Figure 168: Correlation plot

A.1.45 $\Lambda_c^+ \to p^+\pi^-\pi^+K_S^0$

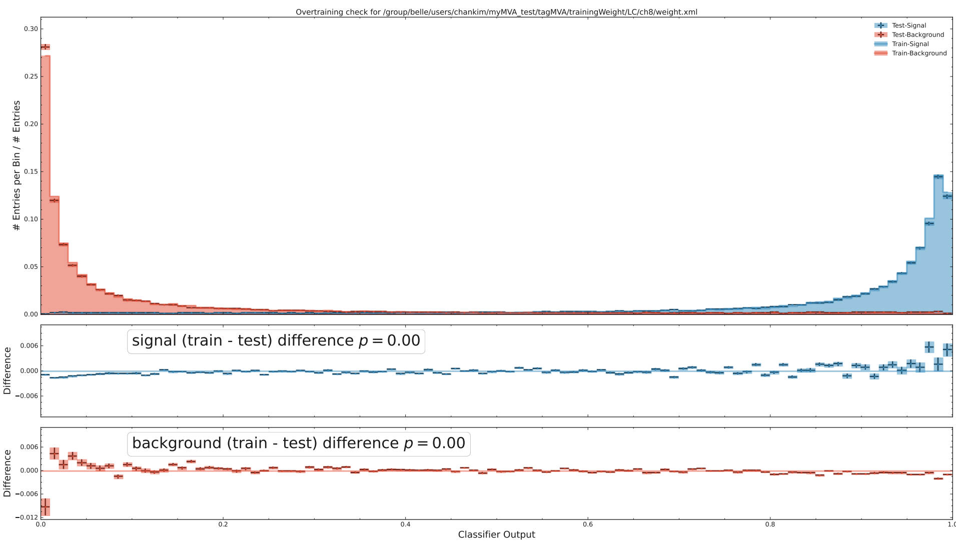

Figure 169: BDT output

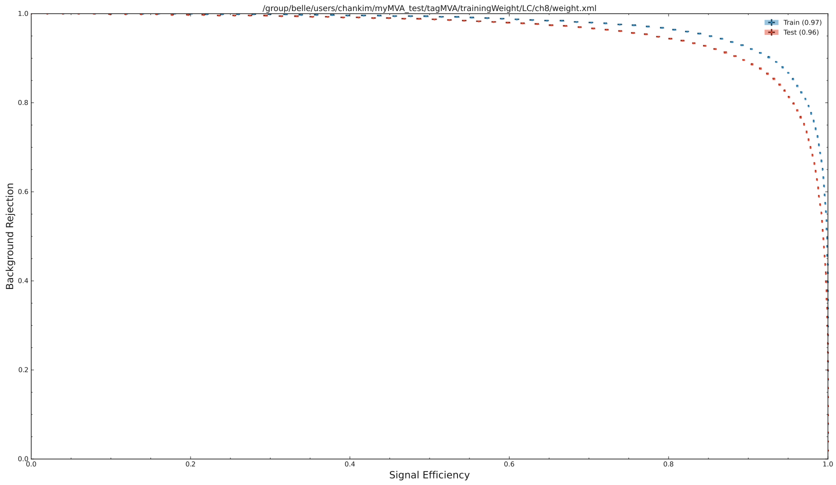

Figure 170: ROC Curve

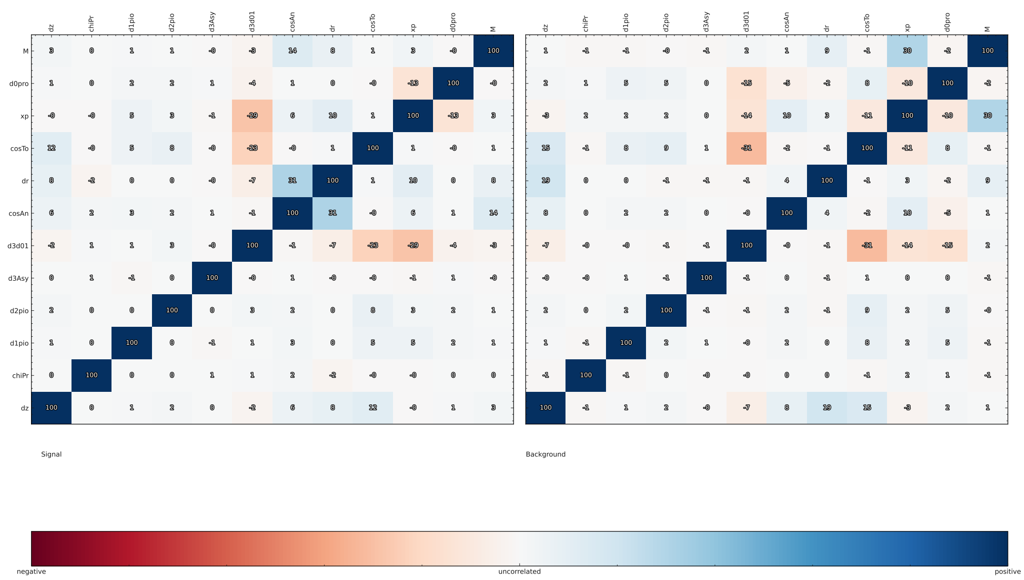

Figure 171: Correlation plot

A.1.46 $\Lambda_c^+ \to \pi^+\Lambda^0$

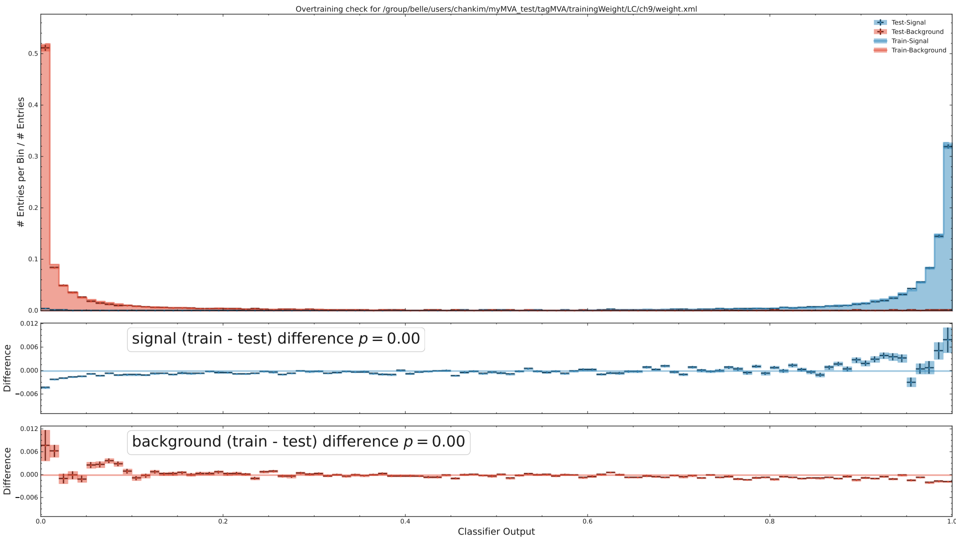

Figure 172: BDT output

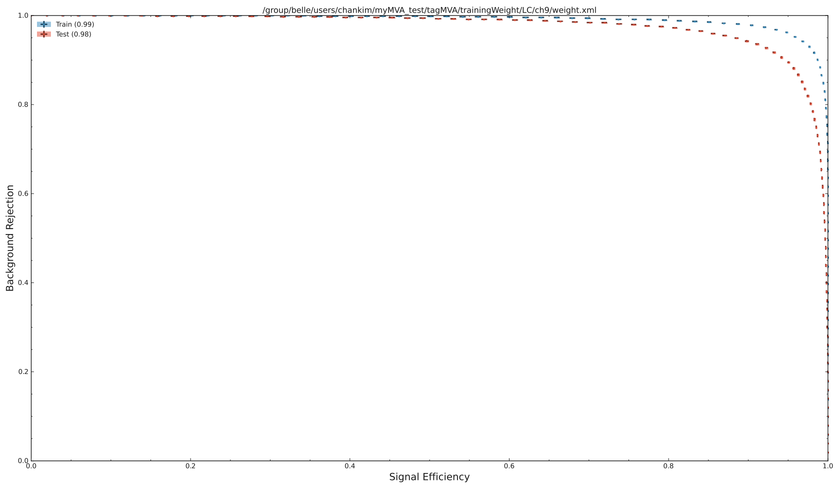

Figure 173: ROC Curve

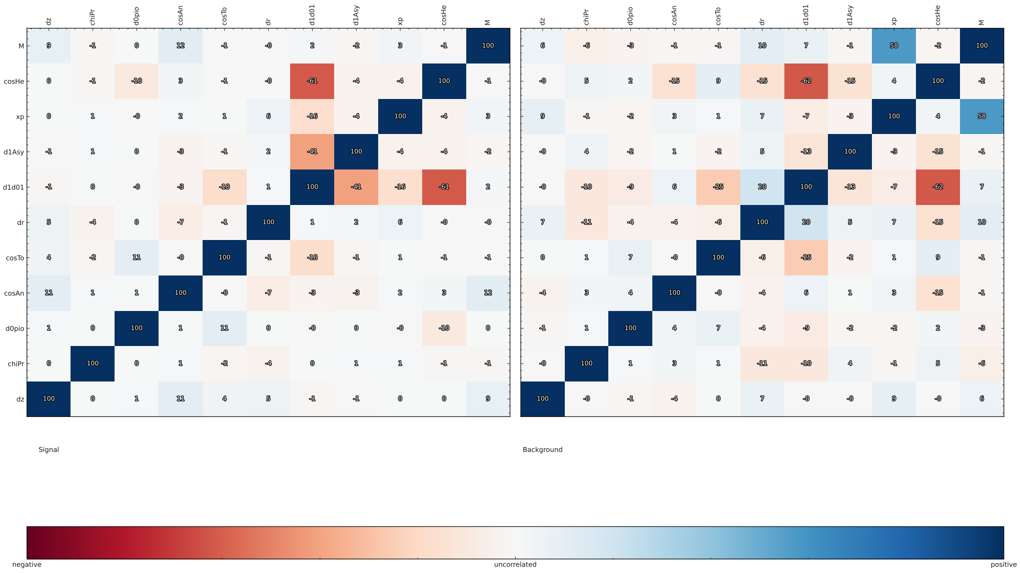

Figure 174: Correlation plot

A.1.47 $\Lambda_c^+ \to \pi^+\pi^0\Lambda^0$

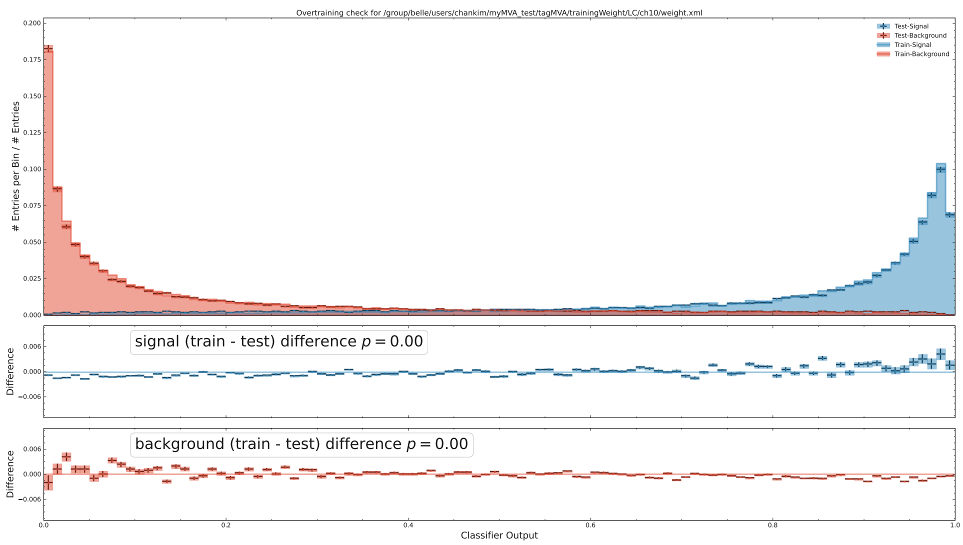

Figure 175: BDT output

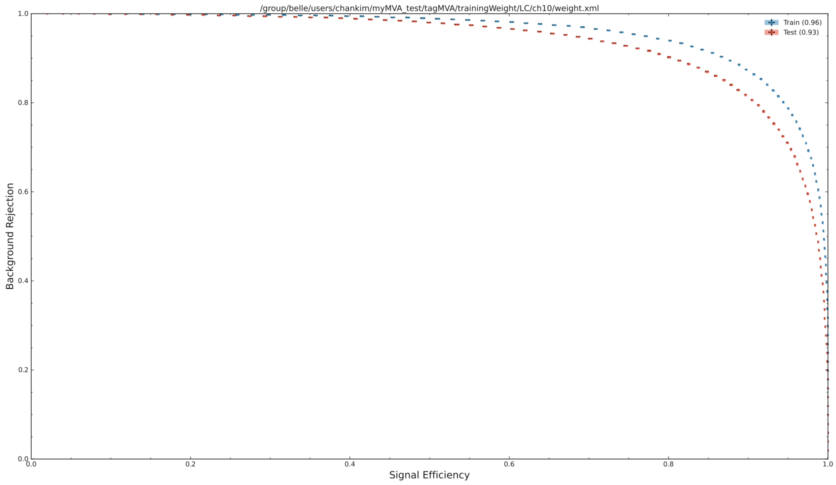

Figure 176: ROC Curve

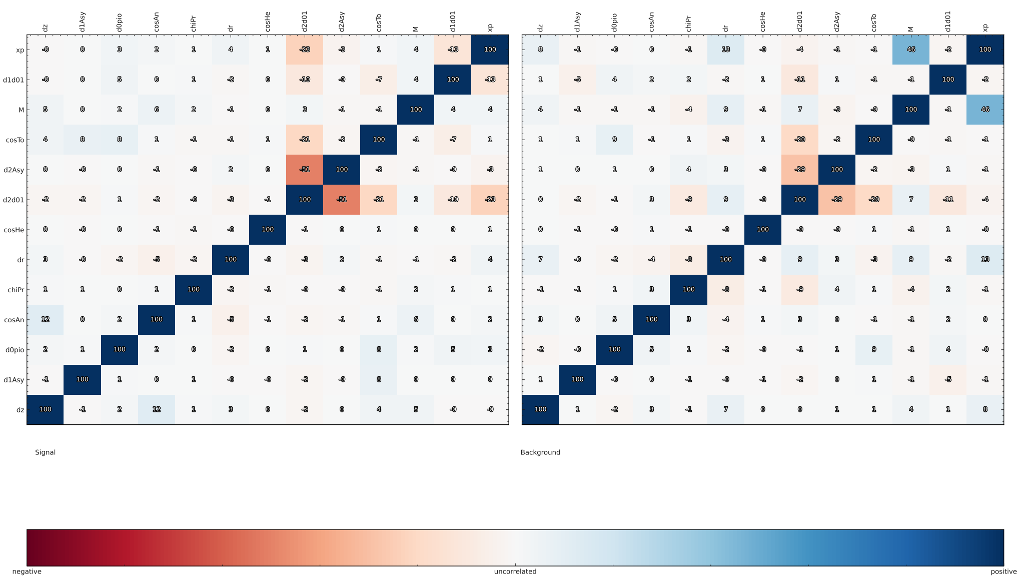

Figure 177: Correlation plot

A.1.48 $\Lambda_c^+ \to \pi^+\pi^-\pi^+\Lambda^0$

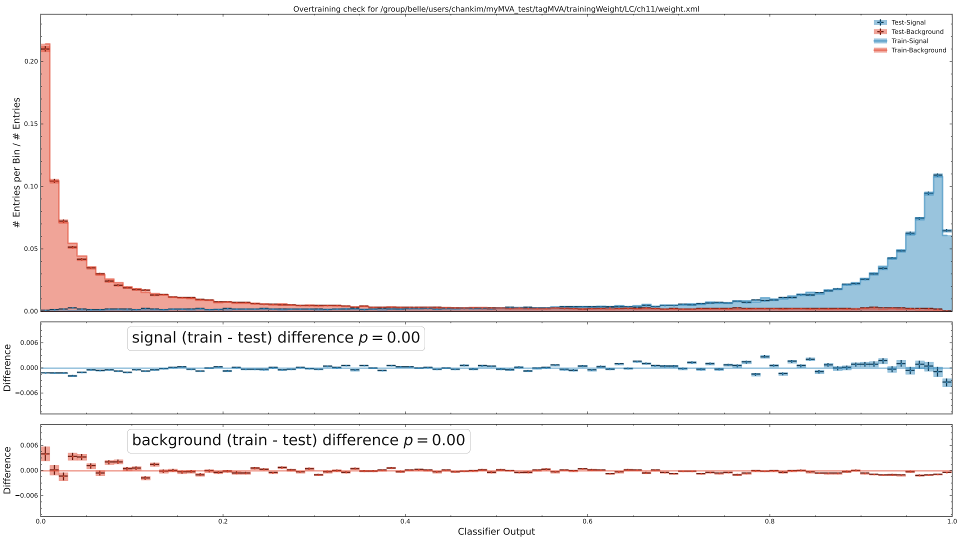

Figure 178: BDT output

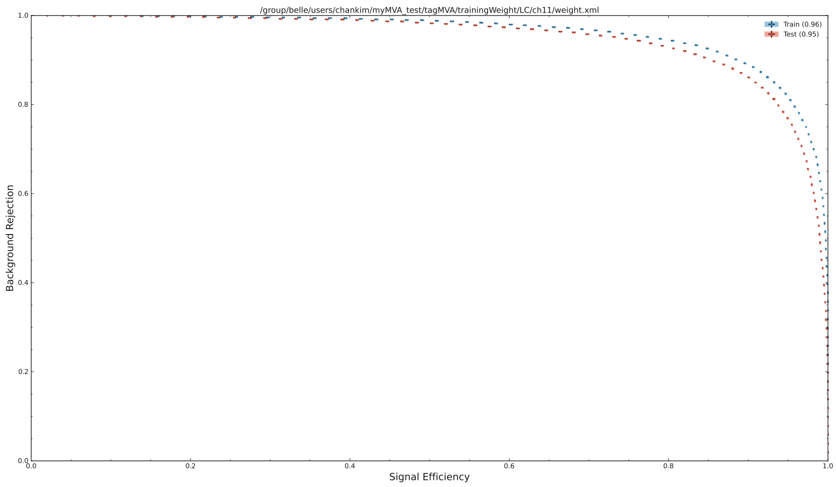

Figure 179: ROC Curve

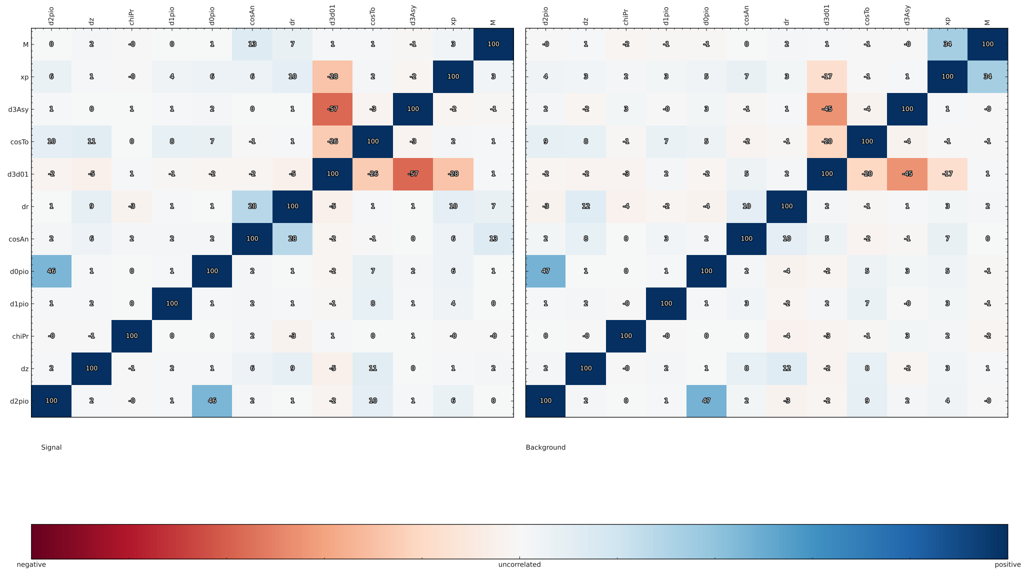

Figure 180: Correlation plot

426 ## A.1.49 $\Lambda_c^+ \to \pi^+\pi^-\Sigma^+$

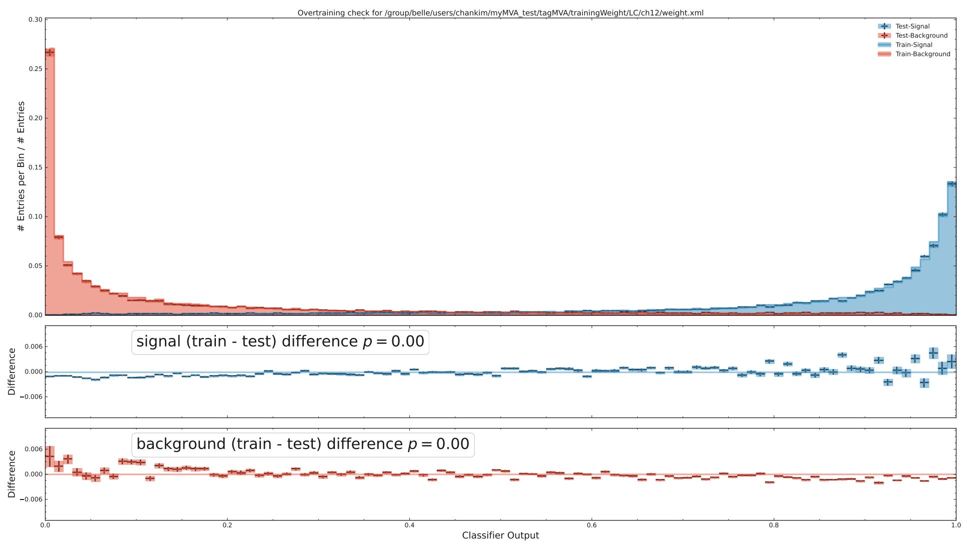

Figure 181: BDT output

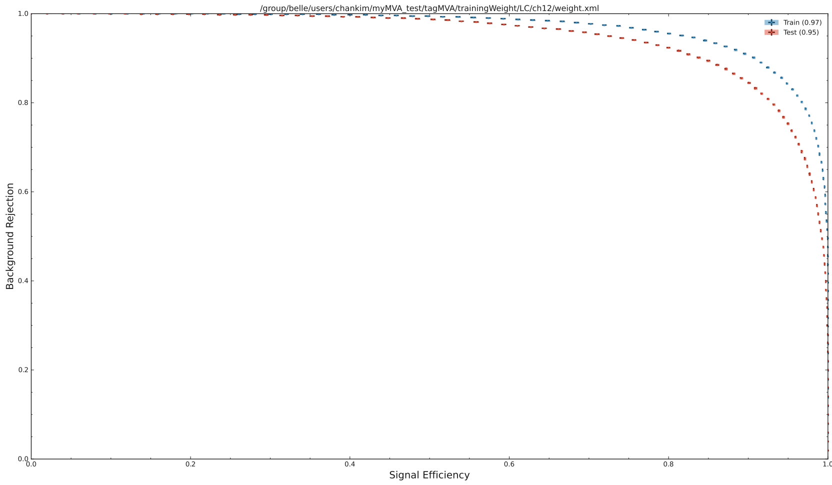

Figure 182: ROC Curve

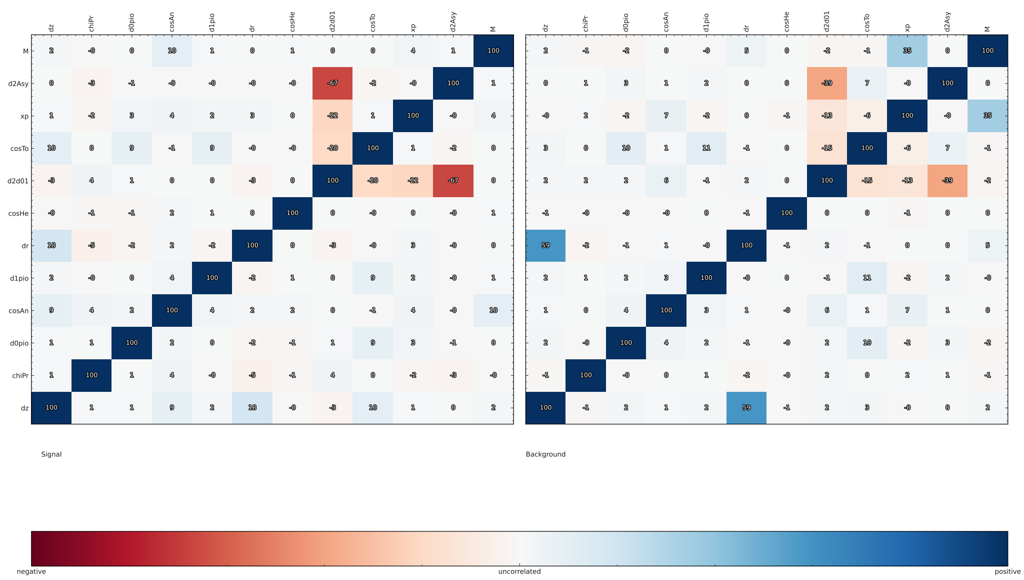

Figure 183: Correlation plot

427 ### A.1.50 $\Lambda_c^+ \to \pi^+\pi^-\pi^0\Sigma^+$

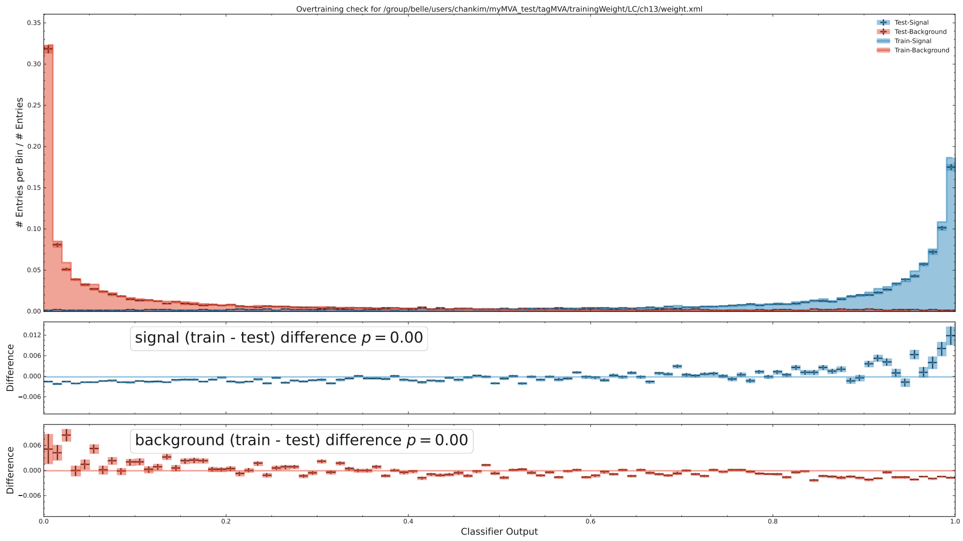

Figure 184: BDT output

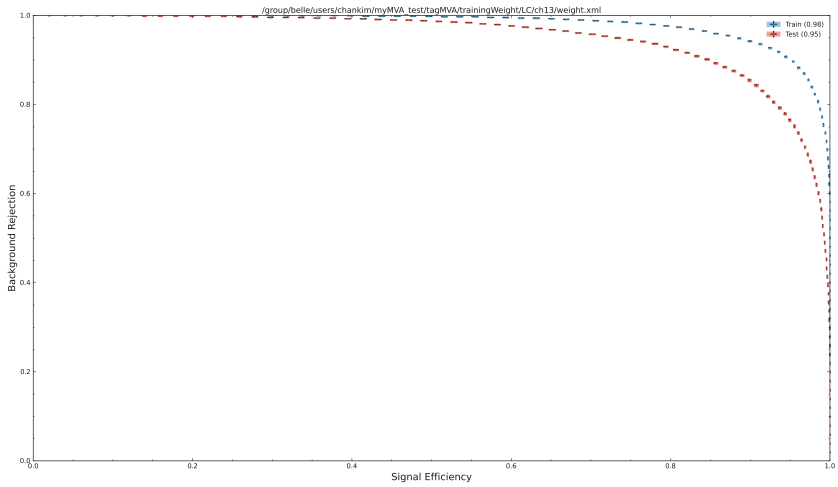

Figure 185: ROC Curve

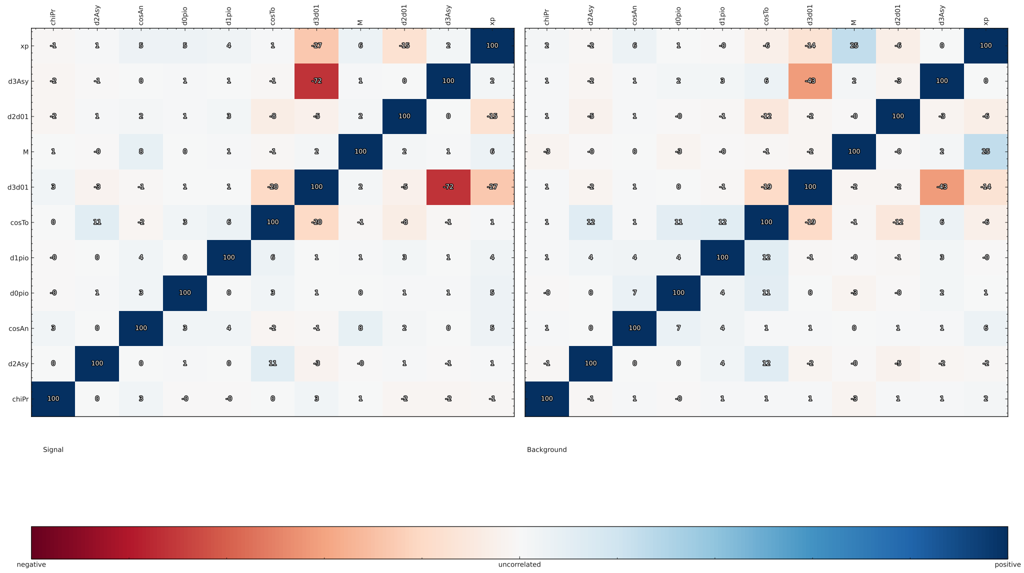

Figure 186: Correlation plot

A.1.51 $\Lambda_c^+ \to \pi^0 \Sigma^+$

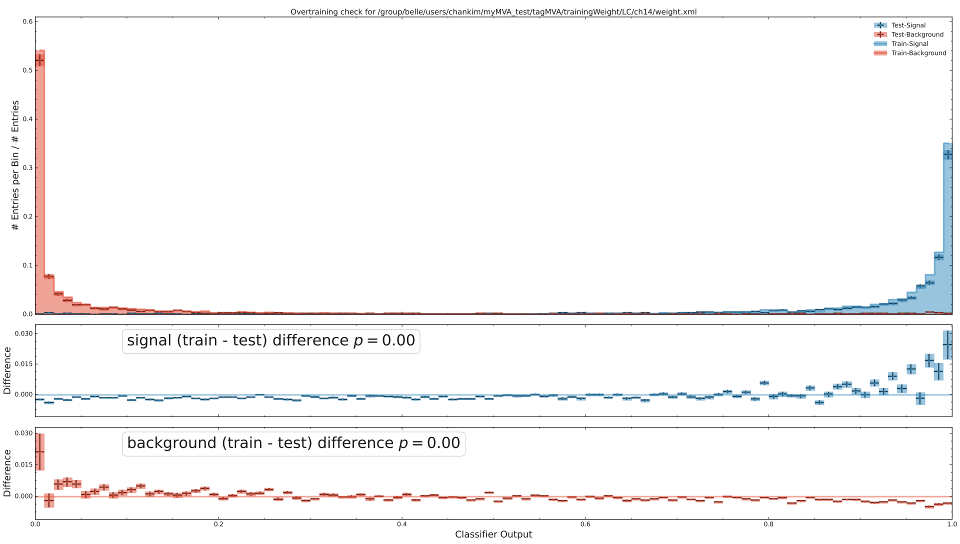

Figure 187: BDT output

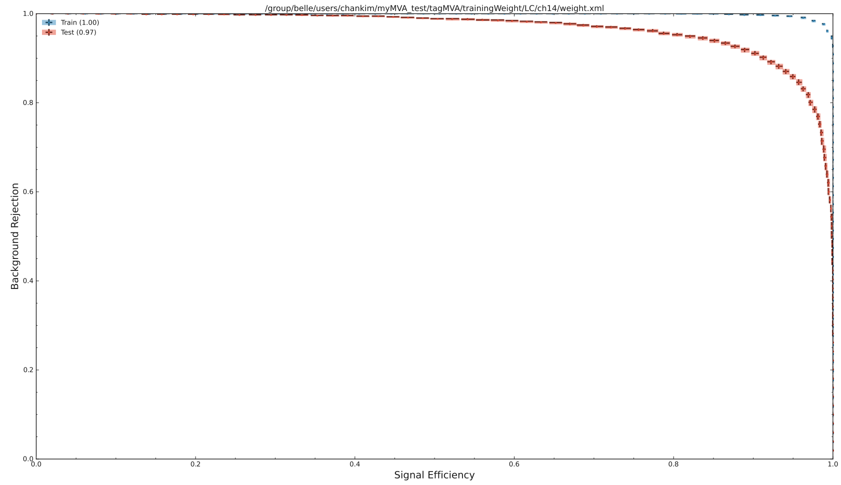

Figure 188: ROC Curve

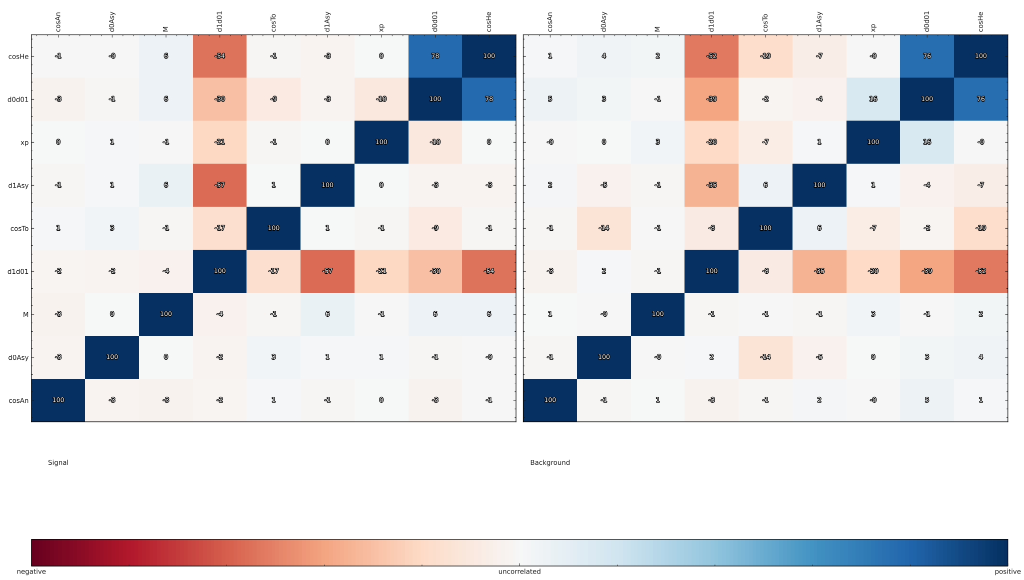

Figure 189: Correlation plot

A.1.52 $D^{*+} \to D^0\pi^+$

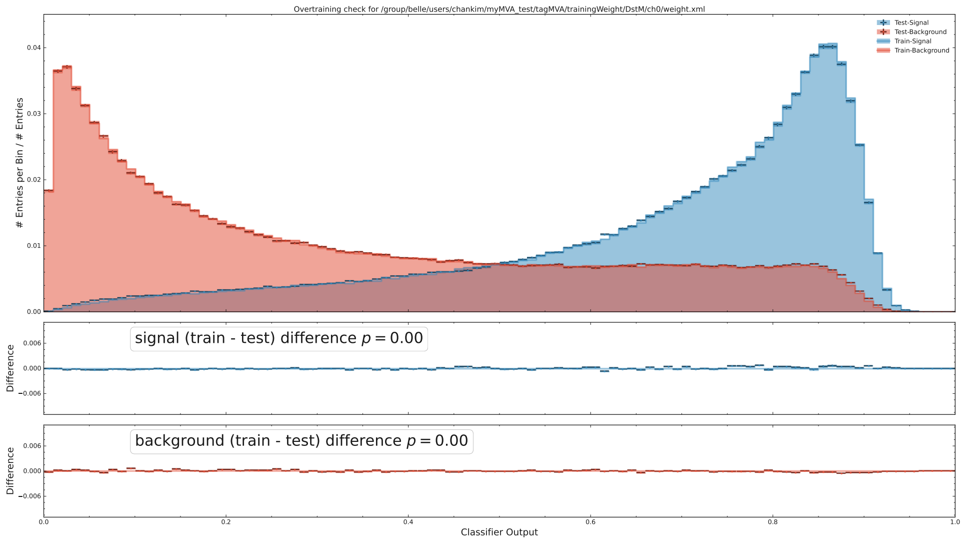

Figure 190: BDT output

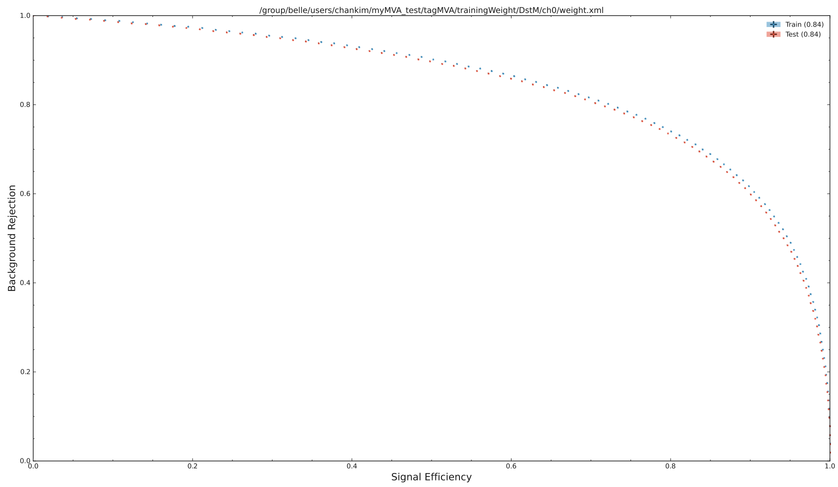

Figure 191: ROC Curve

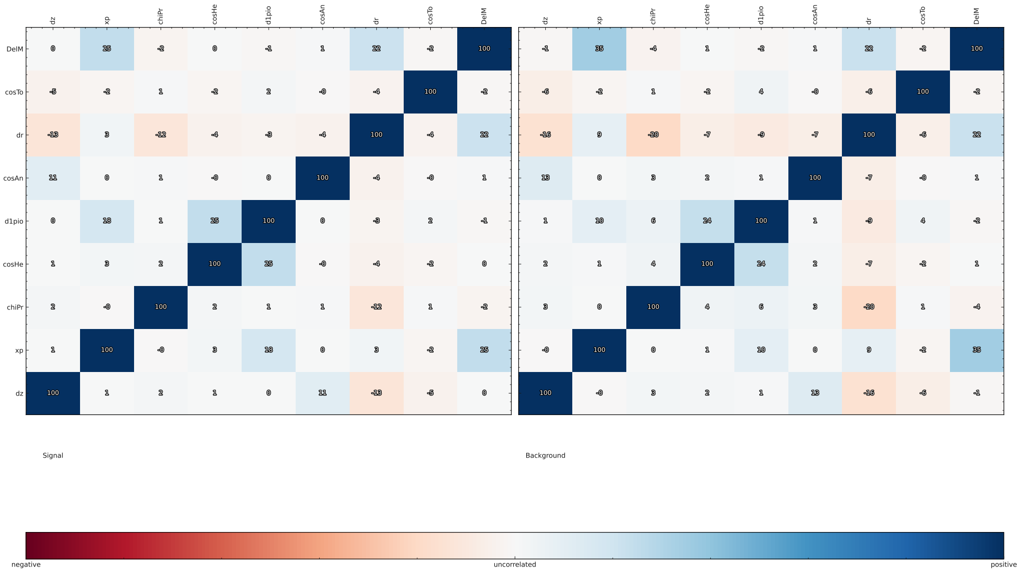

Figure 192: Correlation plot

A.1.53 $D^{*+} \to D^{+}\pi^{0}$

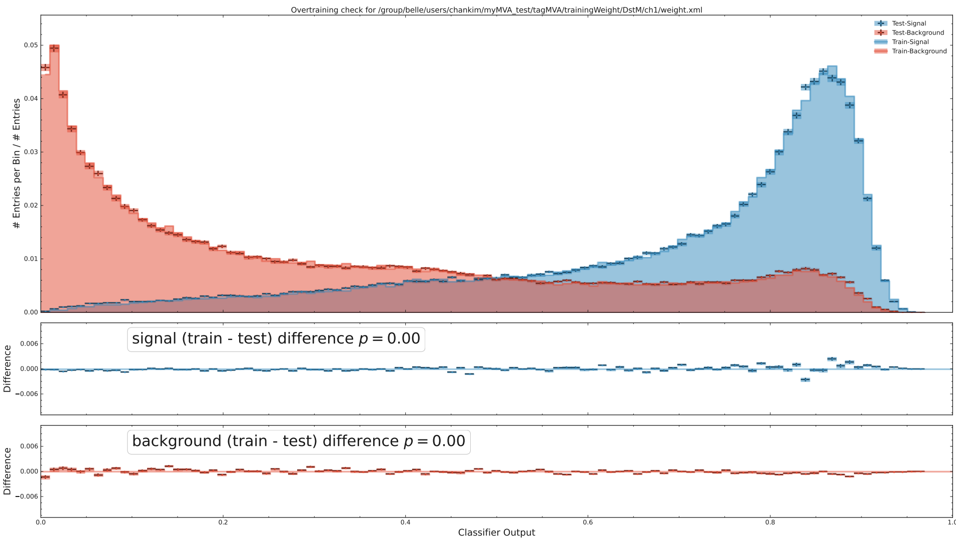

Figure 193: BDT output

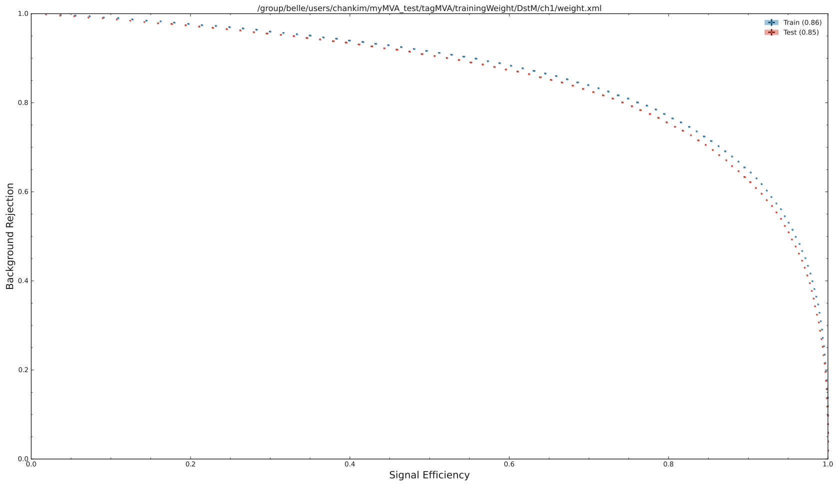

Figure 194: ROC Curve

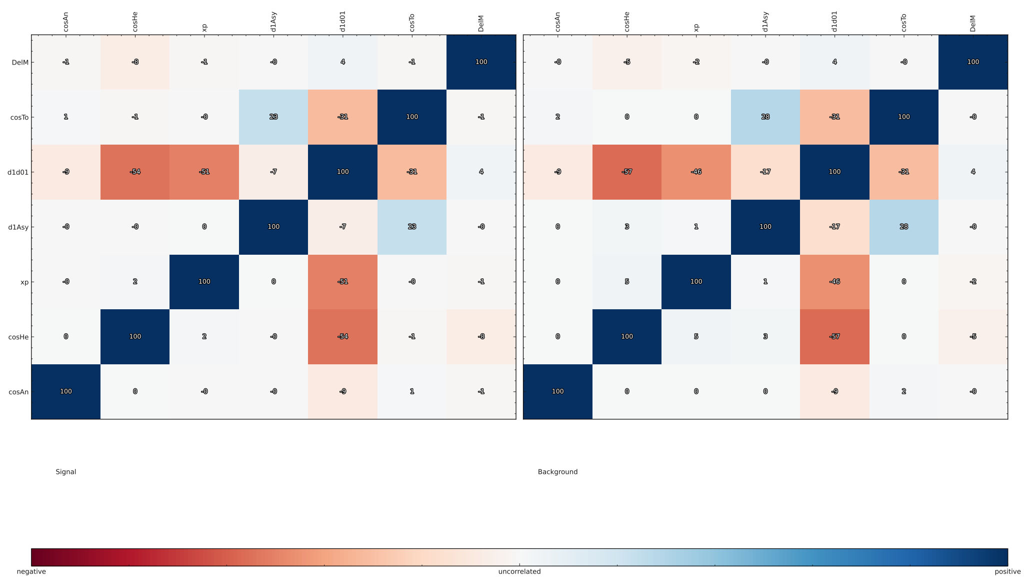

Figure 195: Correlation plot

431 ### A.1.54 $D^{*0} \to D^0\gamma$

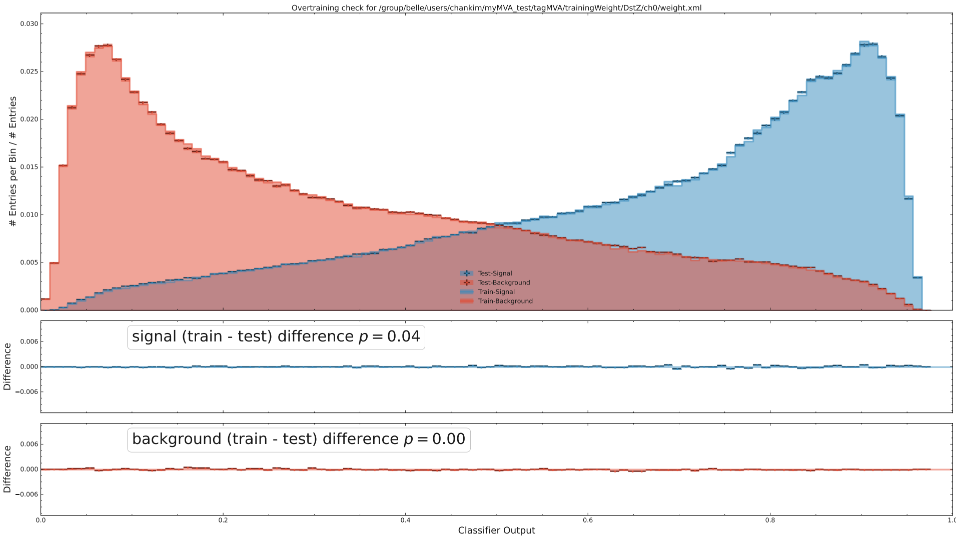

Figure 196: BDT output

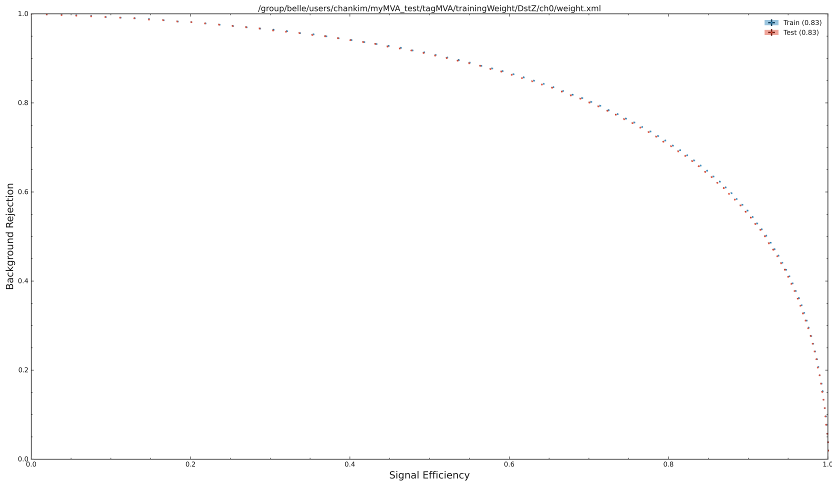

Figure 197: ROC Curve

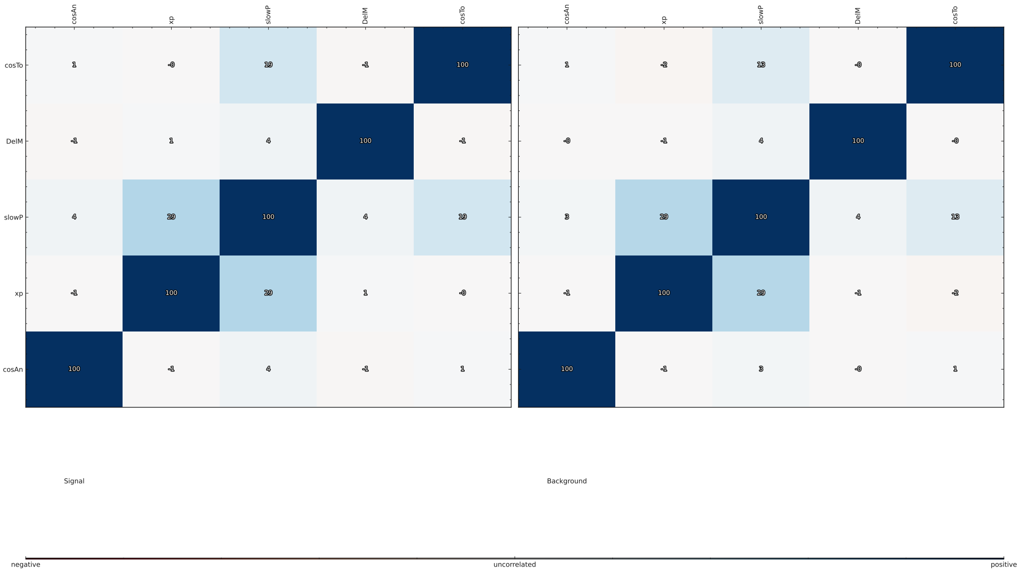

Figure 198: Correlation plot

432 A.1.55 $D^{*0} \to D^0\pi^0$

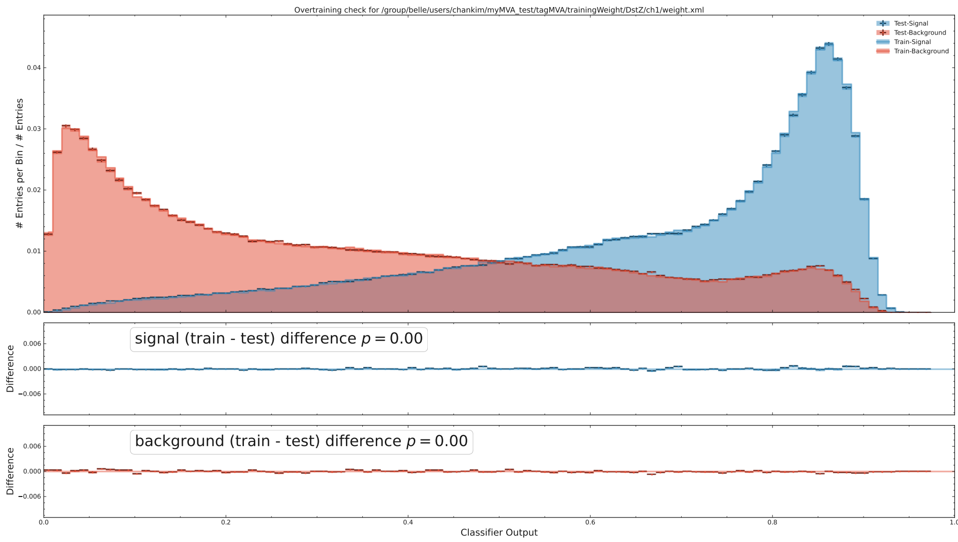

Figure 199: BDT output

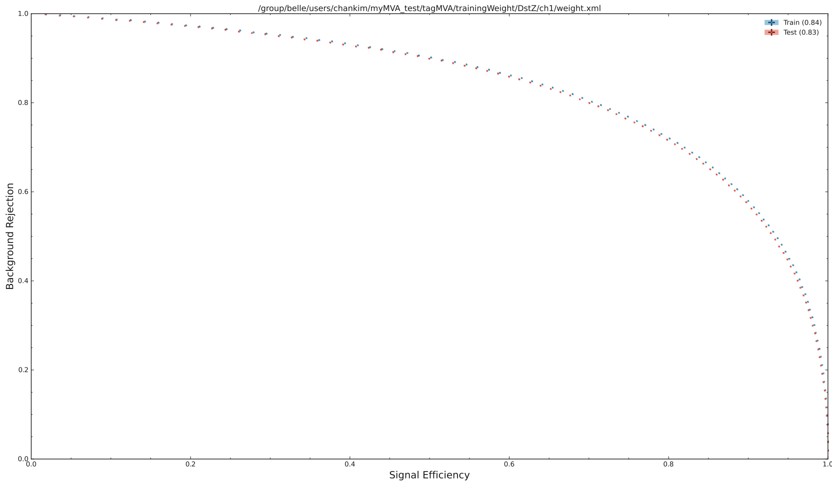

Figure 200: ROC Curve

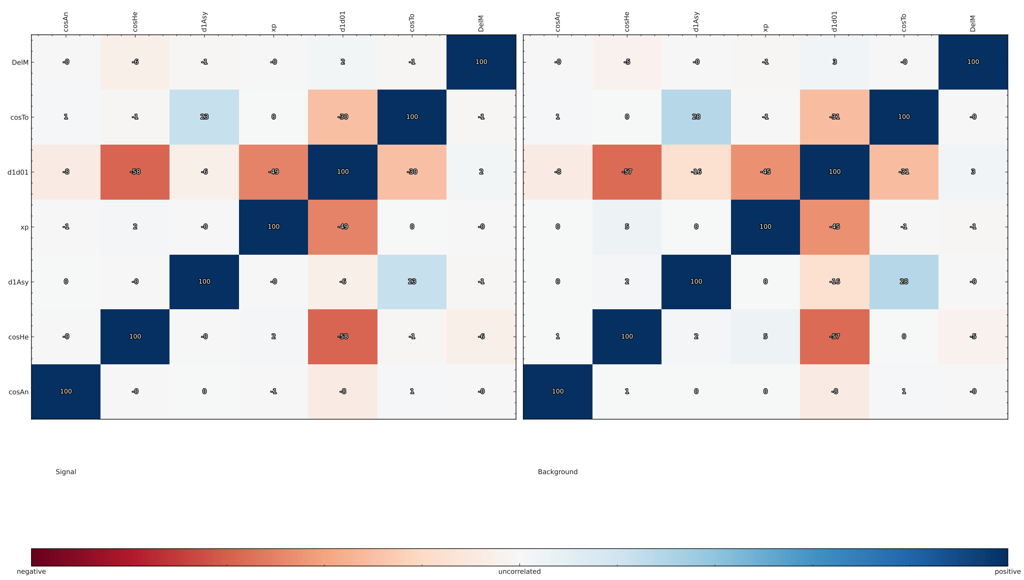

Figure 201: Correlation plot

A.1.56 $D_s^{*+} \to D_s^+ \gamma$

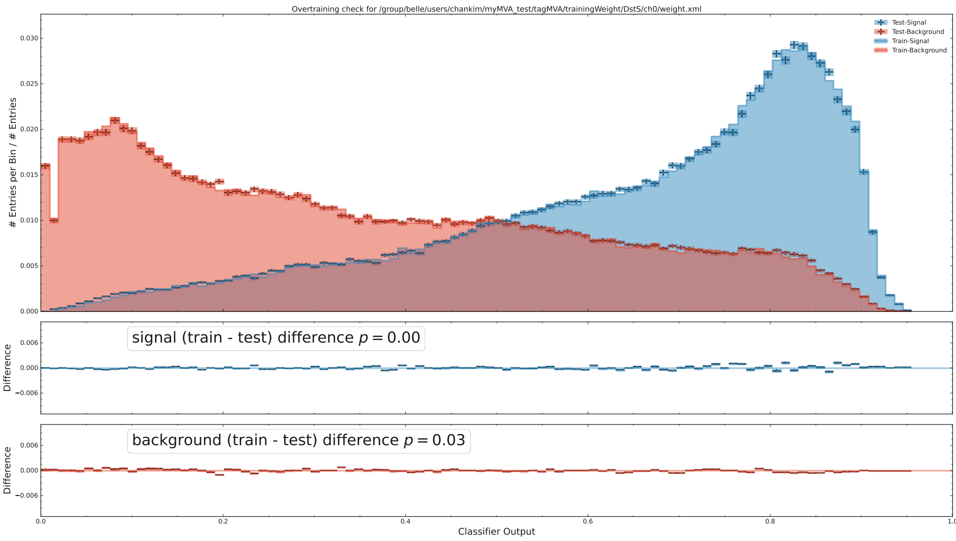

Figure 202: BDT output

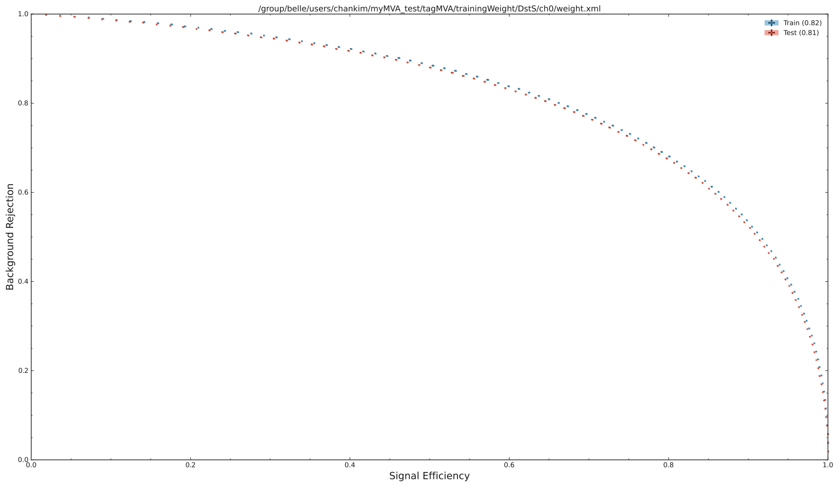

Figure 203: ROC Curve

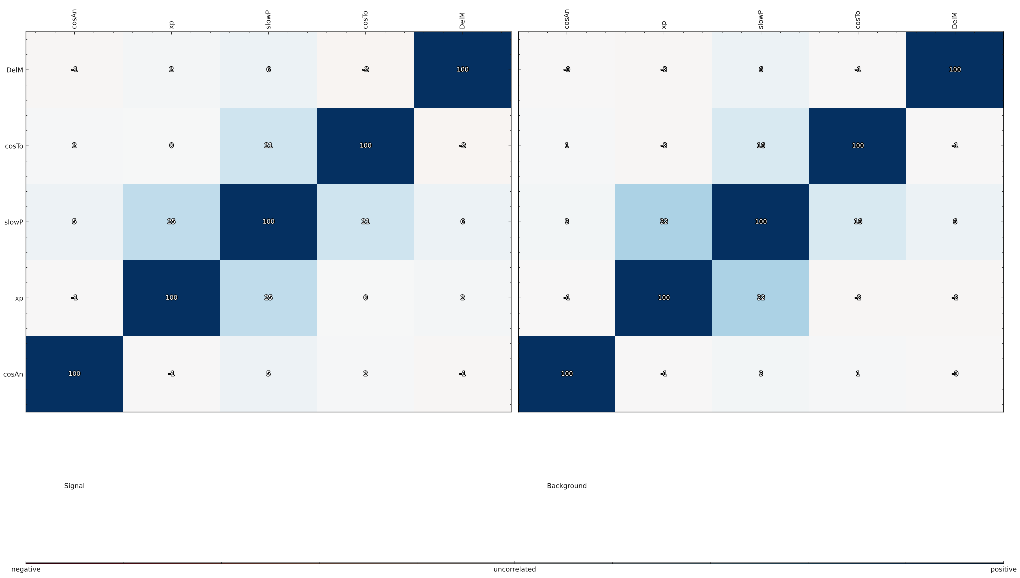

Figure 204: Correlation plot

B.0 Second Appendix

References

recommended references are

- Belle II physics: [1]
- B factories: [2]
- Belle: [3]
- CKM matrix: [4]
- Belle II detector: [5]
- SuperKEKB: [6]
- EvtGen: [7]
- Pythia8: [8]
- KKMC: [9]
- TAUOLA: [10]
- Photos: [11]
- Geant4: [12]
- basf2: [13]

- FEI: [14]
- PDG: [15]
- HFLAV: [16]

Some other standard references are available in `references.bib`. To add your own references to the bibtex file use the command `./addref` with the arXiv number or inspire ID as argument. The added entries are might still need some editing:

- check that Latex symbols in the titles are properly rendered (use Belle II symbols whenever possible);
- page ranges should in many cases be shortened to just having the start page;
- collaborations might need to be added or indeed just the word "collaboration" put after them;
- for errata and/or addenda use the fields `extraPrefix`, `extraVolume`, `extraPages`, `extraYear`, and `extraDoi`, as done for example in Ref. [1].

References

[1] W. Altmannshofer *et al.*, *The Belle II physics book*, PTEP **2019** (2019) 123C01, Erratum ibid. **2020** (2020) 029201, `arXiv:1808.10567`.

[2] Ed. A. J. Bevan, B. Golob, Th. Mannel, S. Prell, and B. D. Yabsley, *The physics of the B factories*, Eur. Phys. J. **C74** (2014) 3026, `arXiv:1406.6311`.

[3] Belle collaboration, J. Brodzicka *et al.*, *Physics achievements from the Belle experiment*, PTEP **2012** (2012) 04D001, `arXiv:1212.5342`.

[4] M. Kobayashi and T. Maskawa, *CP violation in the renormalizable theory of weak interaction*, Prog. Theor. Phys. **49** (1973) 652.

[5] Belle II collaboration, T. Abe, *Belle II technical design report*, `arXiv:1011.0352`.

[6] K. Akai, K. Furukawa, and H. Koiso, *SuperKEKB collider*, Nucl. Instrum. Meth. **A907** (2018) 188, `arXiv:1809.01958`.

[7] D. J. Lange, *The EvtGen particle decay simulation package*, Nucl. Instrum. Meth. **A462** (2001) 152.

[8] T. Sjöstrand *et al.*, *An Introduction to PYTHIA 8.2*, Comput. Phys. Commun. **191** (2015) 159, `arXiv:1410.3012`.

[9] S. Jadach, B. F. L. Ward, and Z. Wąs, *The precision Monte Carlo event generator KK for two-fermion final states in* e^+e^- *collisions*, Comput. Phys. Commun. **130** (2000) 260, `arXiv:hep-ph/9912214`.

[10] S. Jadach, J. H. Kuhn, and Z. Wąs, *TAUOLA: A library of Monte Carlo programs to simulate decays of polarized tau leptons*, Comput. Phys. Commun. **64** (1990) 275.

[11] E. Barberio, B. van Eijk, and Z. Wąs, *PHOTOS: A universal Monte Carlo for QED radiative corrections in decays*, Comput. Phys. Commun. **66** (1991) 115.

[12] GEANT4 collaboration, S. Agostinelli *et al.*, *GEANT4: A simulation toolkit*, Nucl. Instrum. Meth. **A506** (2003) 250.

[13] Belle II Framework Software Group, T. Kuhr *et al.*, *The Belle II Core Software*, Comput. Softw. Big Sci. **3** (2019) 1, `arXiv:1809.04299`.

[14] T. Keck *et al.*, *The Full Event Interpretation*, Comput. Softw. Big Sci. **3** (2019) 6, `arXiv:1807.08680`.

[15] Particle Data Group, P. A. Zyla *et al.*, *Review of Particle Physics*, PTEP **2020** (2020) 083C01.

[16] Heavy Flavor Averaging Group, Y. S. Amhis *et al.*, *Averages of b-hadron, c-hadron, and* τ*-lepton properties as of 2018*, Eur. Phys. J. **C81** (2021) 226, `arXiv:1909.12524`, updated results and plots available at `https://hflav.web.cern.ch/`.

Additional Material

This sections contains all figures and numbers that are requested to be approved for public presentation.